LA-UR-12-20901
Approved for public release; distribution is unlimited.

Title: Intrinsic Radiation Source Generation with the ISC Package: Data Comparisons and Benchmarking

Author(s): Solomon, Clell J. Jr.

Intended for: Report

Intrinsic Radiation Source Generation with the ISC Package: Data Comparisons and Benchmarking

Clell J. (CJ) Solomon

April 20, 2012

1 Introduction

The characterization of radioactive emissions from unstable isotopes (intrinsic radiation) is necessary for shielding and radiological-dose calculations from radioactive materials. While most radiation transport codes, e.g., MCNP [X-5 Monte Carlo Team, 2003], provide the capability to input user prescribed source definitions, such as radioactive emissions, they do not provide the capability to calculate the correct radioactive-source definition given the material compositions. Special modifications to MCNP have been developed in the past to allow the user to specify an intrinsic source, but these modification have not been implemented into the primary source base [Estes et al., 1988]. To facilitate the description of the intrinsic radiation source from a material with a specific composition, the Intrinsic Source Constructor library (LIBISC) and MCNP Intrinsic Source Constructor (MISC) utility have been written. The combination of LIBISC and MISC will be herein referred to as the ISC package.

LIBISC is a statically linkable C++ library that provides the necessary functionality to construct the intrinsic-radiation source generated by a material. Furthermore, LIBISC provides the ability use different particle-emission databases, radioactive-decay databases, and natural-abundance databases allowing the user flexibility in the specification of the source, if one database is preferred over others. LIBISC also provides functionality for aging materials and producing a thick-target bremsstrahlung photon source approximation from the electron emissions.

The MISC utility links to LIBISC and facilitates the description of intrinsic-radiation sources into a format directly usable with the MCNP transport code. Through a series of input keywords and arguments the MISC user can specify the material, age the material if desired, and produce a source description of the radioactive emissions from the material in an MCNP readable format. Further details of using the MISC utility can be obtained from the user guide [Solomon, 2012].

The remainder of this report presents a discussion of the databases available to LIBISC and MISC, a discussion of the models employed by LIBISC, a comparison of the thick-target bremsstrahlung model employed, a benchmark comparison to plutonium and depleted-uranium spheres, and a comparison of the available particle-emission databases.

2 Available Databases

The types of data files used by the ISC package fall into three categories:

1. *natural abundance* files that contain fractions of a naturally occurring isotope (these files typically have a ".na" extension)

2. *radioactive decay* files that contain the half lives, decay mechanisms, branching ratios, and daughters of a given isotope (these files typically have a ".dk" extension)

3. *particle emission* files that contain the types, energies, and intensities of radioactive emissions from an isotope (these files typically have an extension corresponding to the database name, e.g., ".endf7" for the ENDF-B/VII data)

2.1 Natural Abundance Data Files

Currently, only one natural-abundance data file has been compiled for use with the ISC package. The natural abundance data was obtained from the National Institute of Standards and Technology [NIST, 2011].

2.2 Radioactive Decay Data Files

Four radioactive-decay data files have been compiled for use with the ISC package. These data files contain information about the half lives, branching ratios, and daughter isotopes. The three primary radioactive-decay data files are "endf6.dk," "endf7.dk," and "radsrc.dk." The endf6.dk file was compiled from data in the ENDF-B/VI radioactive-decay sublibrary [Reich et al., 1991]. The endf7.dk file was compiled from data in the ENDF-B/VII radioactive-decay sublibrary [Johnson et al., 2011]. The radsrc.dk file was compiled from data distributed with the RadSrc utility [Hiller et al., 2007]. The final file "none.dk" contains the same information as that in the endf7.dk file without any of the daughter nuclide information. Using the none.dk file provides only the information necessary for activity calculations but not for decaying a material.

2.3 Particle Emission Data Files

Five sets of particle-emission data files have been compiled for use with the ISC package. These data files contain information about the types, energies, and intensities of radioactive emissions from an isotope. Each of the data sets contain varying levels of detail with regard to the radioactive emissions, e.g., some data sets only contain gamma decay information.

The particle emission data sets are "ENDF6," "ENDF7," "RadSrc," "IRTAPE11E," and "IRTAPE11L." The ENDF6 and ENDF7 data sets contain particle emissions from the ENDF-B/VI and ENDF-B/VII radioactive-decay sublibraries, respectively Reich et al. [1991]; Johnson et al. [2011]. The RadSrc data set contains particle-emission information extracted from the data shipped with the RadSrc utility [Hiller et al., 2007]. The IRTAPE11E data was compiled from Erdtmann and Soyka [1979], and the IRTAPE11L data was compiled from Gunnick and Tinney [1971] and Gunnick et al. [1976]. Unlike all the other data sets, the IRTAPE11L data contains pre-decayed particle emissions and care should be taken not to age materials when this data set is utilized.

3 Physics Models in the ISC Package

Three physics models have been implemented into the ISC package: radioactive decay, Fermi theory of beta decay, and a thick-target bremsstrahlung model. Each of the models is discussed below.

3.1 Radioactive Decay Model

The radioactive decay model solves the Bateman equations for a strictly decaying system, i.e., no burn-up or transmutation in the presence of a neutron flux can be performed. For such a system, the number of atoms of the jth daughter in the decay chain N_j after a time t can be expressed as [Shultis and Faw, 2002]

$$N_j(t) = \frac{N_1(0)}{\lambda_j} \sum_{m=1}^{j} C_m e^{-\lambda_m t}, \tag{1}$$

where λ_j is the decay constant of the jth isotope and C_m is given as

$$C_m = \frac{\prod_{i=1}^{j} \lambda_j}{\prod_{i=1, i\neq m}^{j} (\lambda_i - \lambda_m)}. \tag{2}$$

The ISC package solves the equation above for each initial parent nuclide specified in the material description and the resulting daughters are summed to obtained the aged material description.

3.2 Fermi Theory of Beta Decay

The beta particles are emitted with a continuous spectrum of kinetic energies ranging from zero up to the Q value for decay. The particle emission data sets do not tabulate the full beta particle spectra; rather, only the end-point energies (Q values) are tabulated. Fermi's theory of beta decay provides a description of the beta particle spectrum in terms of the end-point energy of the spectrum. Fermi's theory of beta decay states that the number of beta particles $n(W)$ in dW about W for a fixed Q is given by [Evans, 1955]

$$n(W)dW = \left(\frac{16\pi m_o^5 c^4}{h^6}\right)(W^2 - 1)^2 (W_o - W)^2 F(Z, W) dW, \tag{3}$$

where W is a dimensionless unit of energy given by

$$W = \frac{E + m_o c^2}{m_o c^2}. \tag{4}$$

$F(Z, W)$ is a nuclear coulomb factor that accounts for deceleration of electrons and acceleration of positrons out of the nucleus and is given by

$$F(Z, W) = \left[\frac{4(1 + s/2)}{[\Gamma(3 + 2s)]^2}\left(\frac{4\pi R}{h/m_o c}\right)^{2s}\right] \times \left[(W^2 - 1)^{2s} e^{\pi y} |\Gamma(1 + s + iy)|^2\right], \tag{5}$$

where $s = \sqrt{1 - (Z\alpha)^2} - 1$ and $y = \pm Z\alpha W/(W^2 - 1)$ ($+Z$ for electrons and $-Z$ for positrons).

Using Fermi's theory of beta decay, the tabulated end-point beta particle energies in the particle emission data sets can be converted into an approximate spectrum of kinetic energies. This continuous spectrum of electron energies can then be used to describe the particle source for the calculation or converted into an approximate bremsstrahlung photon source by means of a thick-target bremsstrahlung approximation.

3.3 Thick-Target Bremsstrahlung Model

The ISC package has a model for converting electron emissions into thick-target bremsstrahlung (TTB) photon emissions. The intensity (number × energy quanta) $I(E)$ of bremsstrahlung photons emitted at energy dE about E from a material with an atomic number Z by an electron with energy E_e can be estimated by [McCall, 1982]

$$I(E)dE = CZ(E_e - E)dE. \tag{6}$$

Thus, the number of photons $N(E)$ emitted at energy dE about E is

$$N(E)dE = CZ\frac{E_e - E}{E}dE. \tag{7}$$

Here, the parameter C is a function of Z and is tabulated for various Z's by McCall [1982]. The values of C provided by McCall [1982] are augmented with an additional value for $Z = 92$ which was determined by trying to match experimental data taken by Bendt and Jurney [1979]. A plot of the value of C versus Z is presented in Fig. 1 where it is observed that the additional point follows the trend of data determined by McCall [1982].

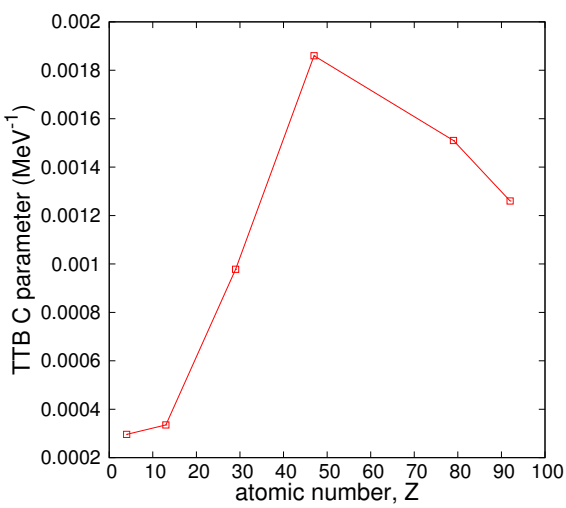

Fig. 1. Thick-target bremsstrahlung C parameter as a function of atomic number as determined by McCall [1982] with added point at $Z = 92$

The TTB photon emission by electrons emitted at discrete energies can be calculated by direct substitution of the electron energy into Eq. (7). The TTB photon emission by beta particles emitted

in a beta spectrum can be calculated by integrating Eq. (7) with the beta-particle emission spectrum $n(E_e)$, namely

$$N_\beta(E)dE = CZ \int_0^{E_e^{max}} dE_e n(E_e) \frac{E_e - E}{E}. \tag{8}$$

4 Thick-Target Bremsstrahlung Model Comparison

The TTB model was compared to full electron-photon coupled transport with MCNP. The depleted ^{238}U benchmark sphere (discussed below) was used for a comparison problem. The ISC package was used to generate a photon source for each of four cases: 1. electron only source, 2. photon line source, 3. TTB photon source, and 4. the combined TTB photon and photon line source. For each case a calculation of the photon current and dose-equivalent rate at 2 m from the source was performed. With a perfect TTB model, cases 1 and 3 would match exactly and the sum of cases 1 and 2 would match case 4.

The current tally results and dose-equivalent-rate tally results are presented in Figs. 2 and 3, respectively. Over the full range of emission energies (0 to 4.5 MeV) there is reasonable agreement between the TTB model results and full transport results. The most notable discrepancies are in the range of 0 to 2 MeV where the TTB model under estimates the bremsstrahlung photon production, especially around 0.1 MeV at the K_α X-ray intensities.

5 Benchmark Comparison to ^{239}Pu and ^{238}U Spheres

Experimental measurements of the gamma emissions from spheres of ^{239}Pu and ^{238}U were performed by Bendt and Jurney in 1979. The gamma spectra were measured for three different spheres—two plutonium spheres, the first with a 2.65 w/o ^{240}Pu content and the second with a 5.93 w/o ^{240}Pu content, and a depleted ^{238}U sphere. The spectra were obtained with both Ge(Li) and NaI(Tl) detectors, and the data from the NaI(Tl) detector was unfolded to obtain the gamma fluxes. The gamma fluxes were subsequently converted into dose-equivalent values by means of flux-to-dose conversion factors [Battat, 1997]. The fluxes and dose-equivalents at two meters from the spheres were tabulated by Bendt and Jurney [1979].

Dose-equivalent calculations from the spheres were modeled with the MCNP transport code using source definitions obtained from the MISC utility. The initial isotopic compositions of the spheres are given in Table 1. At the time of the measurements, each sphere had aged by approximately 0.5 yr, and the isotopic composition of the isotopes had reached secular equilibrium. The material aging capability of the ISC package was used to age the initial sphere compositions by 0.5 yr.

The comparisons of the calculated spectral dose-equivalent rates to the experimental spectral dose-equivalent rates for each of the benchmark spheres are presented in Figs. 4 through 6. For each figure, a comparison is presented for each of the particle emission data sets. When a radioactive-decay database corresponding to the particle-emission data set existed (i.e., endf6.dk, endf7.dk, and radsrc.dk), that decay database was used for the aging of the material. The endf7.dk database was used for the IRTAPE11E calculations, and no aging was performed for the IRTAPE11L calculations as that data set is "pre-aged."

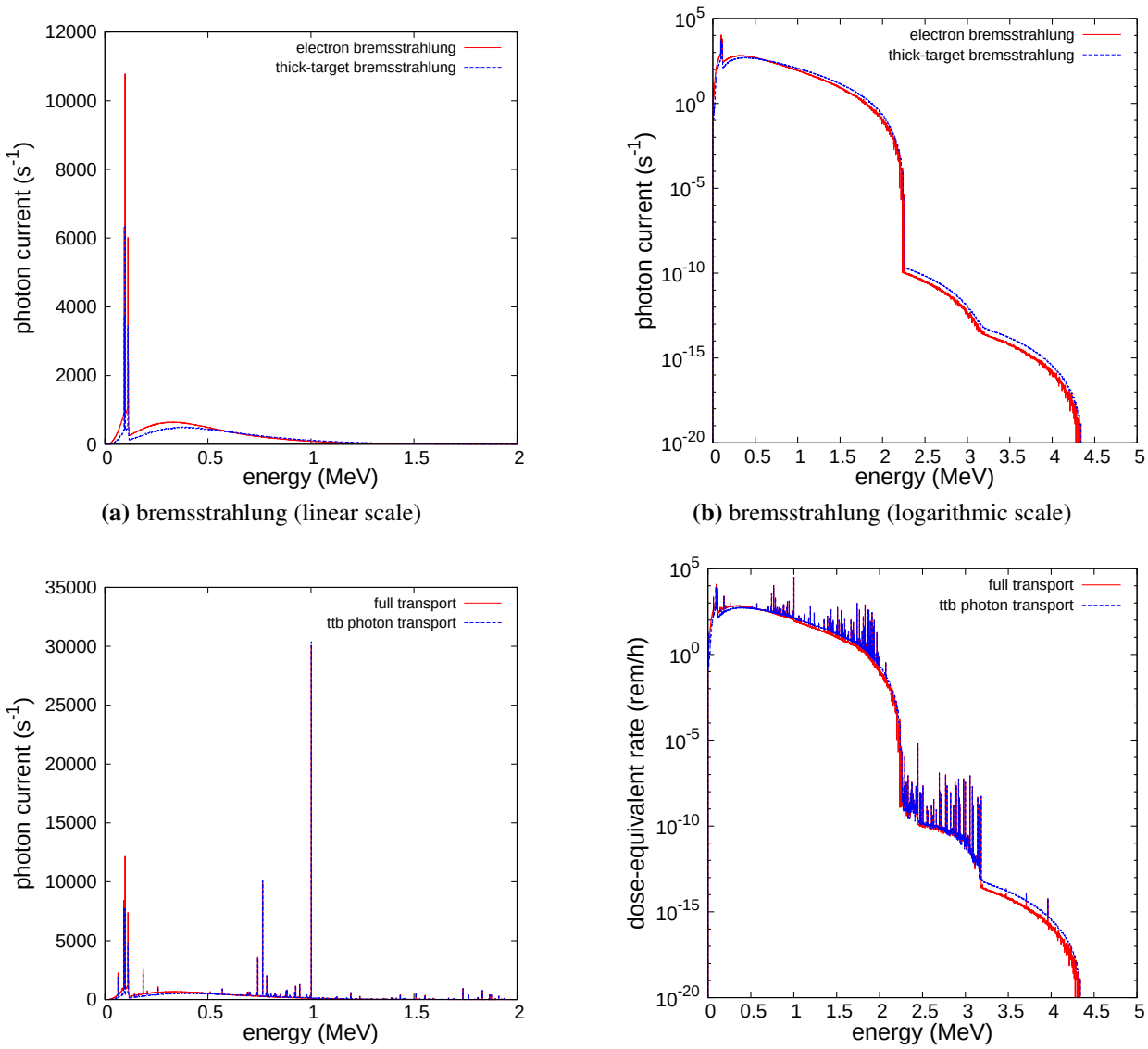

(a) bremsstrahlung (linear scale)

(b) bremsstrahlung (logarithmic scale)

(c) total (linear scale)

(d) total (logarithmic scale)

Fig. 2. Bremsstrahlung and total (bremsstrahlung + discrete lines) current at 2 m from the source

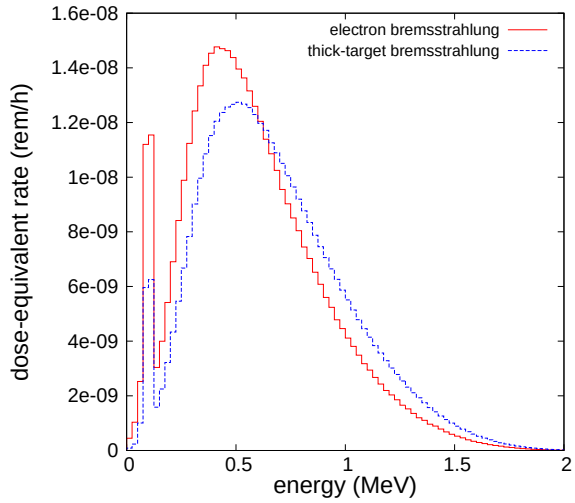

(a) bremsstrahlung (linear scale)

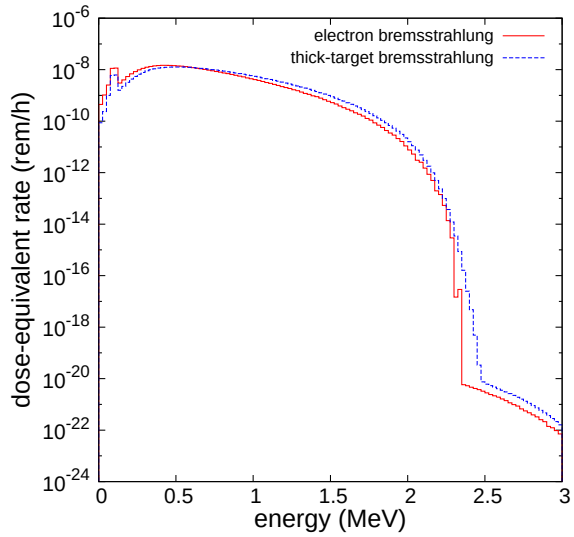

(b) bremsstrahlung (logarithmic scale)

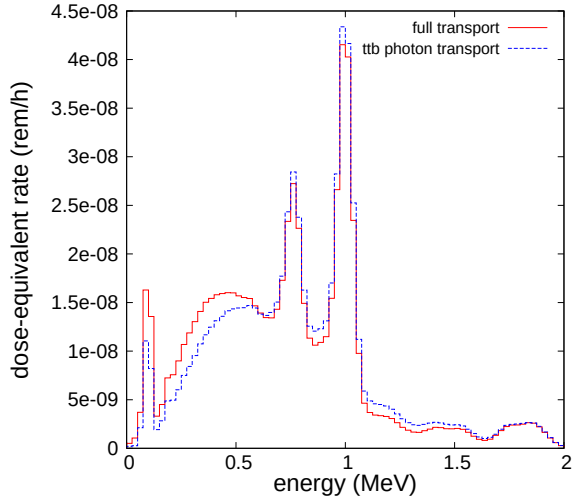

(c) total (linear scale)

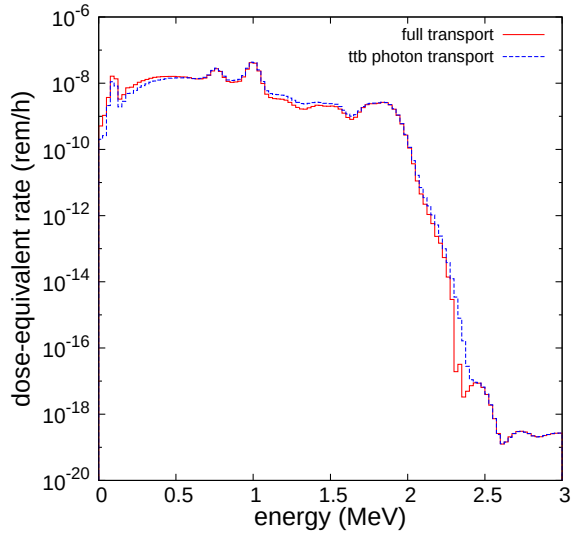

(d) total (logarithmic scale)

Fig. 3. Bremsstrahlung and total (bremsstrahlung + discrete lines) dose-equivalent rate at 2 m from the source

Table 1. Initial isotopic compositions of the benchmark spheres

2.65 w/o Pu-240 Sphere		5.93 w/o Pu-240 Sphere		Depleted U-238 Sphere	
Isotope	**Weight %**	**Isotope**	**Weight %**	**Isotope**	**Weight %**
Pu-239	0.972710	Pu-239	0.937850	U-234	0.000010
Pu-240	0.026541	Pu-240	0.059250	U-235	0.001995
Pu-241	0.000585	Pu-241	0.002950	U-236	0.000030
Pu-242	0.000039	Pu-242	0.000400	U-238	0.998000
Am-241	0.000236	Am-241	0.000384		

In general, there is descent agreement between the calculated and measured spectral dose-equivalent rates, with a few notable exceptions. First, none of the data sets captures the experimentally measured peak at approximately 0.02 MeV in the ^{239}Pu measurements. It is suspected that this feature is a result of detector noise and/or pileup in the NaI(Tl) detector. Second, there are notable differences in the ^{238}U results between 0.1 and 0.6 MeV. Features in that energy range are dominated primarily by bremsstrahlung contributions. Notably, the ENDF6 and ENDF7 results use the TTB model implemented in the ISC package and compare favorably to the experiment, though the selection of the C parameter for $Z = 92$ was calibrated to these experimental results. The RadSrc, IRTAPE11E, and IRTAPE11L[1] data utilize tabulated values of the bremsstrahlung spectrum, each with varying degrees of success (the RadSrc utility uses the bremsstrahlung evaluation of Mitchell et al. [1989]. Lastly, the ENDF6 and IRTAPE11E data sets greatly underestimate the contributions at approximately 0.75 and 1 MeV. ^{238}U α-decays to ^{234}Th which subsequently β-decays to ^{234m}Pa. ^{234m}Pa has a strong 1.001 MeV emission as well as a gamma complex around 0.764 MeV. The similar ENDF6 and IRTAPE11E data have intensities for these emissions almost 40% lower than the newer ENDF7 and RadSrc data, which match the data quite favorably.

The integral dose-equivalent rate comparisons from the benchmark-sphere calculations are presented in Table 2. The best matches to the integrated dose-equivalent rates are obtained with the ENDF7 and IRTAPE11L data sets. Recalling that the IRTAPE11L data set contains pre-decayed data in secular equilibrium with the parent isotope, then, of the non-pre-decayed data sets, the ENDF7 data best matches the integrated dose-equivalent rates. Considering both the spectral dose-equivalent rate and integrated dose-equivalent rates, the ENDF7 data set produces the results best matching experimental data.

6 Comparison of Particle Emission Data Sets

The particle emission data sets were also compared to each other to determine where differences exist. Of the 73 isotopes (the dominant isotopes in the decay chains of ^{238}U and ^{235}U) contained in the RadSrc particle emission data set, 71 of them existed in one or more of the other particle

[1]The IRTAPE11L tabulated bremsstrahlung is multiplied by a scaling factor of 1.2 to obtain a better match with experiment.

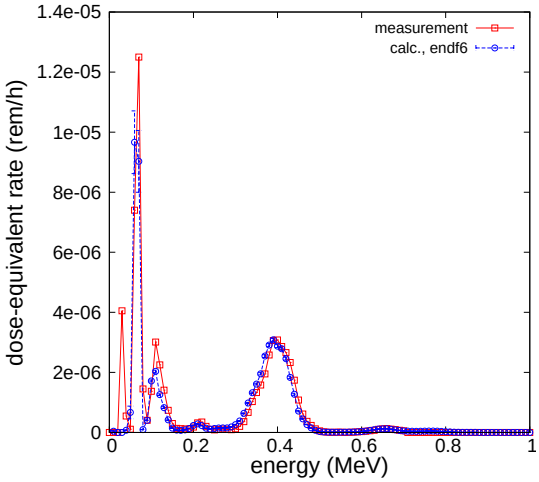

(a) ENDF6

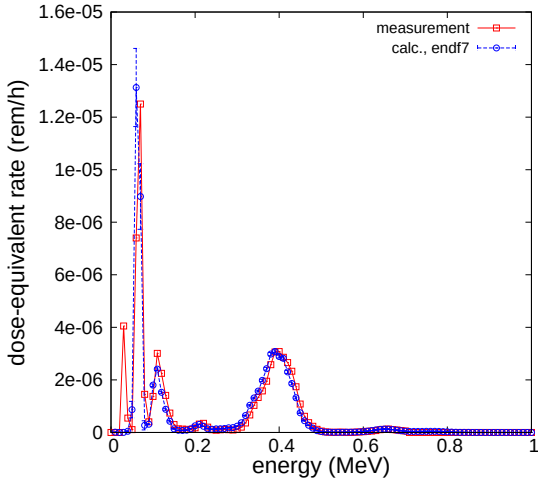

(b) ENDF7

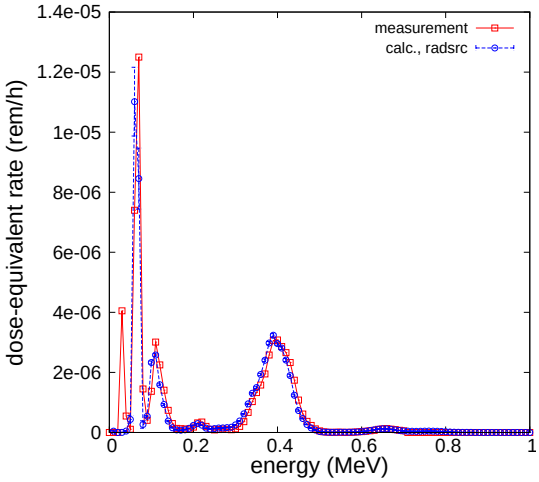

(c) RadSrc

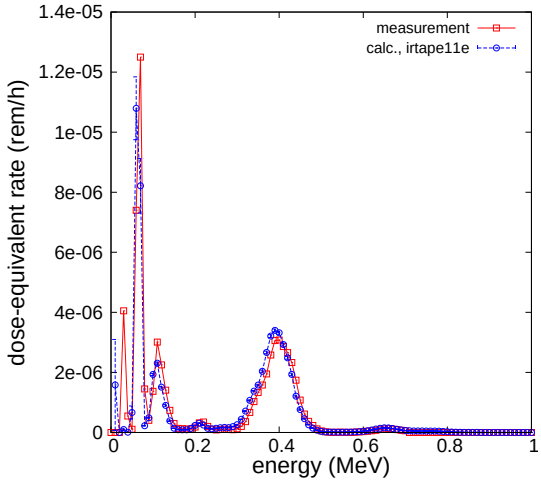

(d) irtape11e

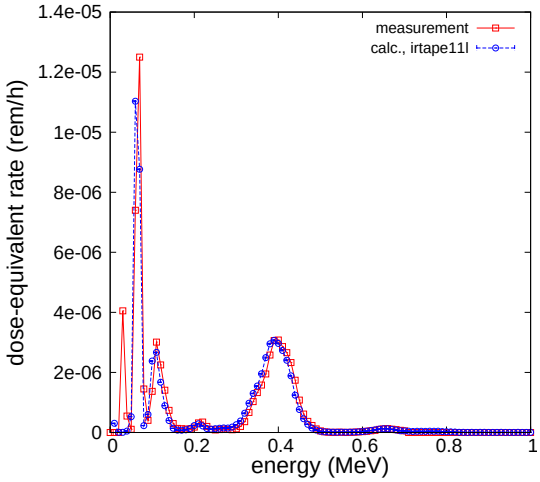

(e) irtape11l

Fig. 4. Spectral dose-equivalent rates from the 2.65 w/o ^{240}Pu sphere using varying particle emission data sets

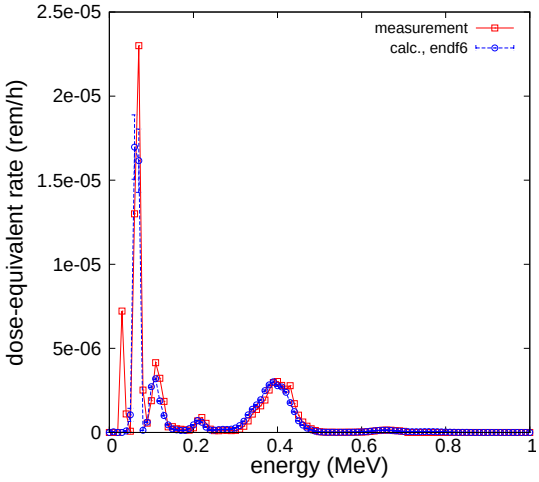

(a) ENDF6

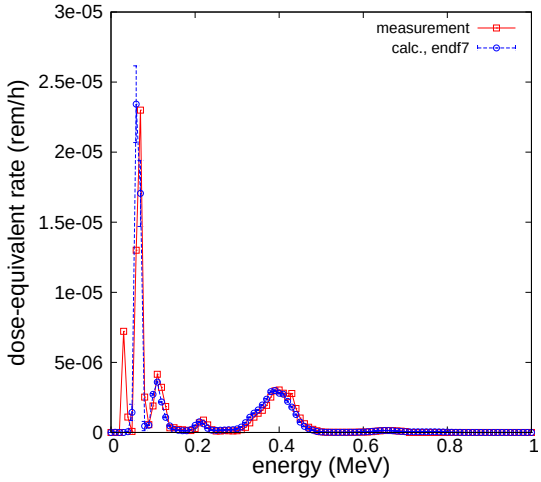

(b) ENDF7

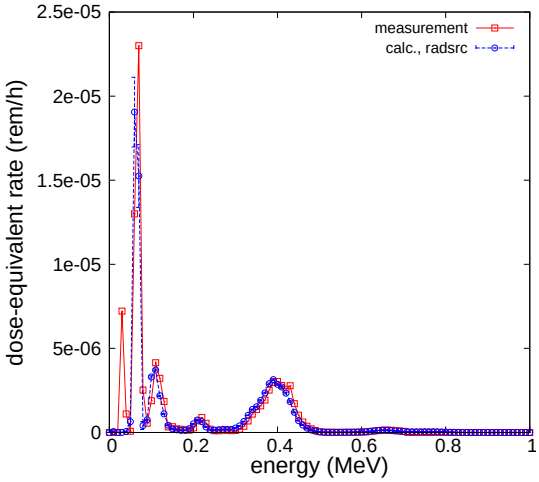

(c) RadSrc

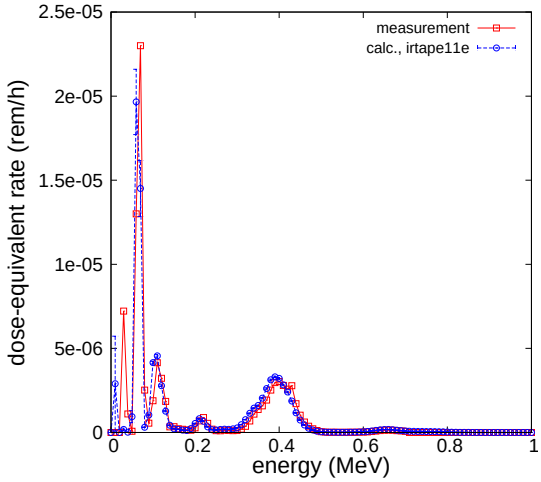

(d) irtape11e

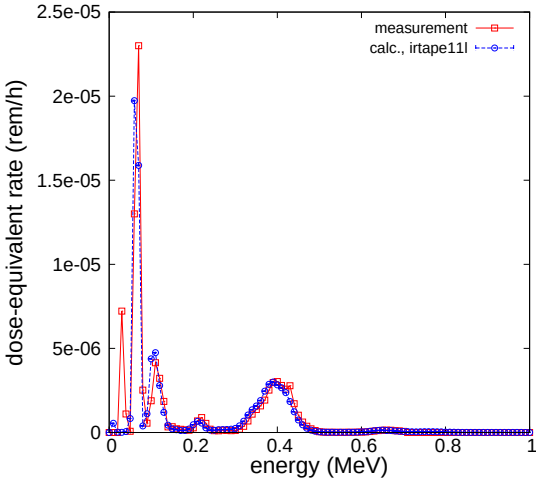

(e) irtape11l

Fig. 5. Spectral dose-equivalent rates from the 5.93 w/o ^{240}Pu sphere using varying particle emission data sets

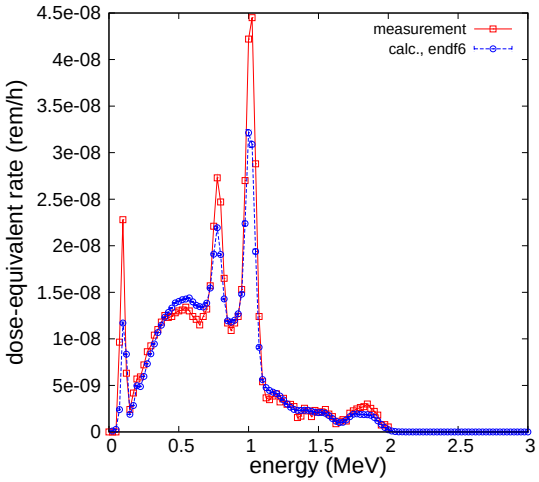

(a) ENDF6

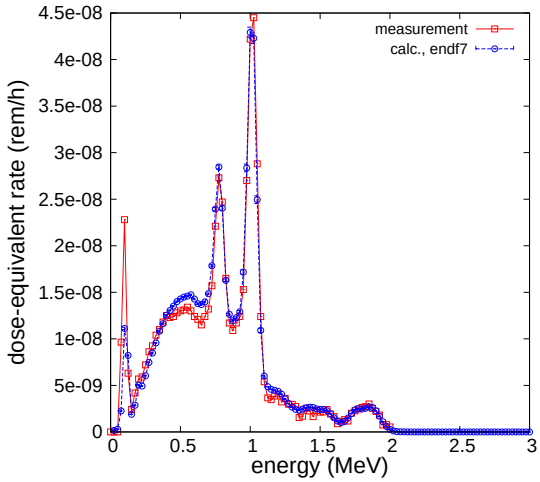

(b) ENDF7

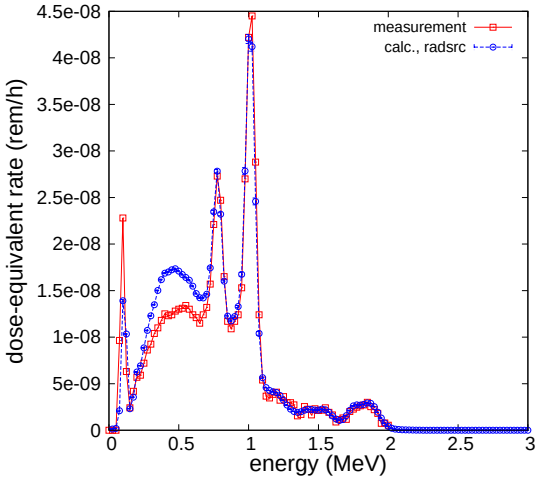

(c) RadSrc

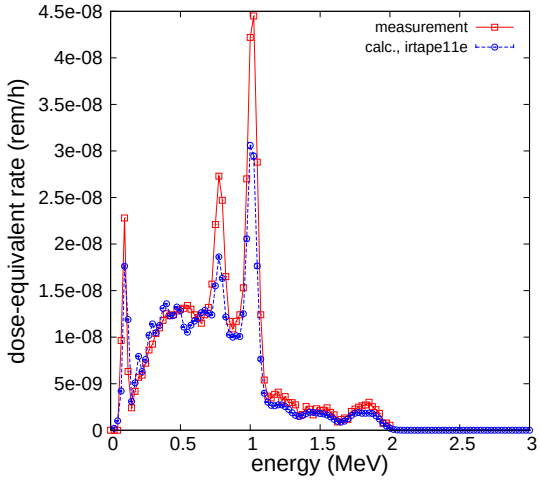

(d) irtape11e

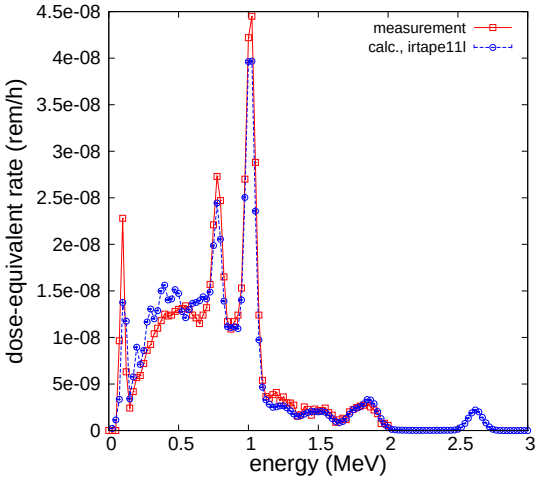

(e) irtape11l

Fig. 6. Spectral dose-equivalent rates from the ^{238}U sphere using varying particle emission data sets

Table 2. Integral dose-equivalent rates in rem/h and calculated-to-measured (C/M) ratios for each of benchmark sphere cases

	2.65 w/o Pu-240		5.93 w/o Pu-240		Depleted U-238	
Data Set	**Rate**	**C/M**	**Rate**	**C/M**	**Rate**	**C/M**
ENDF6	0.0586	0.933	0.0780	0.909	0.000619	0.897
ENDF7	0.0631	1.005	0.0868	1.012	0.000693	1.004
RadSrc	0.0610	0.971	0.0808	0.951	0.000741	1.074
IRTAPE11E	0.0638	1.015	0.0892	1.049	0.000580	0.841
IRTAPE11L	0.0619	0.986	0.0858	1.009	0.000689	0.998
Measurement[a]	0.0628	—	0.0850	—	0.00069	—

[a]The measurement results have the anomalous signal at 0.02 MeV in the Pu sphere results removed from the integrated dose-equivalent rate.

emission data sets. The ISC package was used to generate a source for each of these 71 isotopes individually using each of the particle-emission data sets, except IRTAPE11L because it is pre-decayed, with an arbitrary atom density of 1 b^{-1} cm^{-1}. For each of the sources created, a void MCNP calculation tallying the particle current from a point source on a sphere was performed to collapse the sources to a consistent energy-bin structure. Then, for each of the 71 isotopes, a plot of the emission intensity on the consistent energy-bin structure was created along with a residual-intensity plot on the same consistent energy-bin structure. For the residual-intensity plots, the RadSrc data was taken to be the reference. The intensity and residual-intensity plots for each of the 71 isotopes are presented in Appendix A.

True comparison of emissions from an isotope requires examination of the plots presented in Appendix A. Here, some general observations regarding the overall comparisons are made. Generally, the ENDF6 and IRTAPE11E data sets agree well, and the ENDF7 and RadSrc data sets agree well. However, there is, in many cases, substantial disagreement between the ENDF6 and IRTAPE11E data sets and the ENDF7 and RadSrc data sets. Discrepancies between data sets that are mostly in agreement are largest in the low energy (< 0.1 MeV) regime where x-ray emissions are dominant for the heavier isotopes.

7 Conclusions

The ISC package consisting of LIBISC and the MISC utility have been used to generate source definitions for transport with the MCNP transport code. The thick-target bremsstrahlung model implemented in the ISC package has been shown to compare reasonably well with the full electron transport bremsstrahlung production. Furthermore, comparisons to benchmark sphere experiments using each of the available particle emission data sets indicates that the ENDF7 data set results most closely match the experimental data. Comparisons of each of the particle emission data sets for individual isotopes has been performed to determine where discrepancies between data sets exists,

and such discrepancies are noted to be isotope dependent.

References

M.E. Battat, editor. *American National Standard Neutron and Gamma-Ray Flux-to-Dose Rate Factors*. ANSI/ANS-6.1.1-1977 (N666). American Nuclear Society, LaGrange Park, Illinois, 1997.

P.J. Bendt and E.T. Jurney. Gamma Measurements of Spherical Shells of ^{239}Pu and ^{238}U. LA-8073-MS, Los Alamos National Laboratory, 1979.

G. Erdtmann and Werner Soyka. *The Gamma Rays of the Radionuclides*. Verlag Chemie, 1979.

G.P. Estes, R.G. Schrandt, and J.T. Kriese. Automated MCNP Photon Source Generation for Arbitrary Configurations of Radioactive Materials and First-Principles Calculations of Photon Detector Responses. LA-11153-MS, Los Alamos National Laboratory, 1988.

R.D. Evans. *The Atomic Nucleus*. McGraw-Hill Book Co., 1955.

R. Gunnick and J.F. Tinney. Analysis of Fuel Rods by Gamma-Ray Spectroscopy. UCRL-51086, Lawrence Livermore Laboratory, 1971.

R. Gunnick, J.E. Evans, and A.L. Prindle. A Reevaluation of the Gamma-Ray Energies and Absolute Branching Intensities of ^{237}U, ^{238,239,240,241}Pu, and ^{241}Am. Technical Report UCRL-52139, Lawrence Livermore Laboratory, 1976.

L. Hiller, T. Gosnell, J. Gronberg, and D. Wright. RadSrc Library and Application Manual. UCRL-TM-229497, Lawrence Livermore National Laboratory, 2007.

T.D. Johnson, E.A. McCutchan, and A.A. Sonzogni, editors. *ENDF/B-VII.1 Radioactive Decay Data Files*. National Nuclear Data Center (www.nndc.bnl.gov), 2011.

G.H. McCall. Calculation of x-ray bremsstrahlung and characteristic line emission produced by a Maxwellian electron distribution. *Journal of Physics D: Applied Physics*, 15:823–831, 1982.

D.J. Mitchell, H.L. Scott, K.W. Marlow, and H.M. Sanger. Bremsstrahlung and X-ray Source Terms for Uranium. Sandia National Laboratories MEMO, 1989.

National Institute of Standards and Technology (NIST). Atomic Weights and Isotopic Compositions. http://www.nist.gov/pml/data/comp.cfm, 2011.

C.W. Reich, T.R. England, F.M. Mann, and F. Schmittroth. *ENDF/B-VI Radioactive Decay Data Files*. National Nuclear Data Center (www.nndc.bnl.gov), 1991.

J.K. Shultis and R.E. Faw. *Fundamentals of Nuclear Science and Engineering*. Marcel Dekker, Inc., 2002.

C.J. Solomon. MCNP Intrinsic Source Constructor (MISC): A User's Guide. LA-UR-12-20252, Los Alamos National Laboratory, 2012.

X-5 Monte Carlo Team. MCNP–A General Monte Carlo N-Particle Transport Code, Version 5. LA-UR-03-1987, Los Alamos National Laboratory, 2003.

A Particle Emission Database Comparisons

This appendix contains comparisons between the ISC package particle emission databases: ENDF6, ENDF7, RadSrc, and IRTAPE11E. Table A.1 presents the available isotope comparisons and their location in this appendix. For each isotope there are two plots: 1. a specific intensity plot and 2. a specific residual-intensity plot using the RadSrc data set as the reference. Note that the appearance of approximately equal magnitude residual-intensities on both sides of zero are due to gamma emission energies being tabulated at slightly different energies that fall into different energy bins.

Table A.1. Index to isotope gamma emission comparisons

Isotope	Section	Isotope	Section	Isotope	Section	Isotope	Section
Co-60	A.1	Hg-206	A.2	Tl-206	A.3	Tl-207	A.4
Tl-208	A.5	Tl-209	A.6	Tl-210	A.7	Pb-210	A.8
Pb-211	A.9	Pb-212	A.10	Pb-214	A.11	Bi-210	A.12
Bi-211	A.13	Bi-212	A.14	Bi-213	A.15	Bi-214	A.16
Po-210	A.17	Po-211	A.18	Po-214	A.19	Po-215	A.20
Po-216	A.21	At-215	A.22	Rn-219	A.23	Rn-220	A.24
Rn-222	A.25	Fr-221	A.26	Fr-223	A.27	Fr-224	A.28
Ra-223	A.29	Ra-224	A.30	Ra-225	A.31	Ra-226	A.32
Ra-228	A.33	Ac-225	A.34	Ac-227	A.35	Ac-228	A.36
Th-227	A.37	Th-228	A.38	Th-229	A.39	Th-230	A.40
Th-231	A.41	Th-232	A.42	Th-234	A.43	Pa-231	A.44
Pa-233	A.45	Pa-234	A.46	Pa-234m	A.47	U-232	A.48
U-233	A.49	U-234	A.50	U-235	A.51	U-236	A.52
U-237	A.53	U-238	A.54	Np-237	A.55	Np-239	A.56
Pu-236	A.57	Pu-238	A.58	Pu-239	A.59	Pu-240	A.60
Pu-241	A.61	Pu-242	A.62	Am-241	A.63	Am-243	A.64
Am-245	A.65	Cm-244	A.66	Cm-245	A.67	Cm-249	A.68
Bk-249	A.69	Cf-249	A.70	Es-253	A.71		

A.1 Co-60

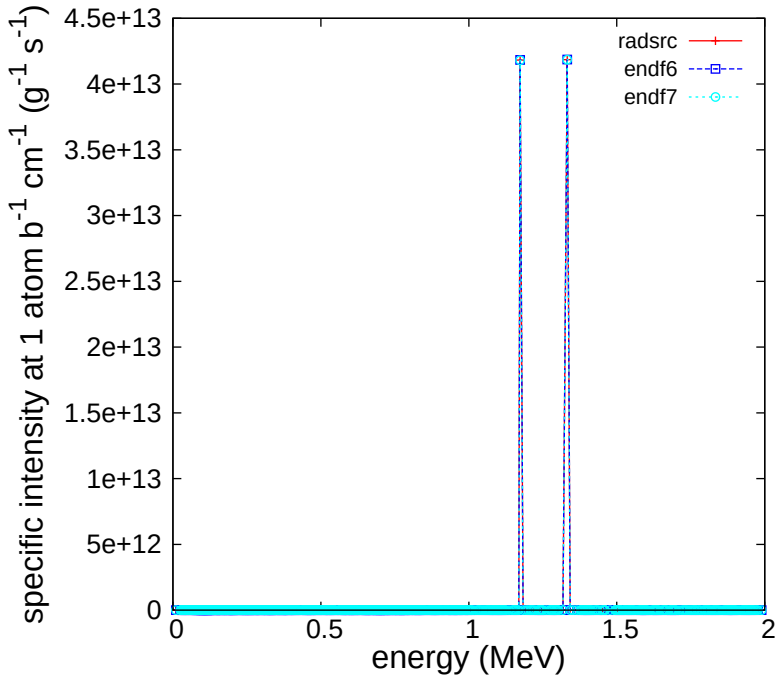

(a)

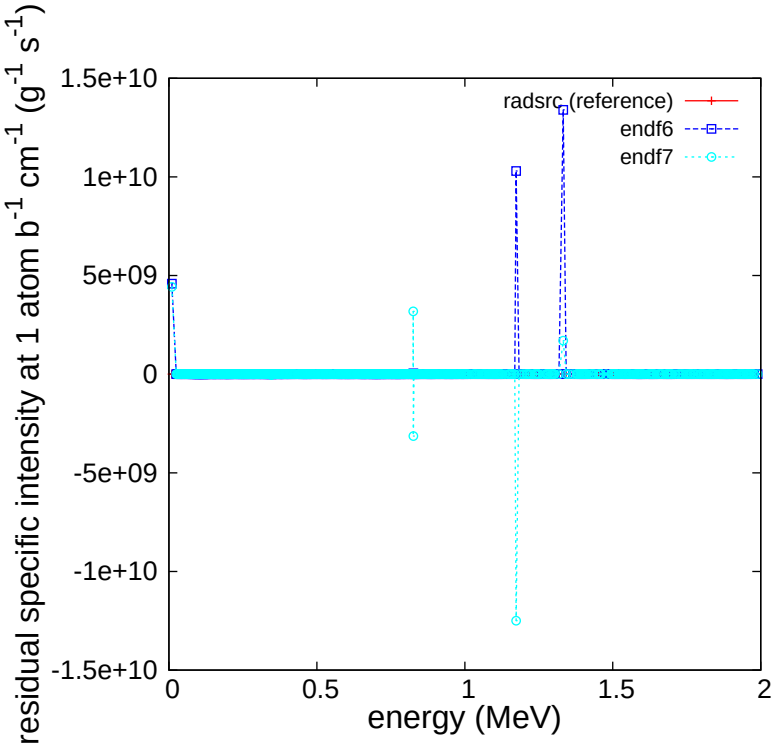

(b)

Fig. A.1. (a) photon emission intensity and (b) residual photon emission intensity with respect to the RadSrc database for Co-60

A.2 Hg-206

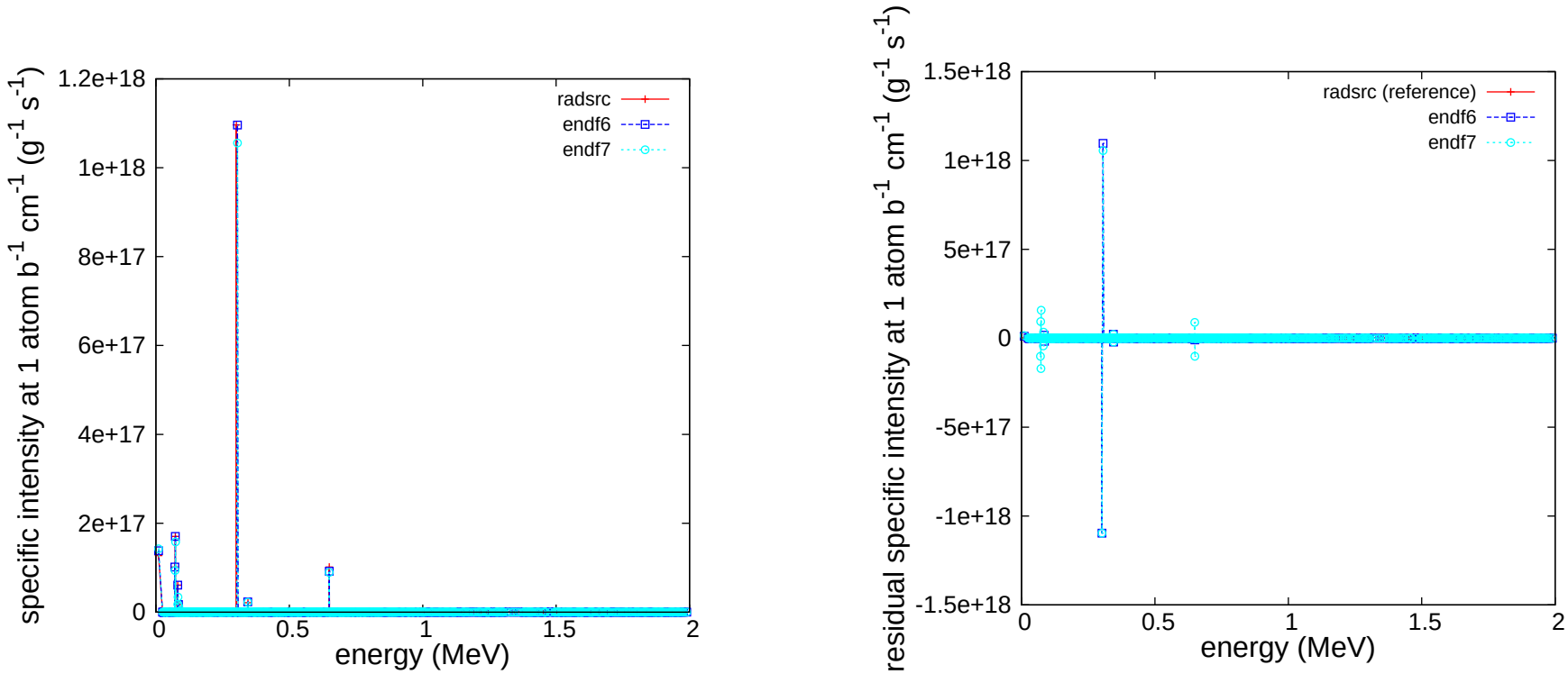

(a) (b)

Fig. A.2. (a) photon emission intensity and (b) residual photon emission intensity with respect to the RadSrc database for Hg-206

A.3 Tl-206

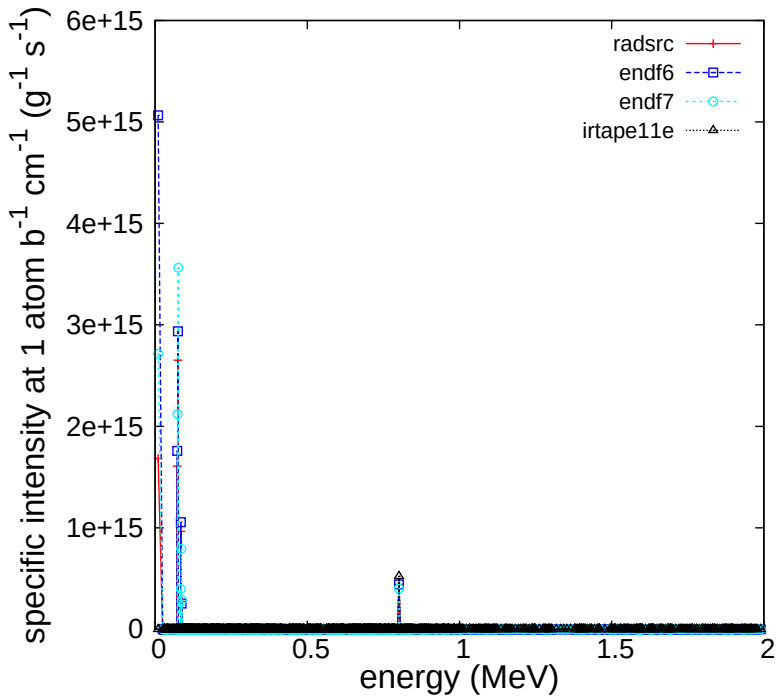

(a)

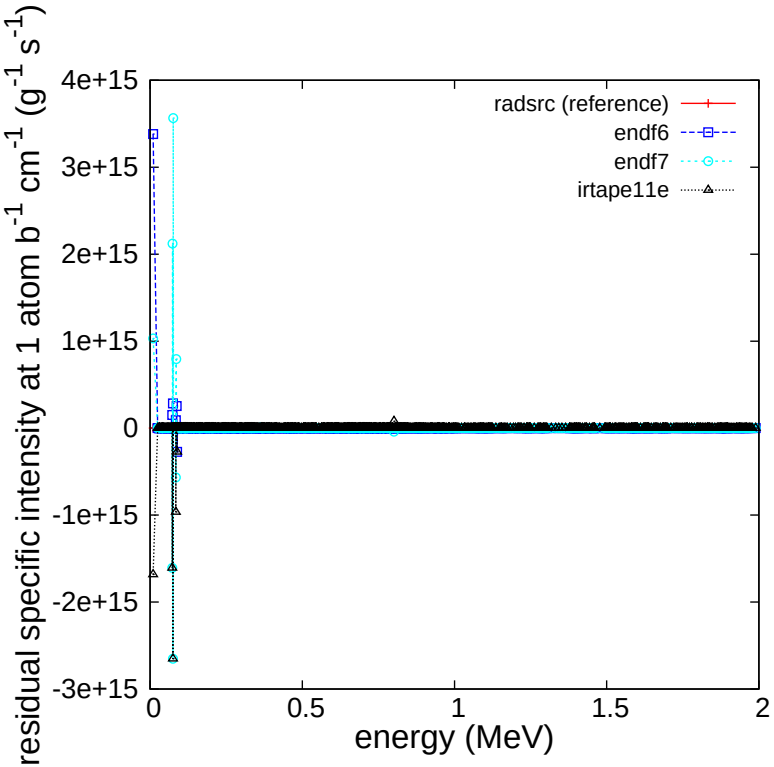

(b)

Fig. A.3. (a) photon emission intensity and (b) residual photon emission intensity with respect to the RadSrc database for Tl-206

A.4 Tl-207

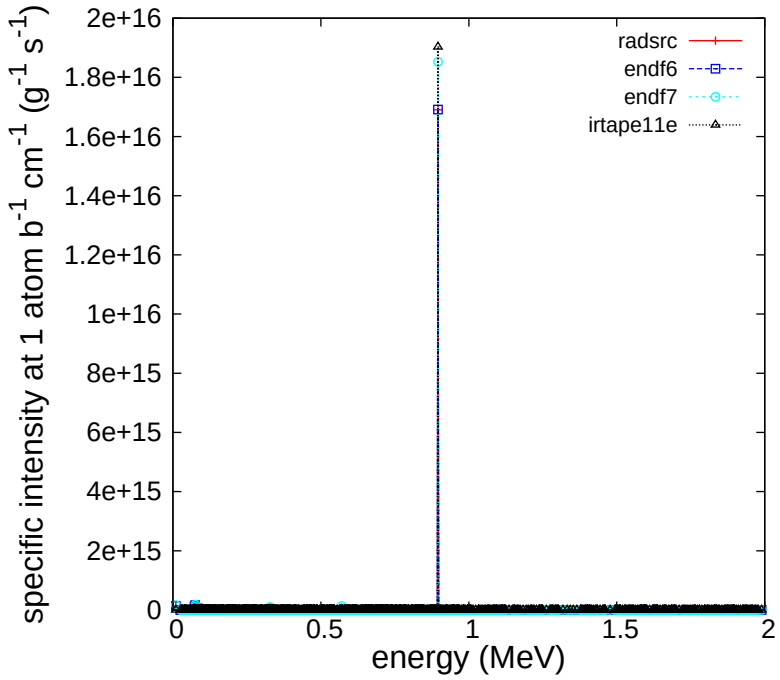

(a)

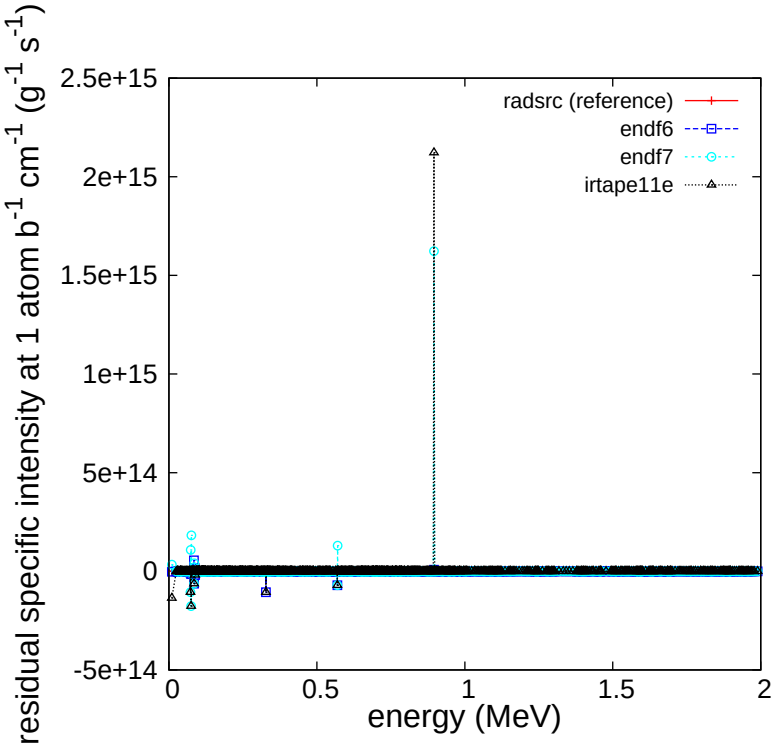

(b)

Fig. A.4. (a) photon emission intensity and (b) residual photon emission intensity with respect to the RadSrc database for Tl-207

A.5 Tl-208

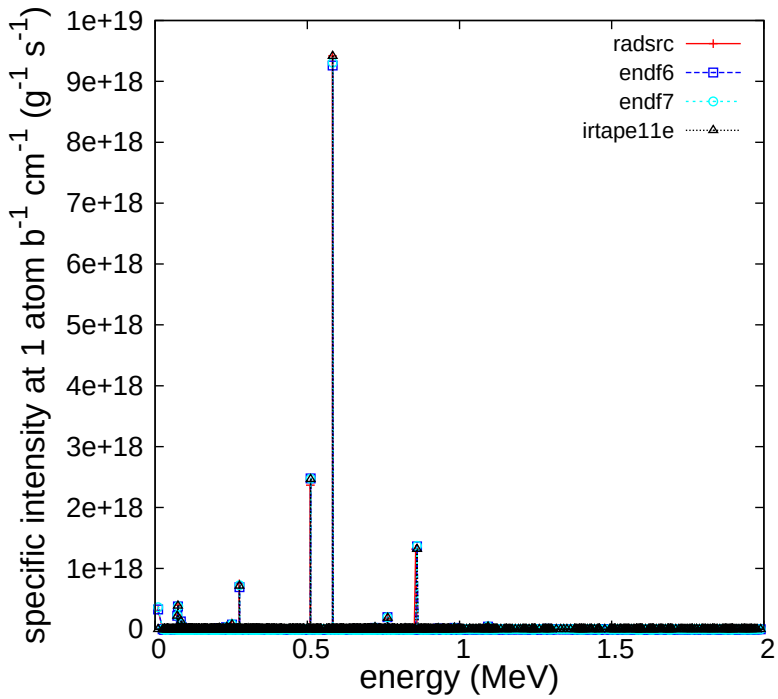

(a)

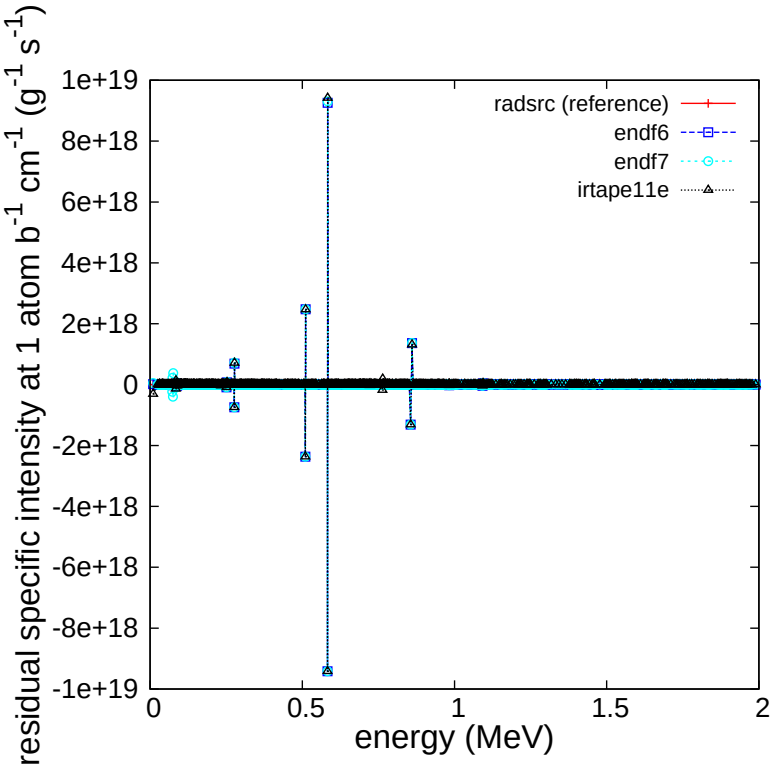

(b)

Fig. A.5. (a) photon emission intensity and (b) residual photon emission intensity with respect to the RadSrc database for Tl-208

A.6 Tl-209

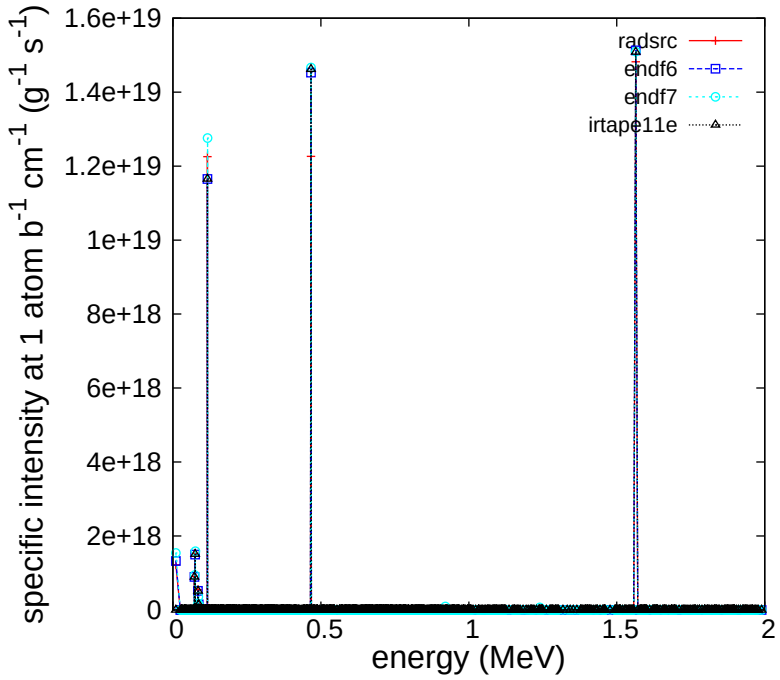

(a)

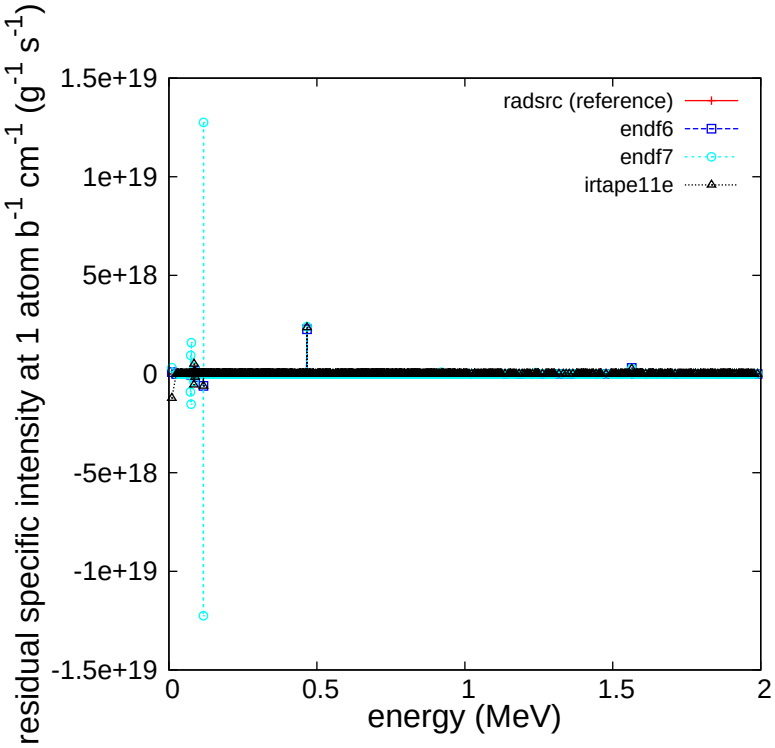

(b)

Fig. A.6. (a) photon emission intensity and (b) residual photon emission intensity with respect to the RadSrc database for Tl-209

A.7 Tl-210

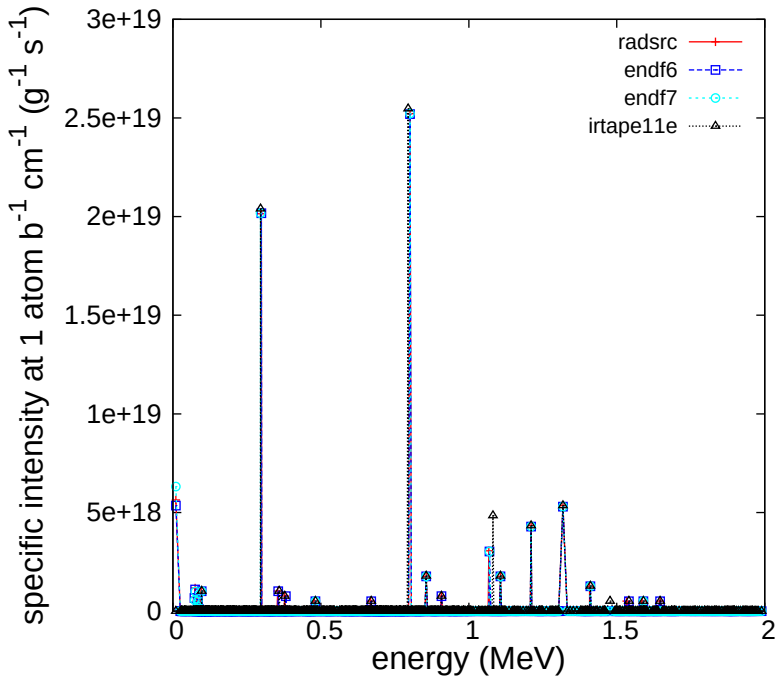

(a)

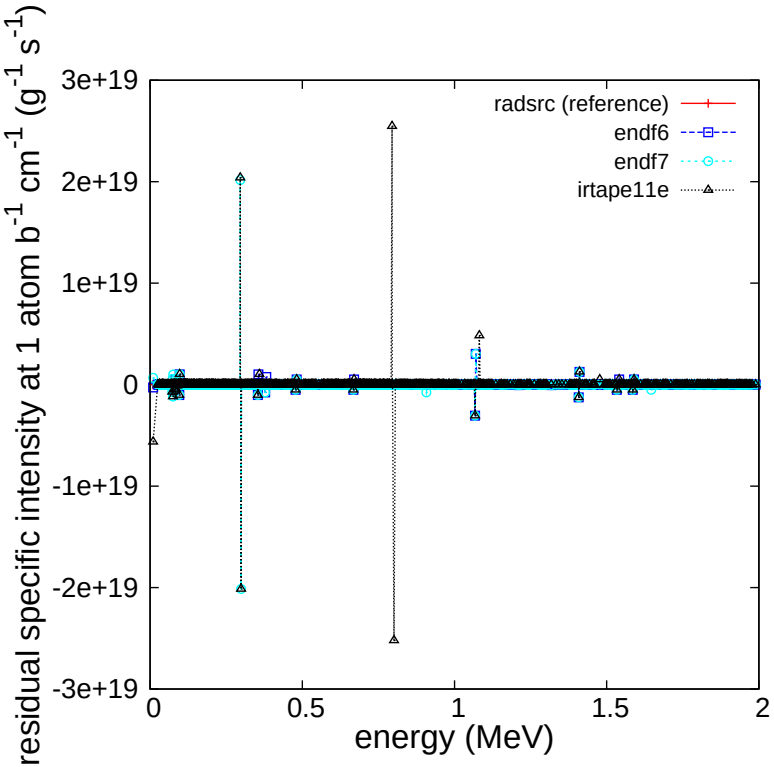

(b)

Fig. A.7. (a) photon emission intensity and (b) residual photon emission intensity with respect to the RadSrc database for Tl-210

A.8 Pb-210

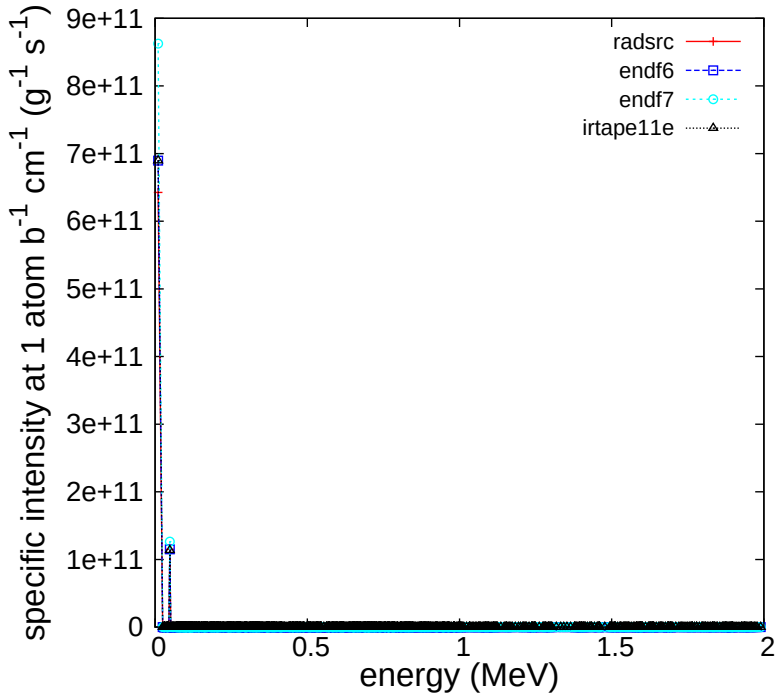

(a)

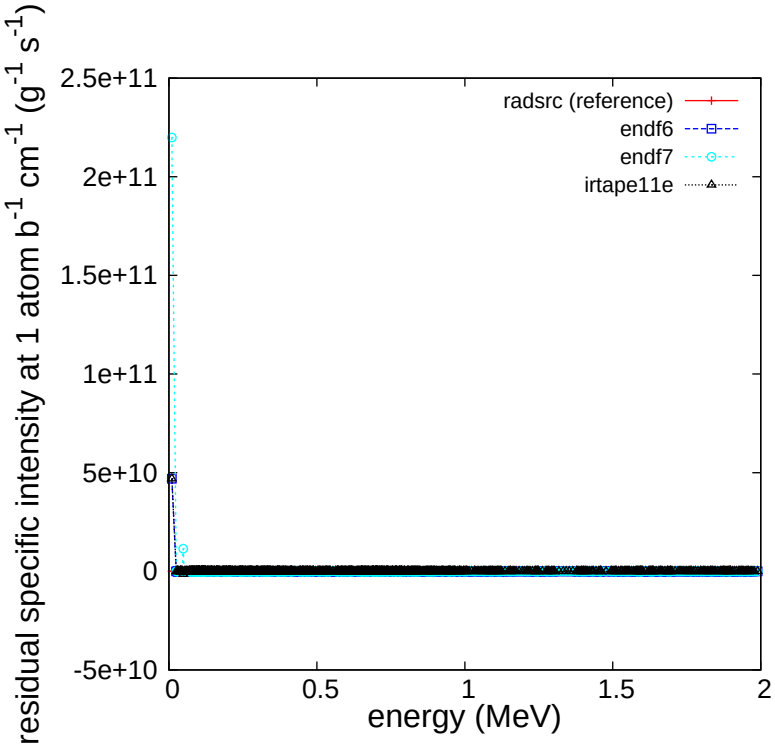

(b)

Fig. A.8. (a) photon emission intensity and (b) residual photon emission intensity with respect to the RadSrc database for Pb-210

A.9 Pb-211

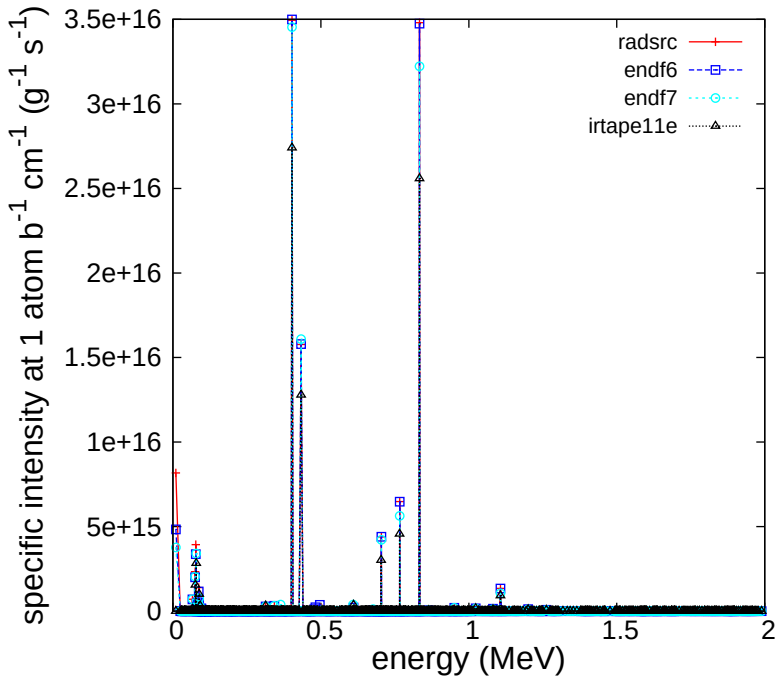

(a)

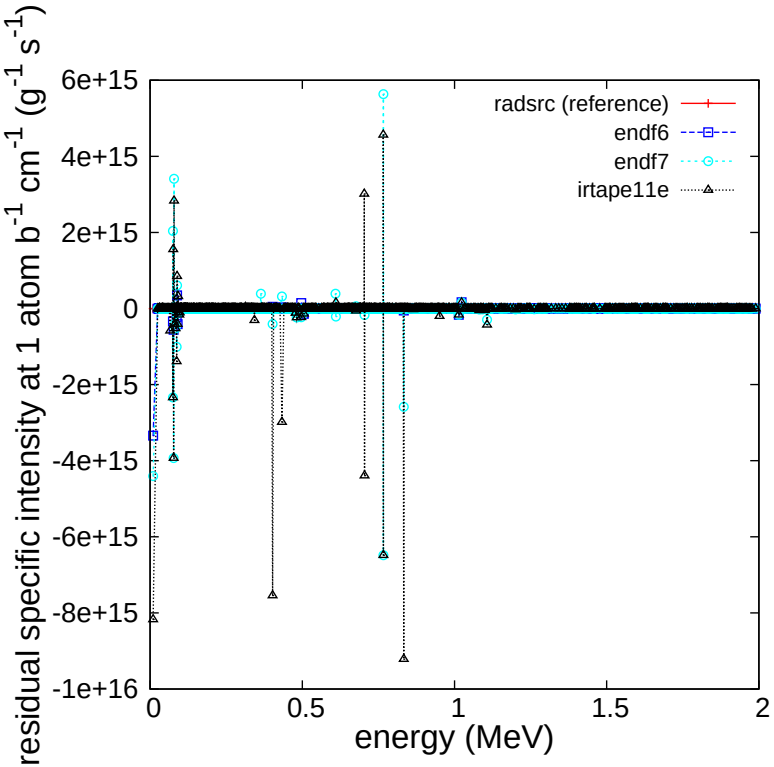

(b)

Fig. A.9. (a) photon emission intensity and (b) residual photon emission intensity with respect to the RadSrc database for Pb-211

A.10 Pb-212

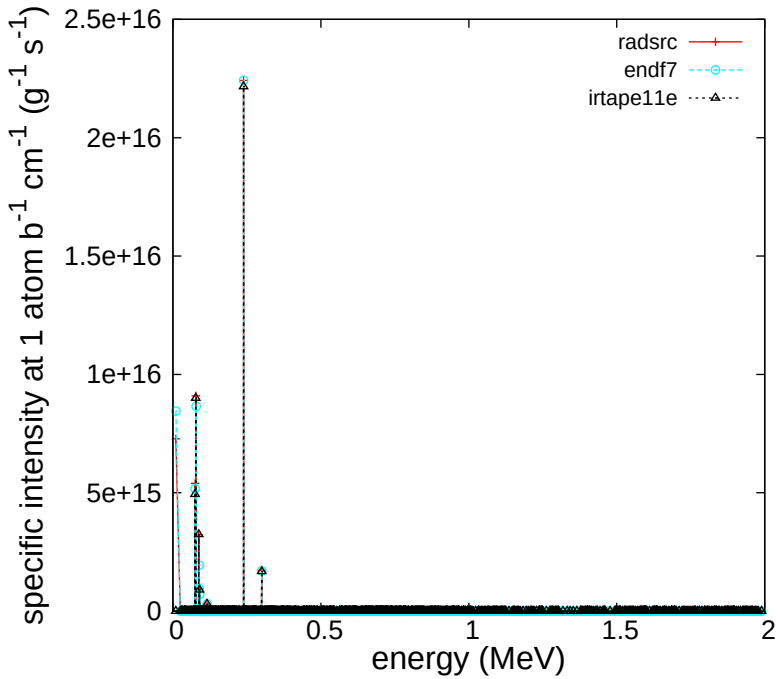

(a)

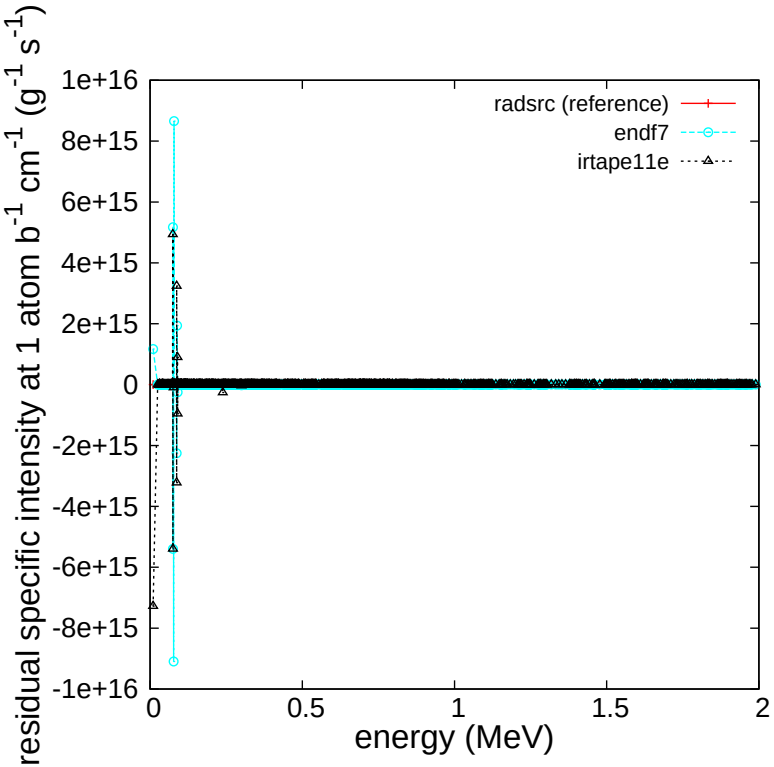

(b)

Fig. A.10. (a) photon emission intensity and (b) residual photon emission intensity with respect to the RadSrc database for Pb-212

A.11 Pb-214

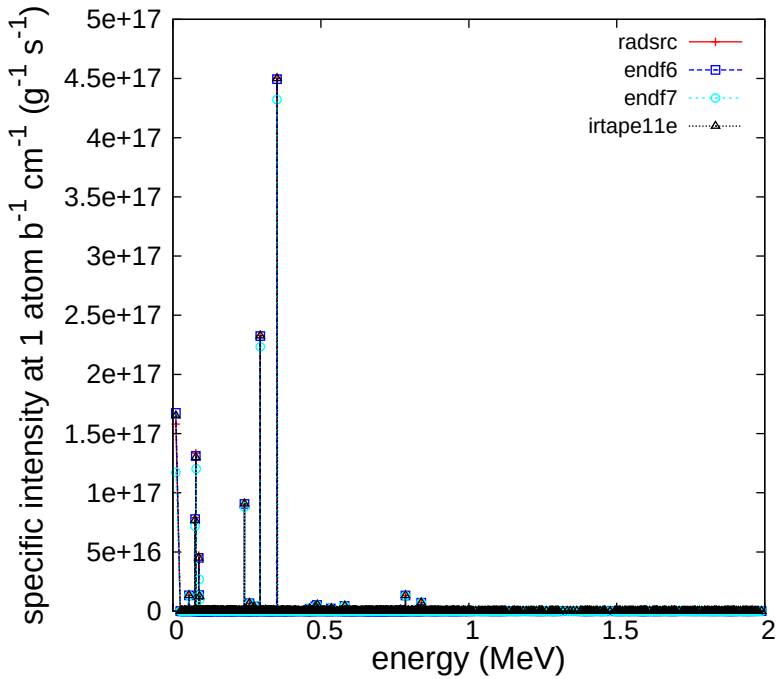

(a)

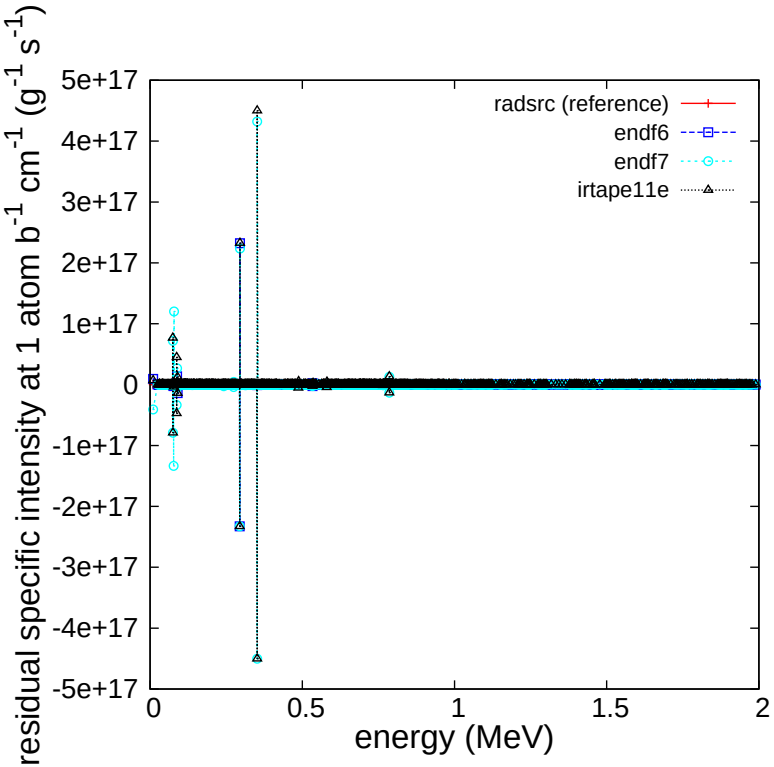

(b)

Fig. A.11. (a) photon emission intensity and (b) residual photon emission intensity with respect to the RadSrc database for Pb-214

A.12 Bi-210

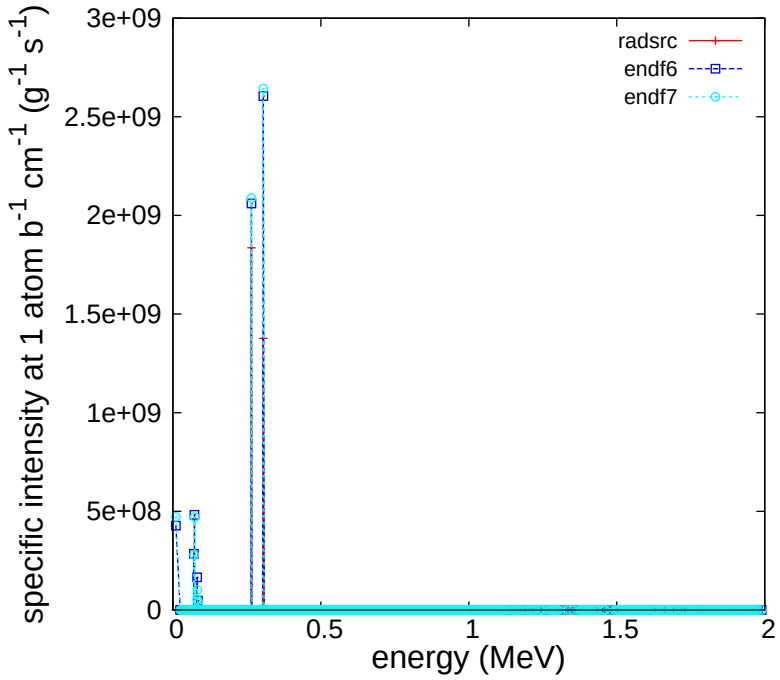

(a)

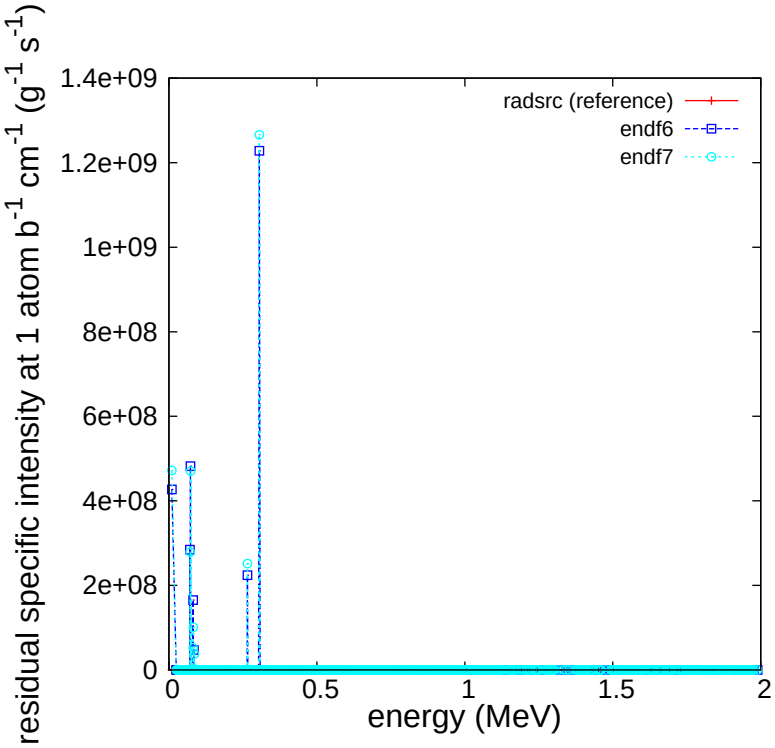

(b)

Fig. A.12. (a) photon emission intensity and (b) residual photon emission intensity with respect to the RadSrc database for Bi-210

A.13 Bi-211

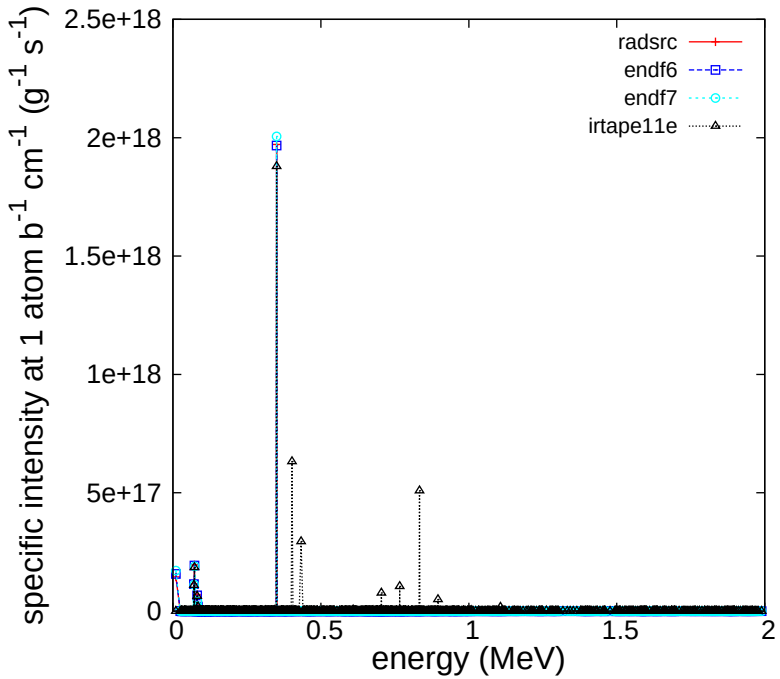

(a)

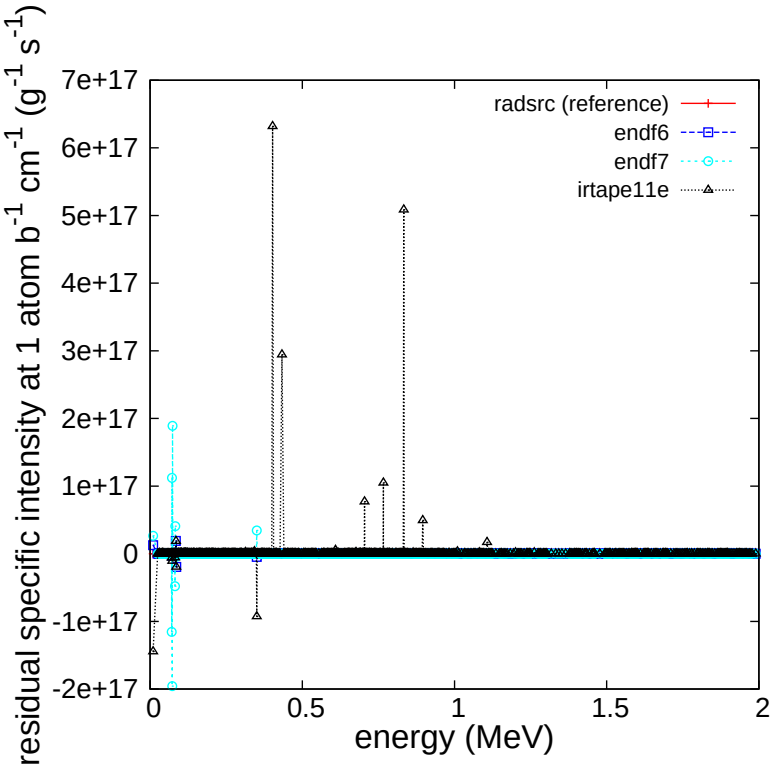

(b)

Fig. A.13. (a) photon emission intensity and (b) residual photon emission intensity with respect to the RadSrc database for Bi-211

A.14 Bi-212

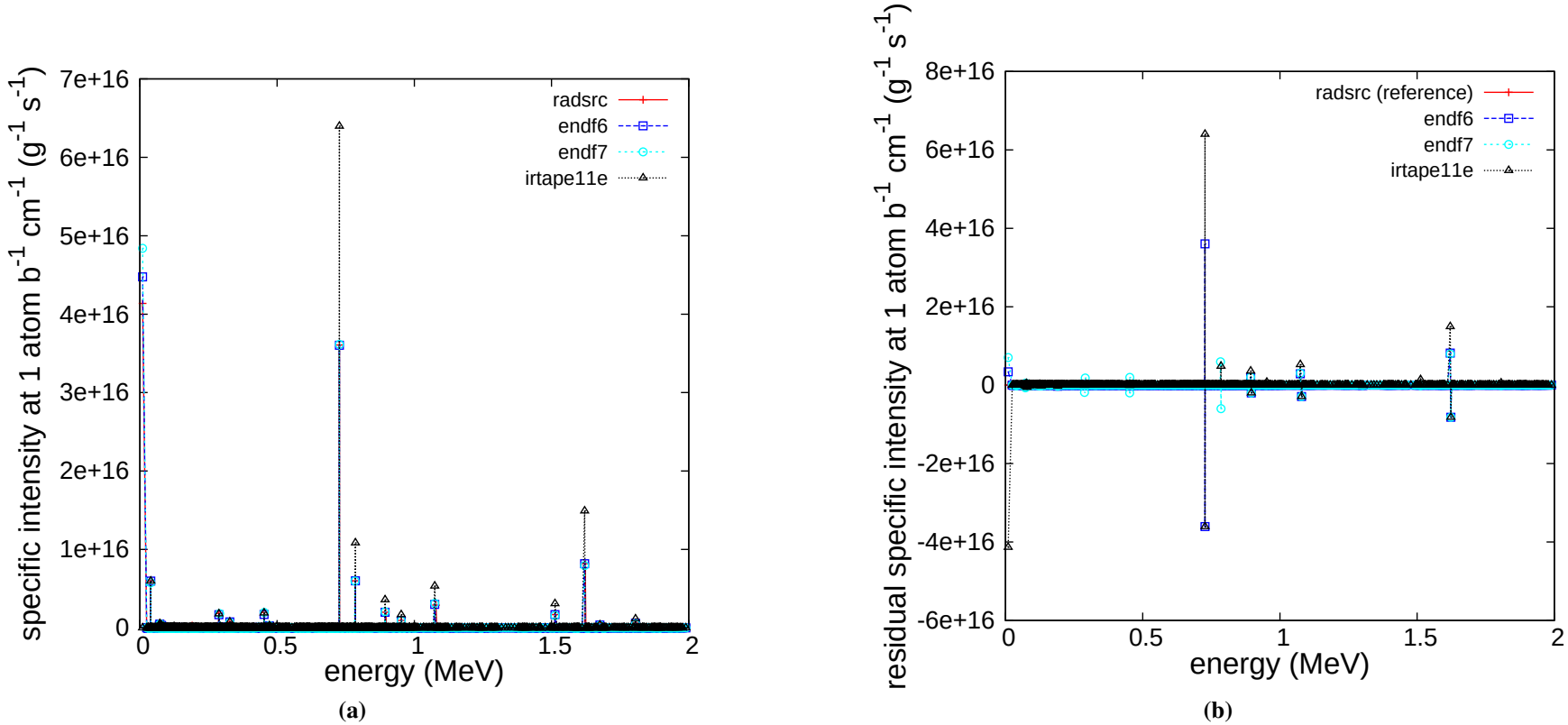

Fig. A.14. (a) photon emission intensity and (b) residual photon emission intensity with respect to the RadSrc database for Bi-212

A.15 Bi-213

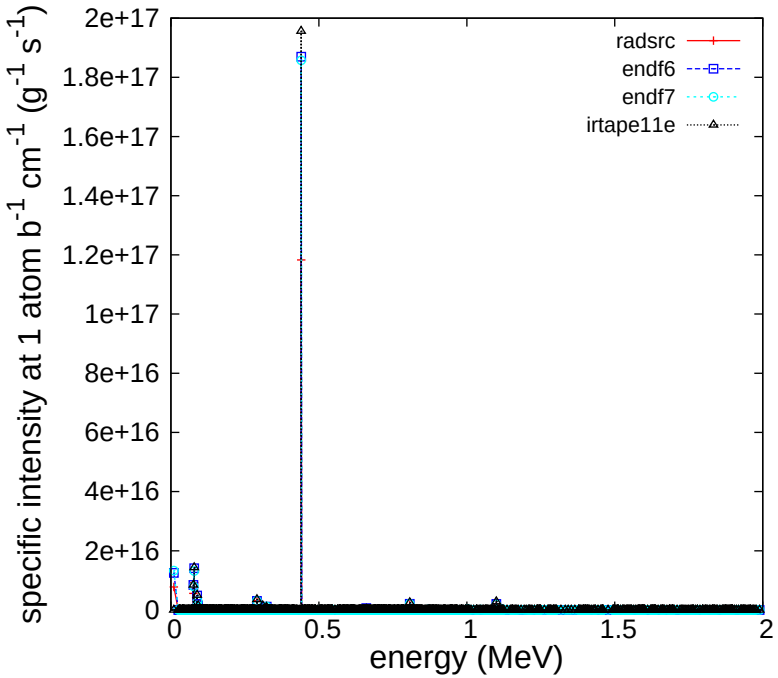

(a)

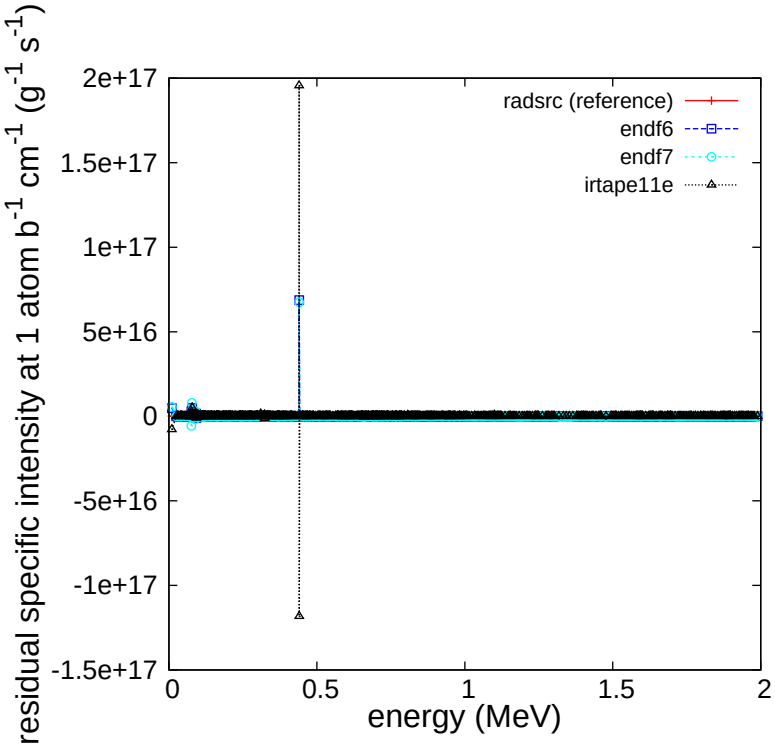

(b)

Fig. A.15. (a) photon emission intensity and (b) residual photon emission intensity with respect to the RadSrc database for Bi-213

A.16 Bi-214

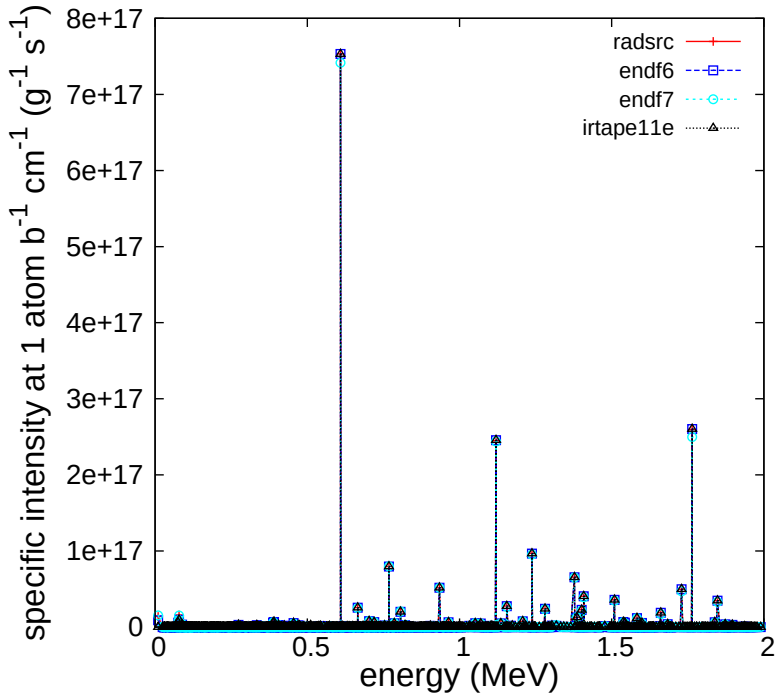

(a)

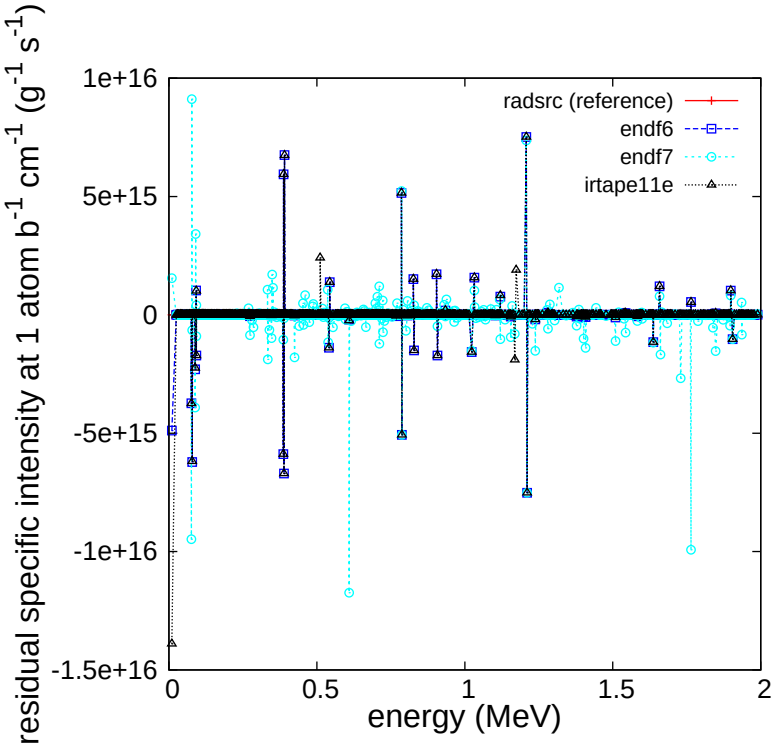

(b)

Fig. A.16. (a) photon emission intensity and (b) residual photon emission intensity with respect to the RadSrc database for Bi-214

A.17 Po-210

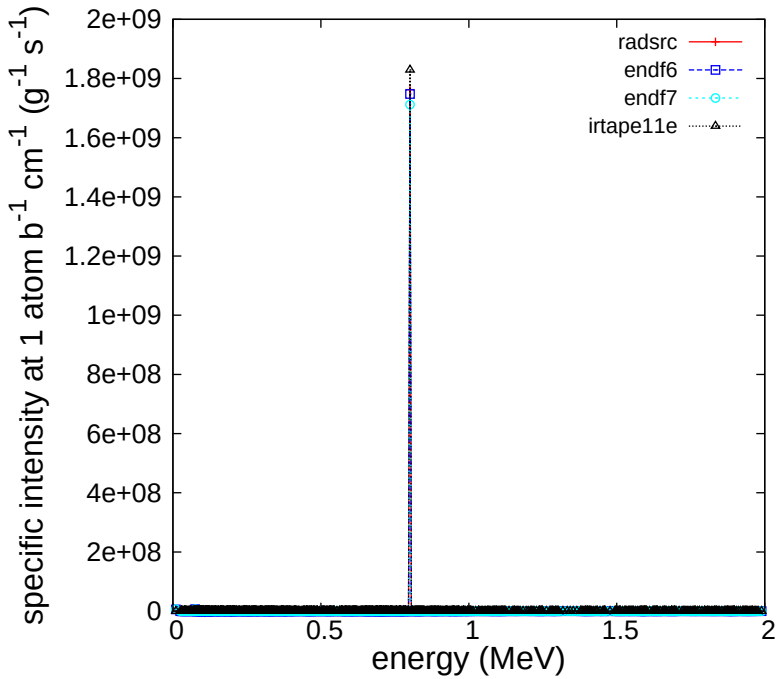

(a)

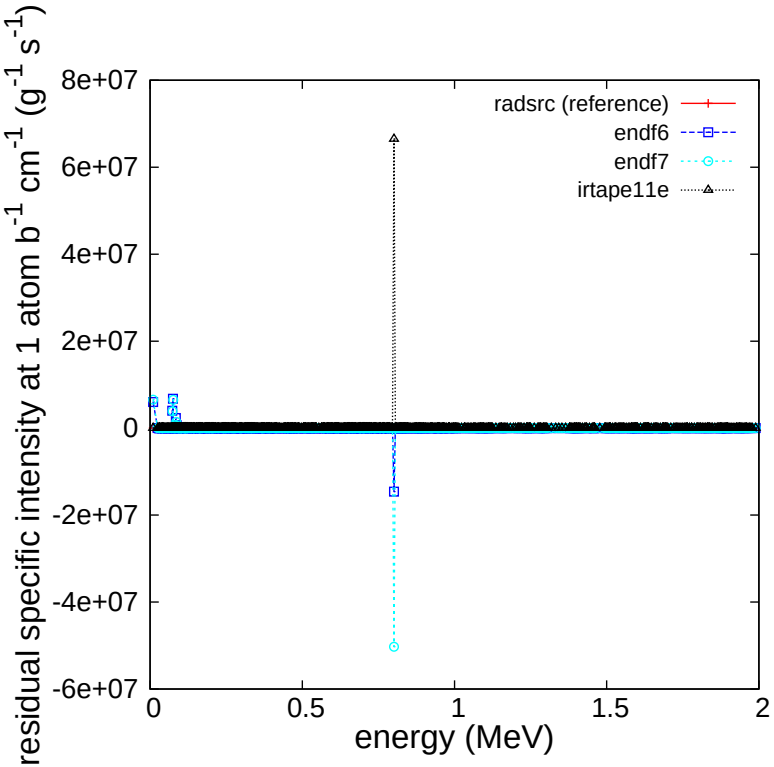

(b)

Fig. A.17. (a) photon emission intensity and (b) residual photon emission intensity with respect to the RadSrc database for Po-210

A.18 Po-211

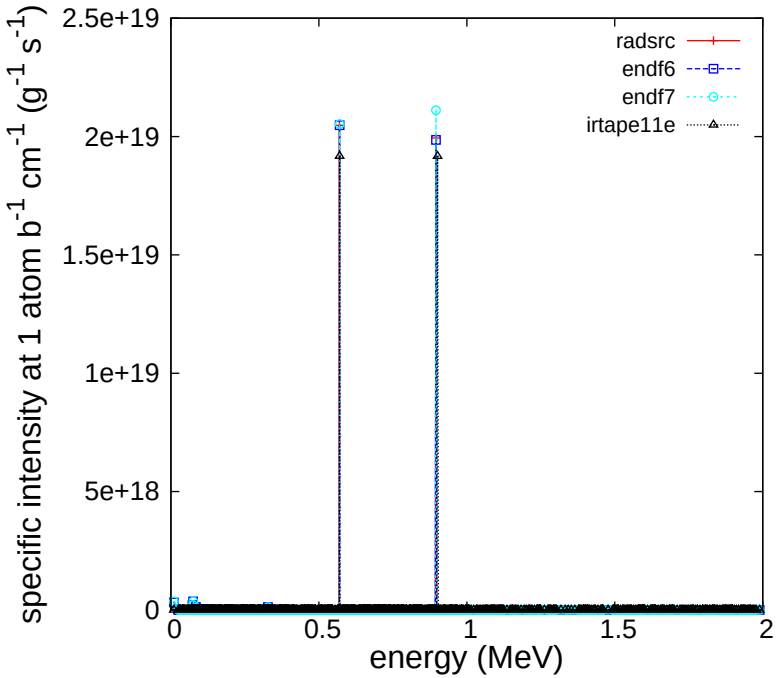

(a)

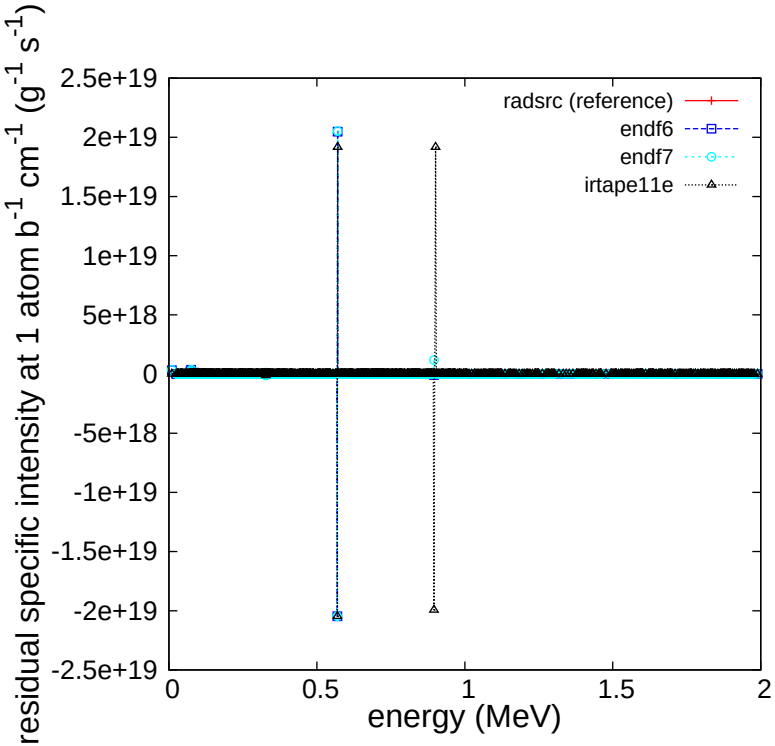

(b)

Fig. A.18. (a) photon emission intensity and (b) residual photon emission intensity with respect to the RadSrc database for Po-211

A.19 Po-214

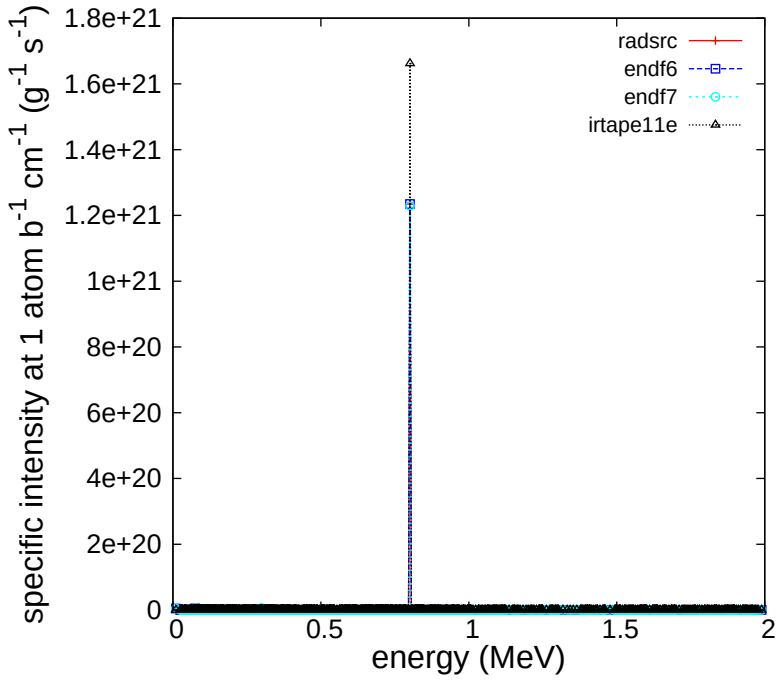

(a)

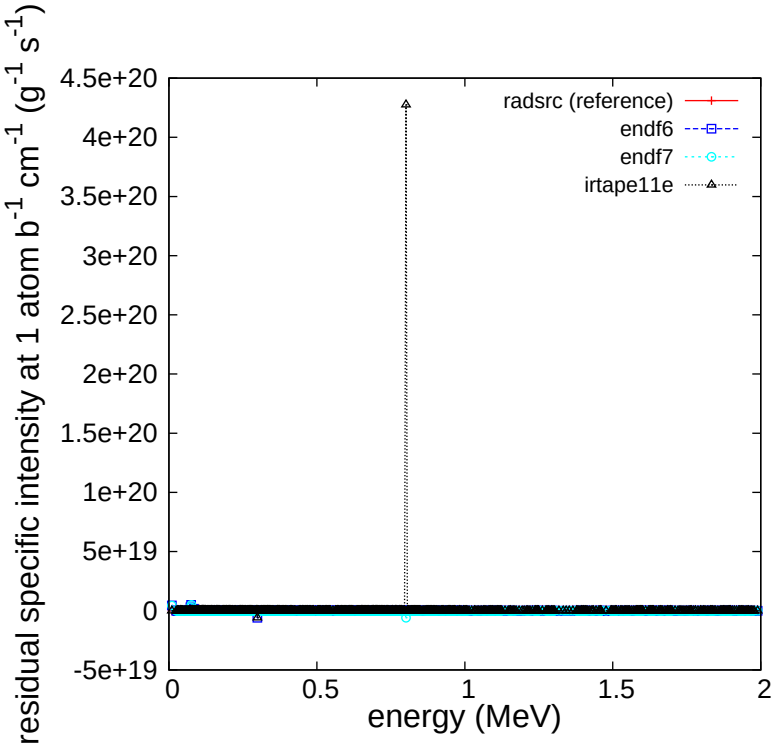

(b)

Fig. A.19. (a) photon emission intensity and (b) residual photon emission intensity with respect to the RadSrc database for Po-214

A.20 Po-215

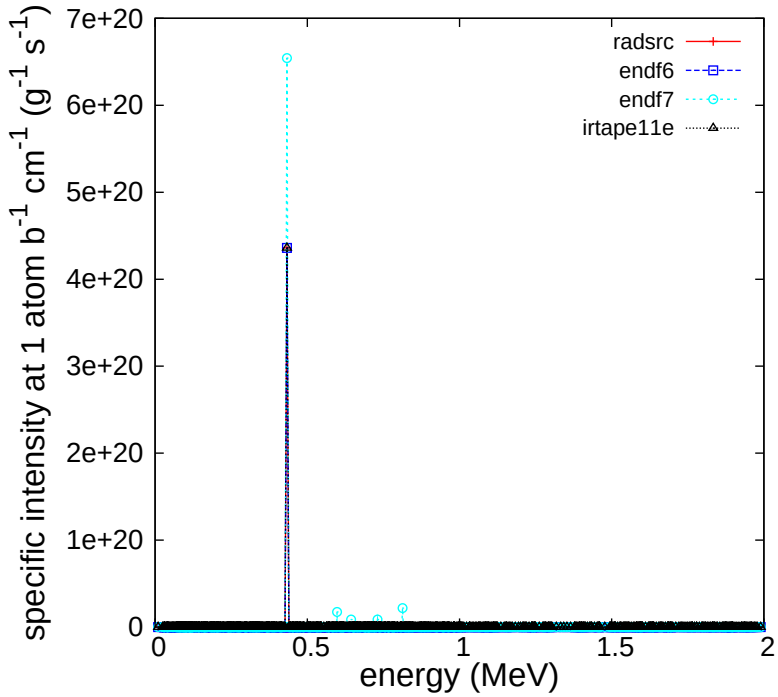

(a)

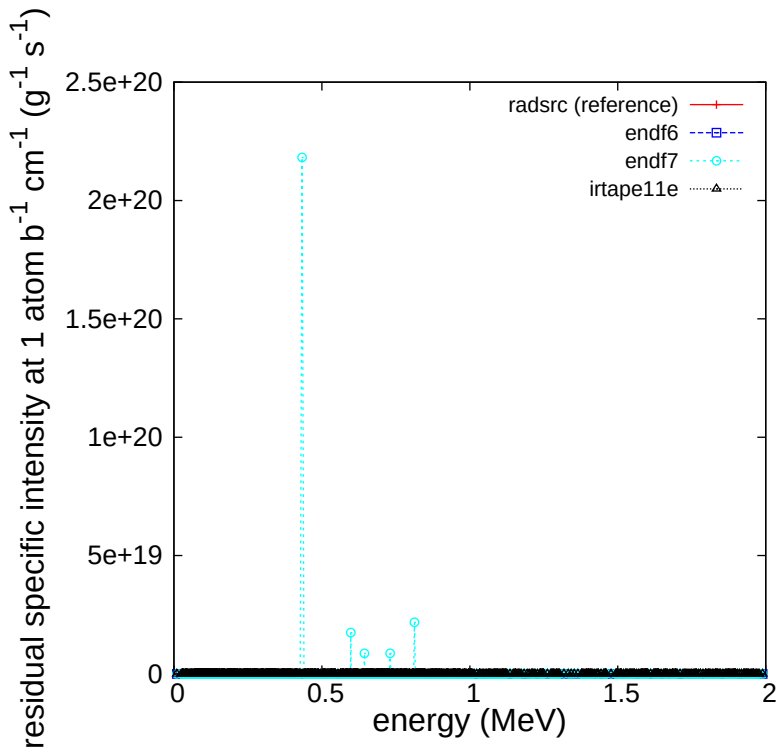

(b)

Fig. A.20. (a) photon emission intensity and (b) residual photon emission intensity with respect to the RadSrc database for Po-215

A.21 Po-216

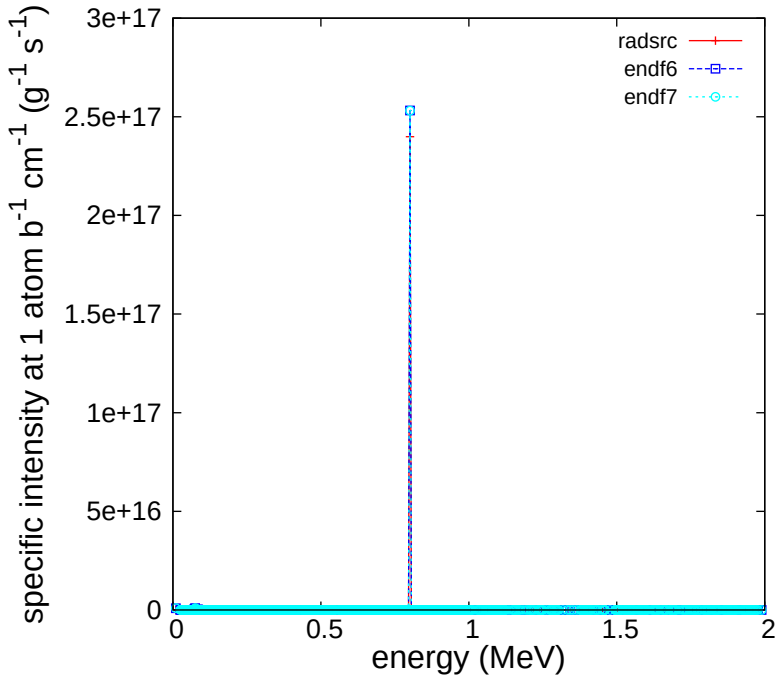

(a)

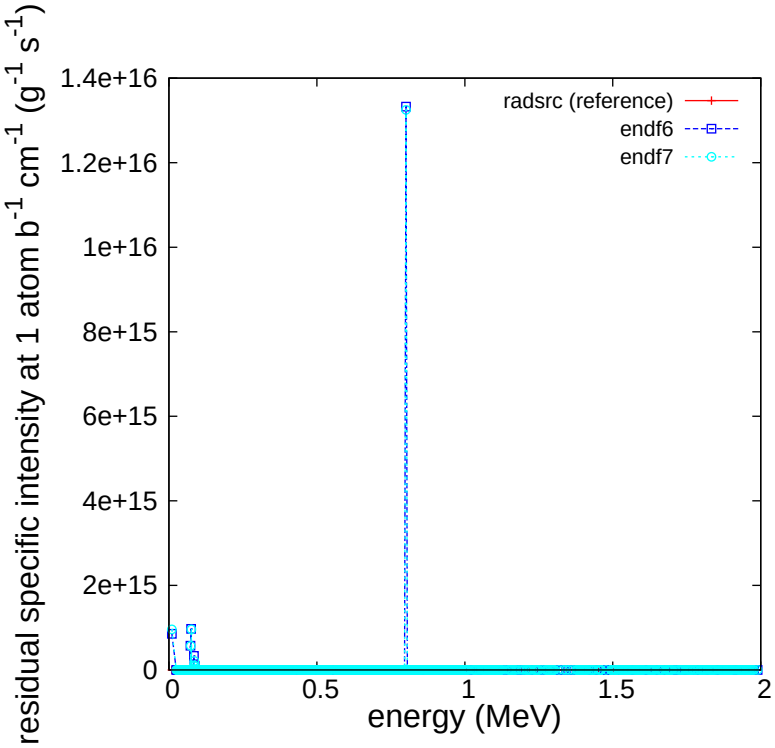

(b)

Fig. A.21. (a) photon emission intensity and (b) residual photon emission intensity with respect to the RadSrc database for Po-216

A.22 At-215

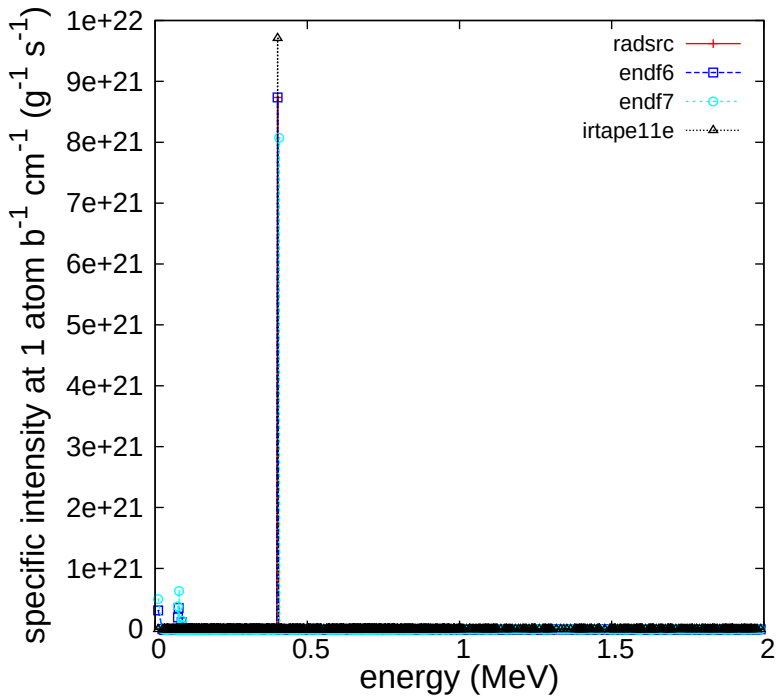

(a)

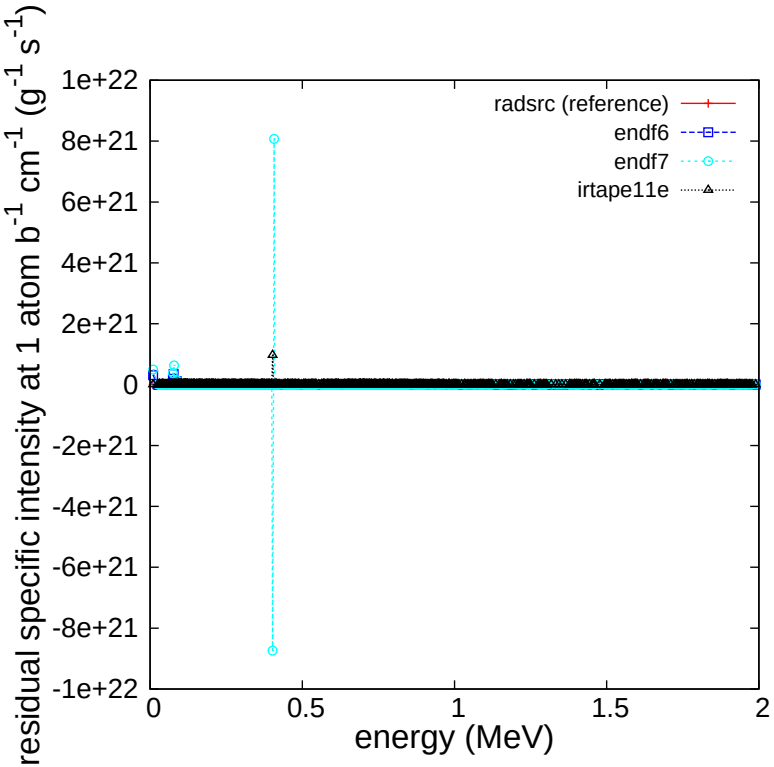

(b)

Fig. A.22. (a) photon emission intensity and (b) residual photon emission intensity with respect to the RadSrc database for At-215

A.23 Rn-219

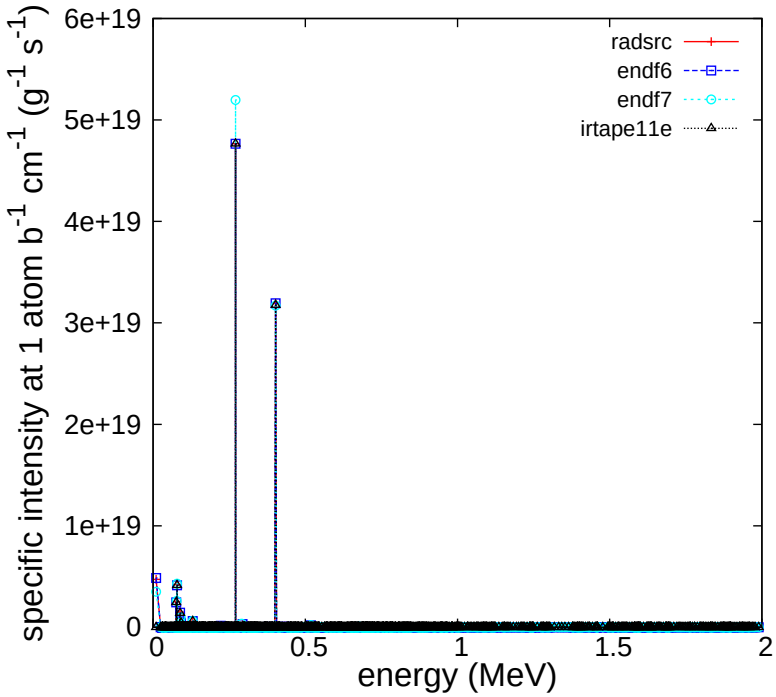

(a)

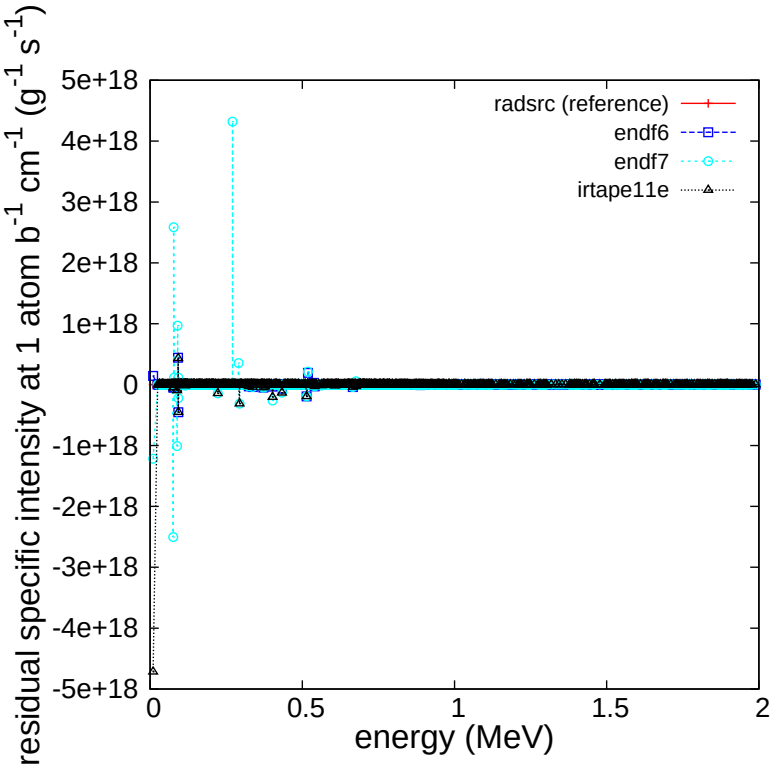

(b)

Fig. A.23. (a) photon emission intensity and (b) residual photon emission intensity with respect to the RadSrc database for Rn-219

A.24 Rn-220

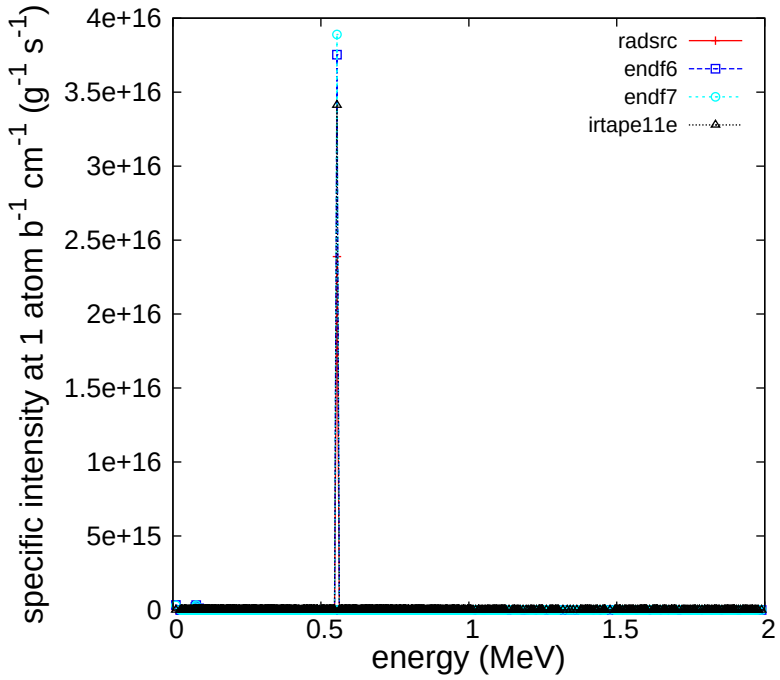

(a)

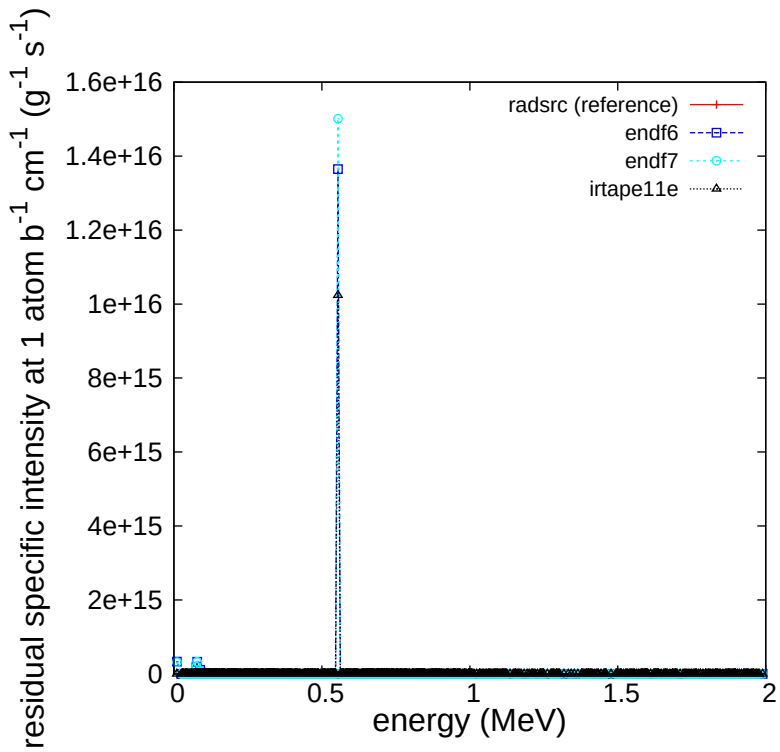

(b)

Fig. A.24. (a) photon emission intensity and (b) residual photon emission intensity with respect to the RadSrc database for Rn-220

A.25 Rn-222

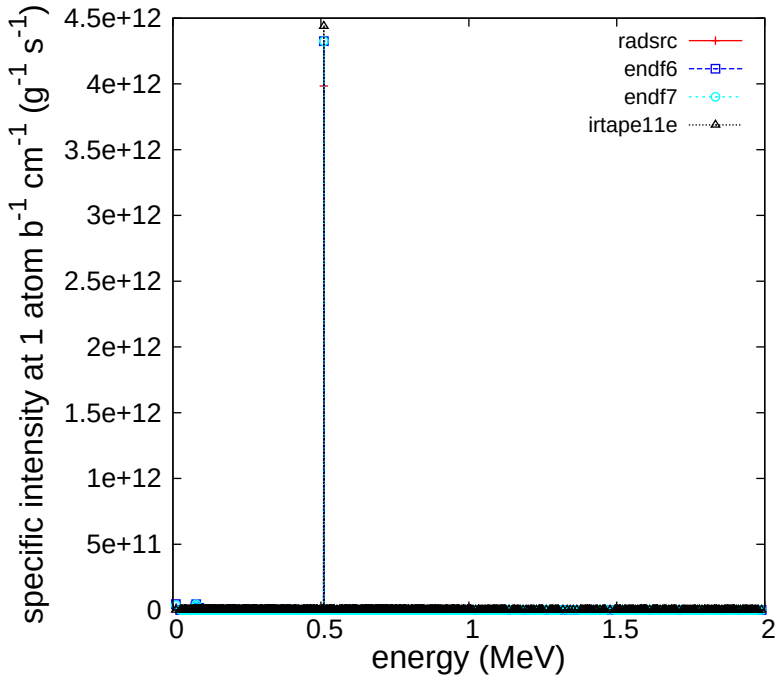

(a)

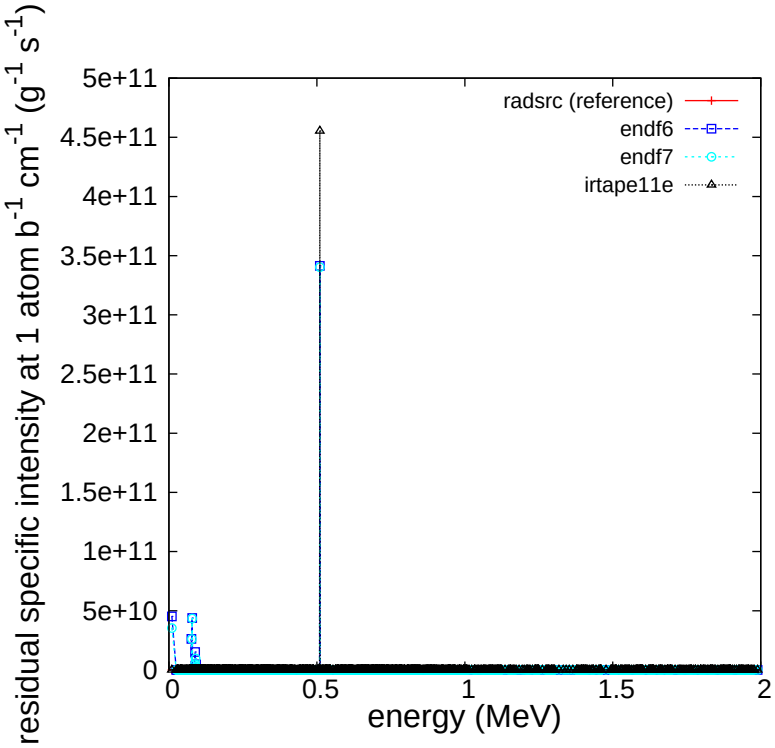

(b)

Fig. A.25. (a) photon emission intensity and (b) residual photon emission intensity with respect to the RadSrc database for Rn-222

A.26 Fr-221

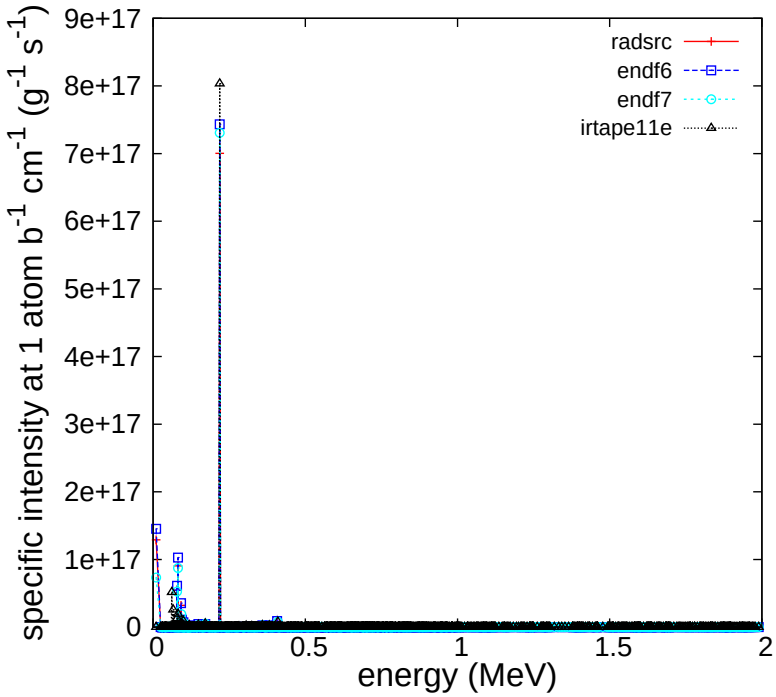

(a)

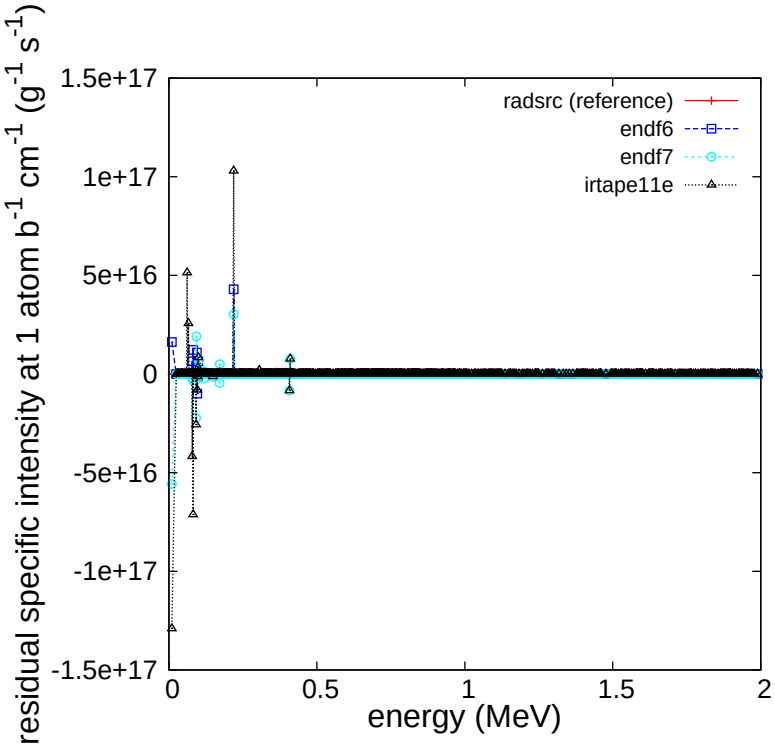

(b)

Fig. A.26. (a) photon emission intensity and (b) residual photon emission intensity with respect to the RadSrc database for Fr-221

A.27 Fr-223

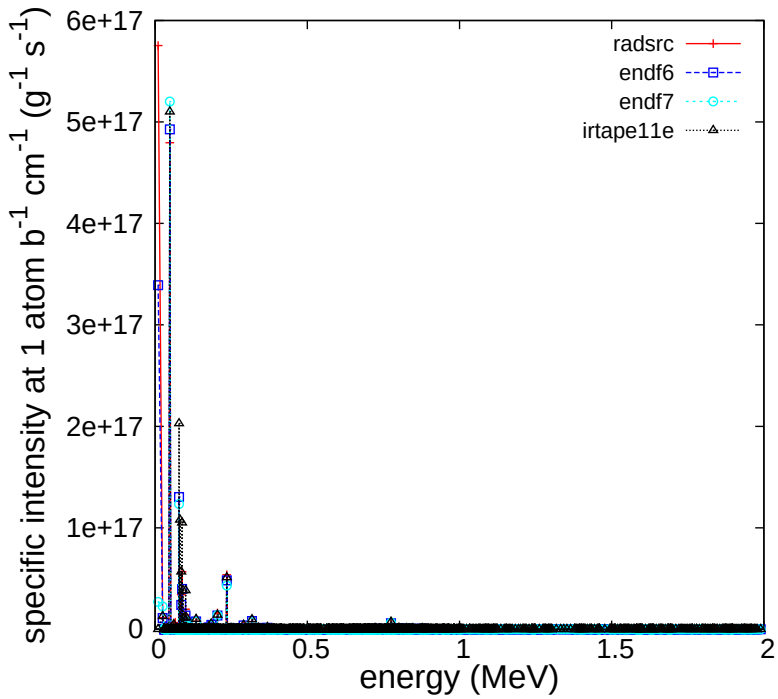

(a)

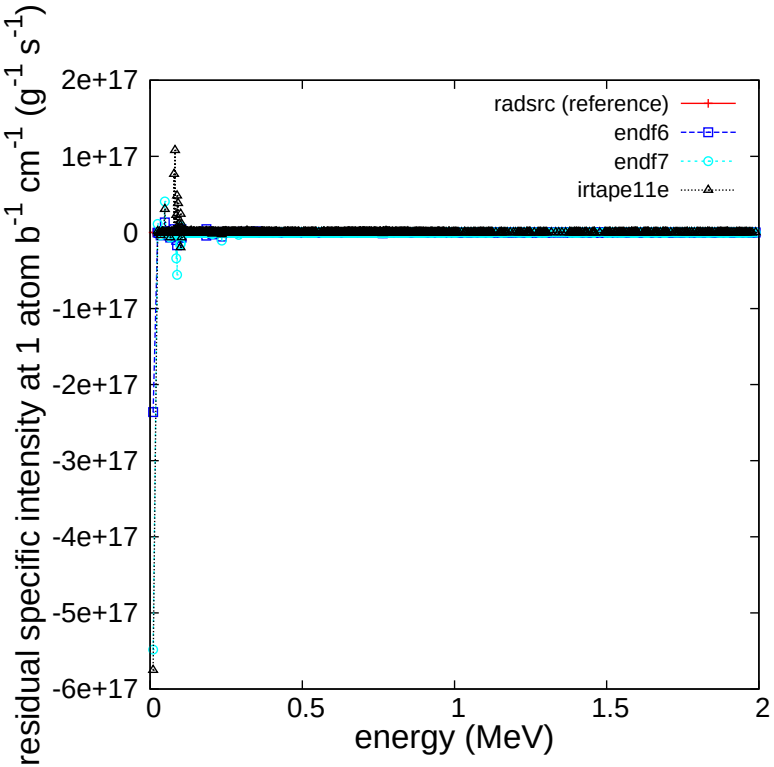

(b)

Fig. A.27. (a) photon emission intensity and (b) residual photon emission intensity with respect to the RadSrc database for Fr-223

A.28 Fr-224

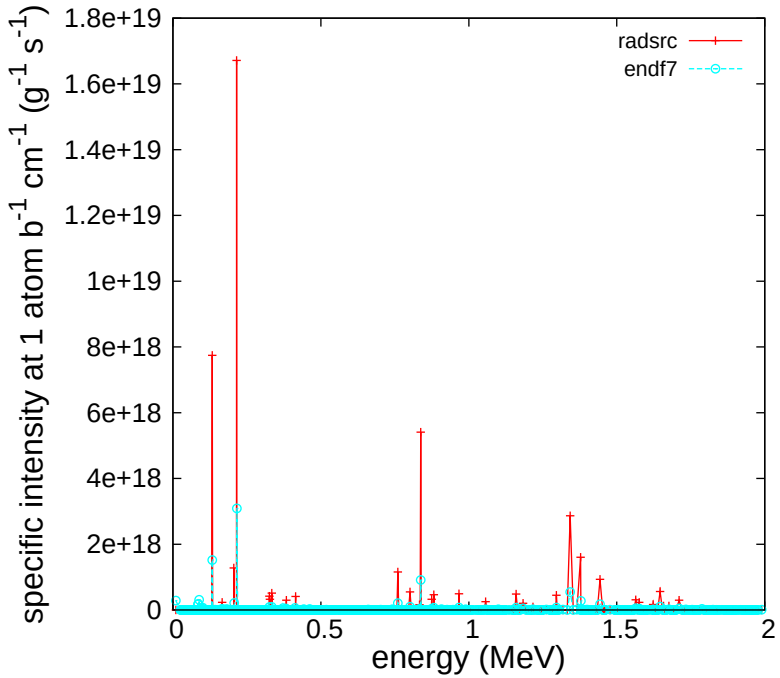

(a)

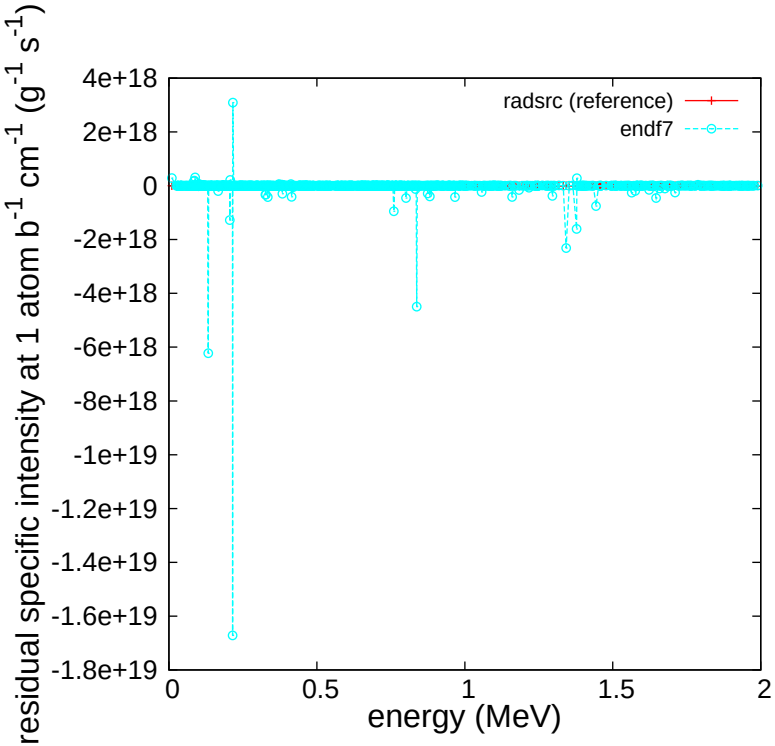

(b)

Fig. A.28. (a) photon emission intensity and (b) residual photon emission intensity with respect to the RadSrc database for Fr-224

A.29 Ra-223

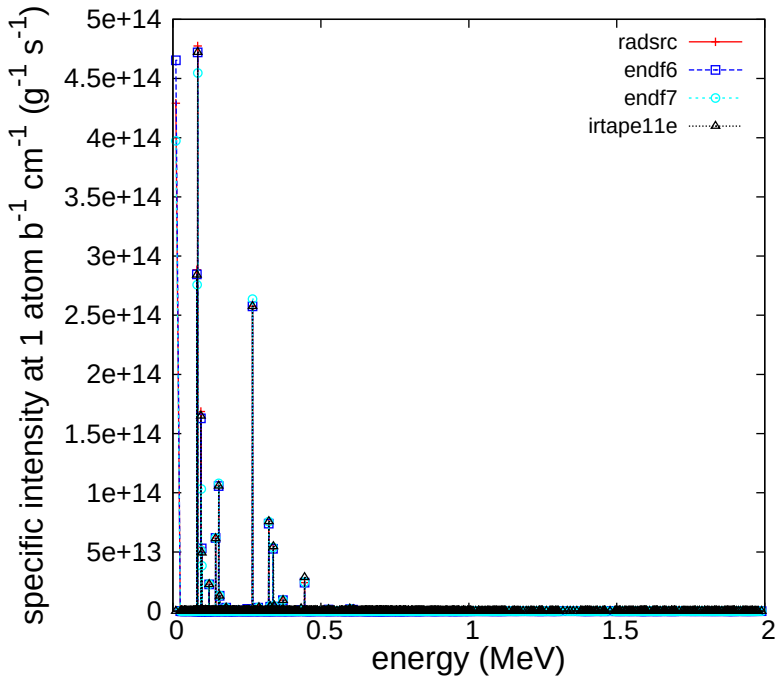

(a)

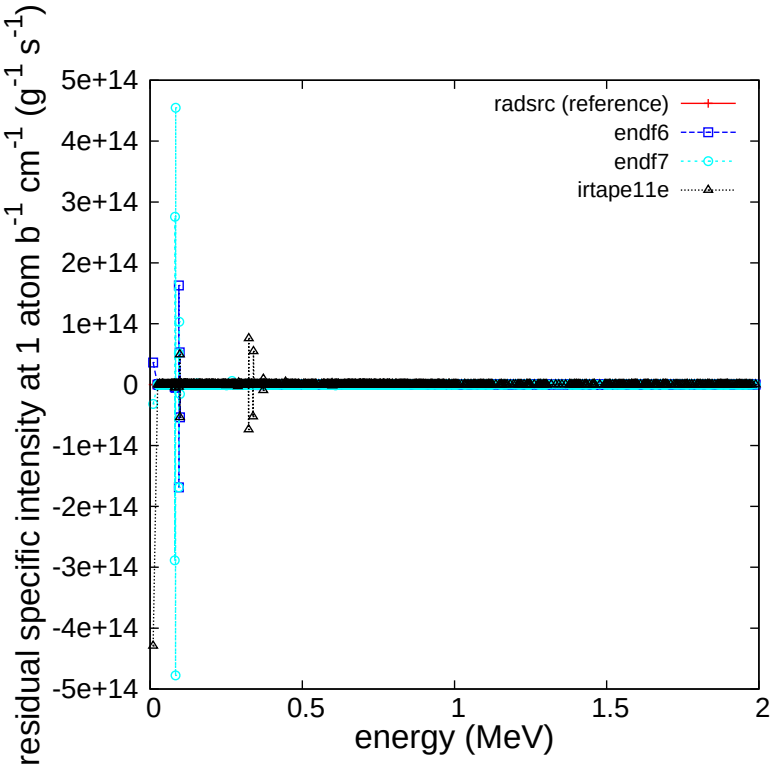

(b)

Fig. A.29. (a) photon emission intensity and (b) residual photon emission intensity with respect to the RadSrc database for Ra-223

A.30 Ra-224

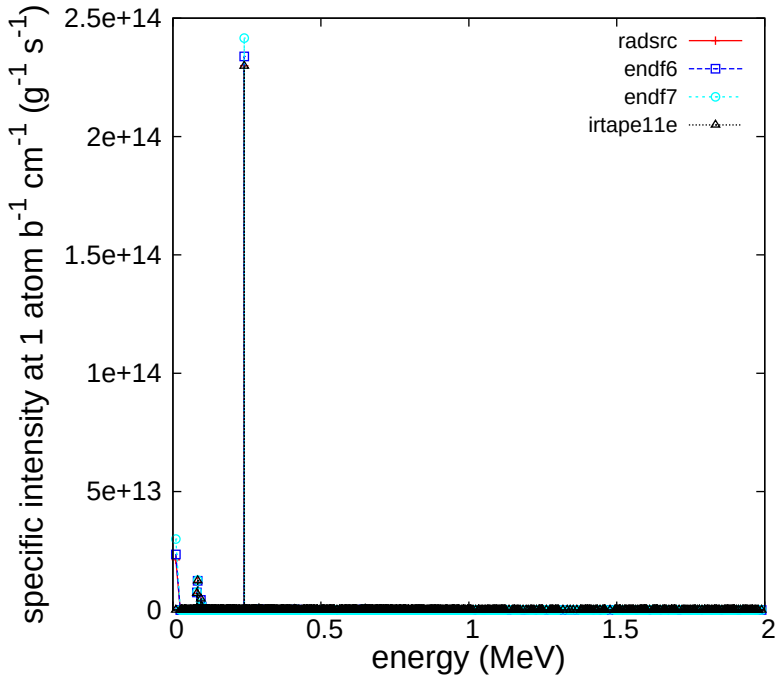

(a)

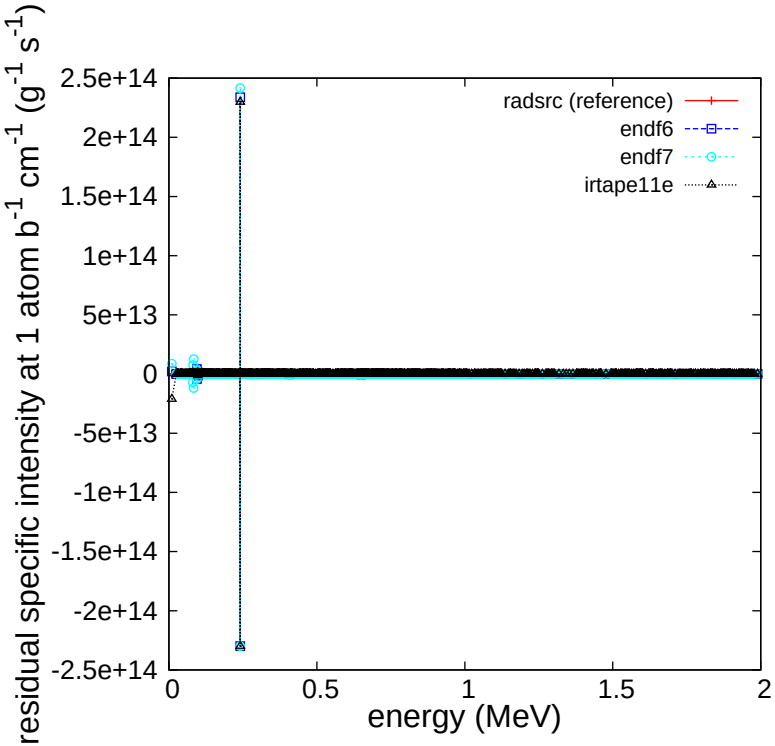

(b)

Fig. A.30. (a) photon emission intensity and (b) residual photon emission intensity with respect to the RadSrc database for Ra-224

A.31 Ra-225

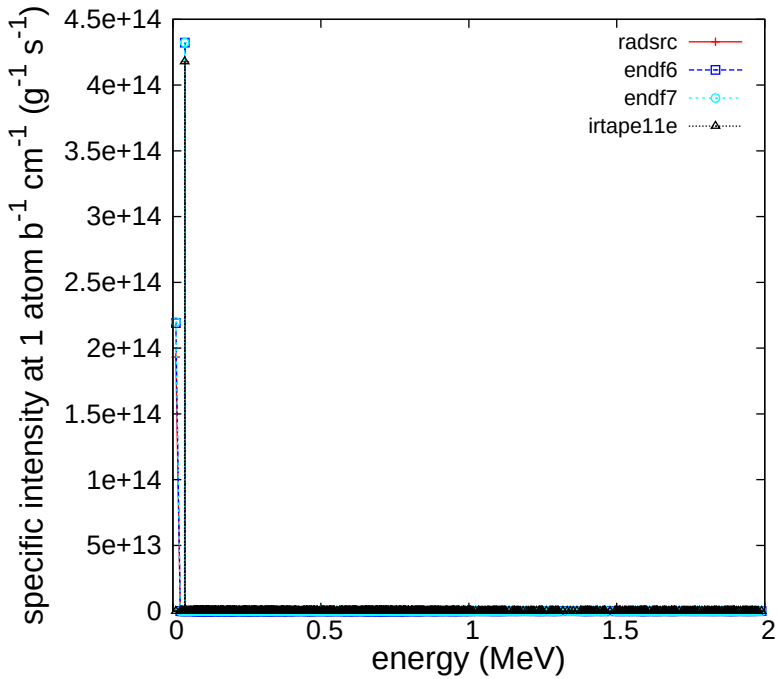

(a)

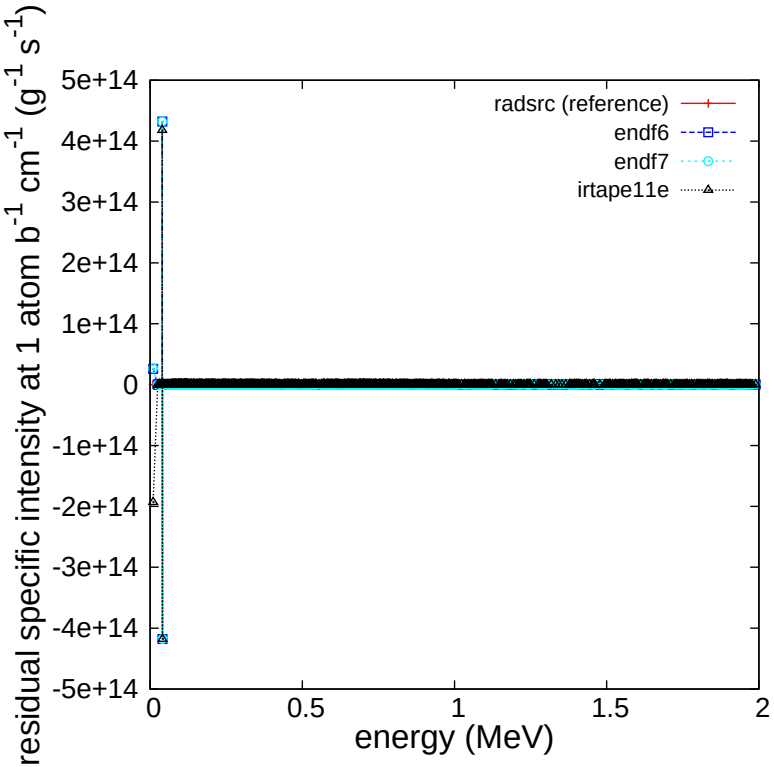

(b)

Fig. A.31. (a) photon emission intensity and (b) residual photon emission intensity with respect to the RadSrc database for Ra-225

A.32 Ra-226

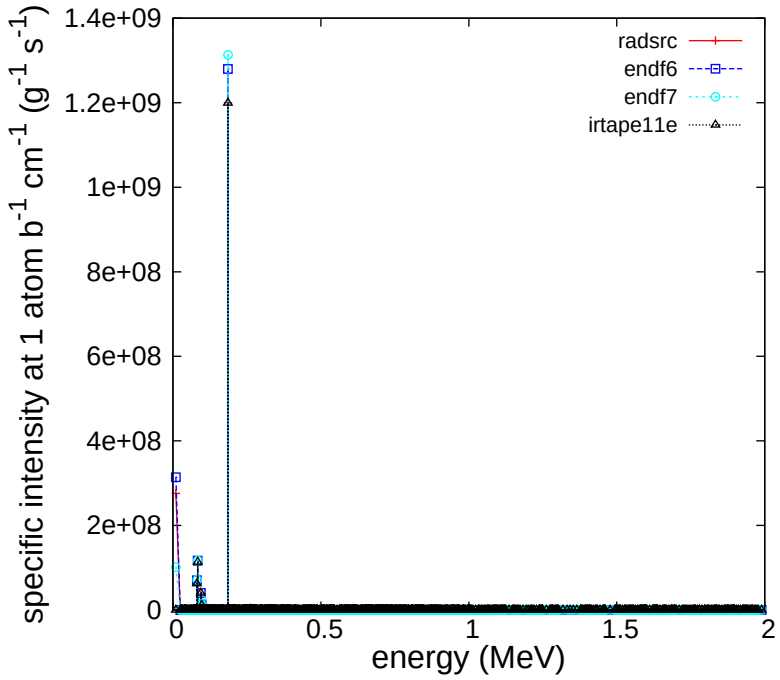

(a)

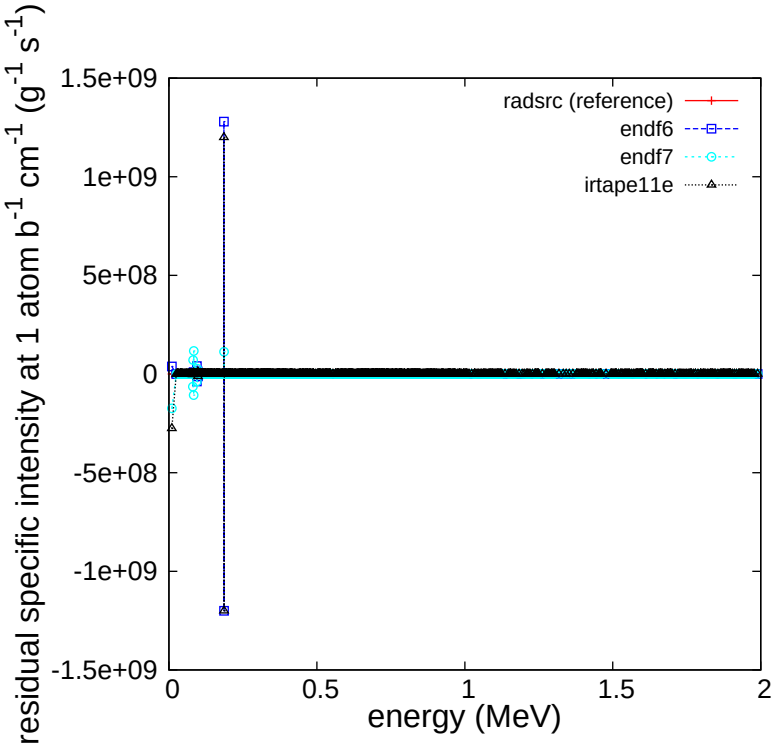

(b)

Fig. A.32. (a) photon emission intensity and (b) residual photon emission intensity with respect to the RadSrc database for Ra-226

A.33 Ra-228

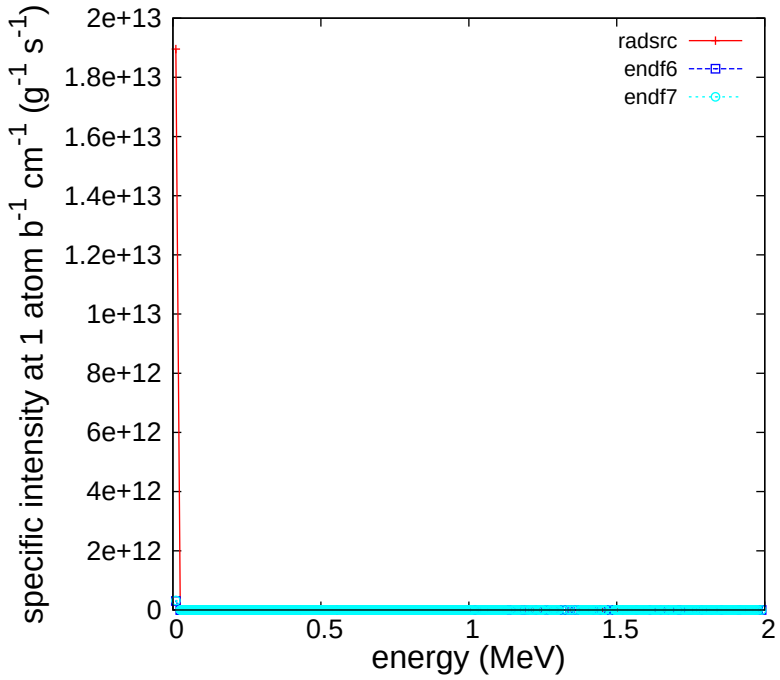

(a)

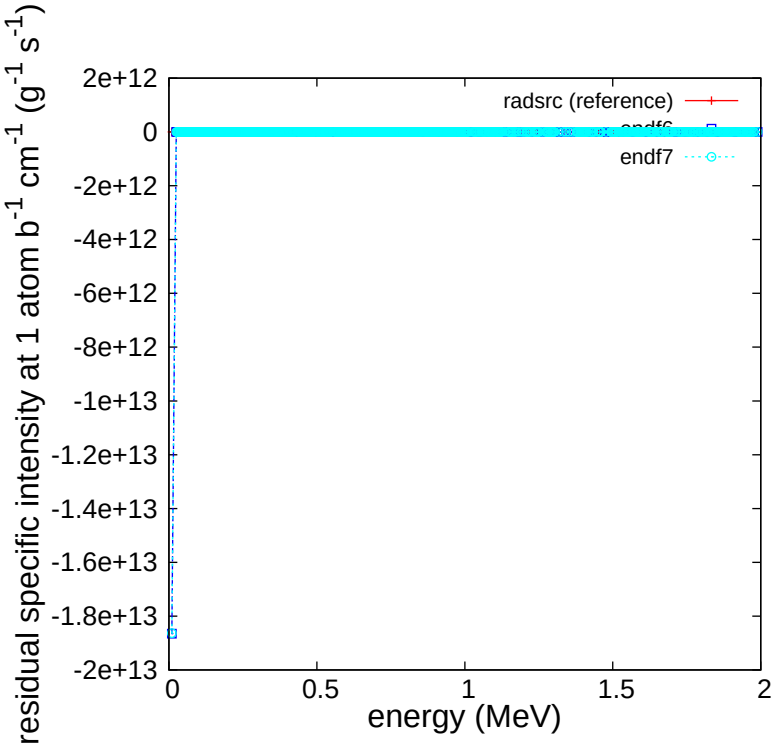

(b)

Fig. A.33. (a) photon emission intensity and (b) residual photon emission intensity with respect to the RadSrc database for Ra-228

A.34 Ac-225

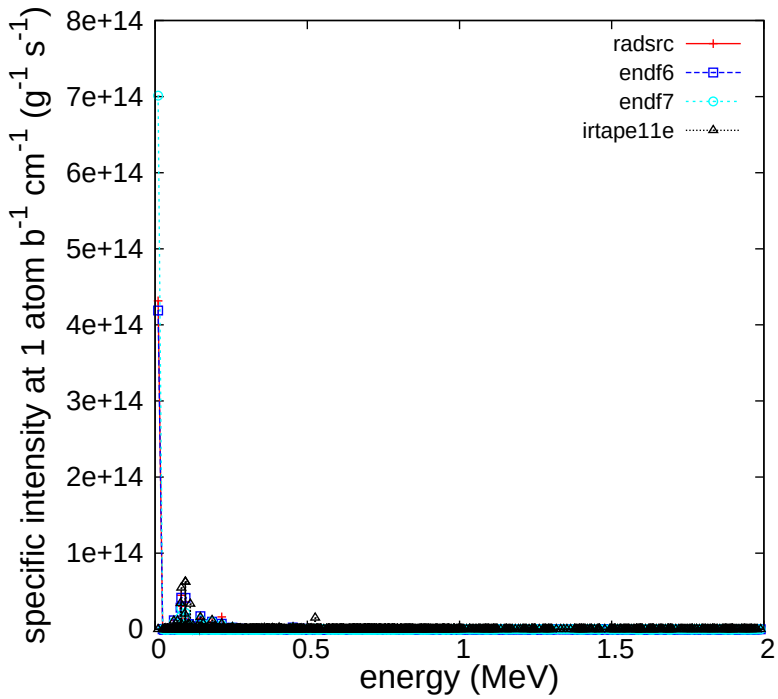

(a)

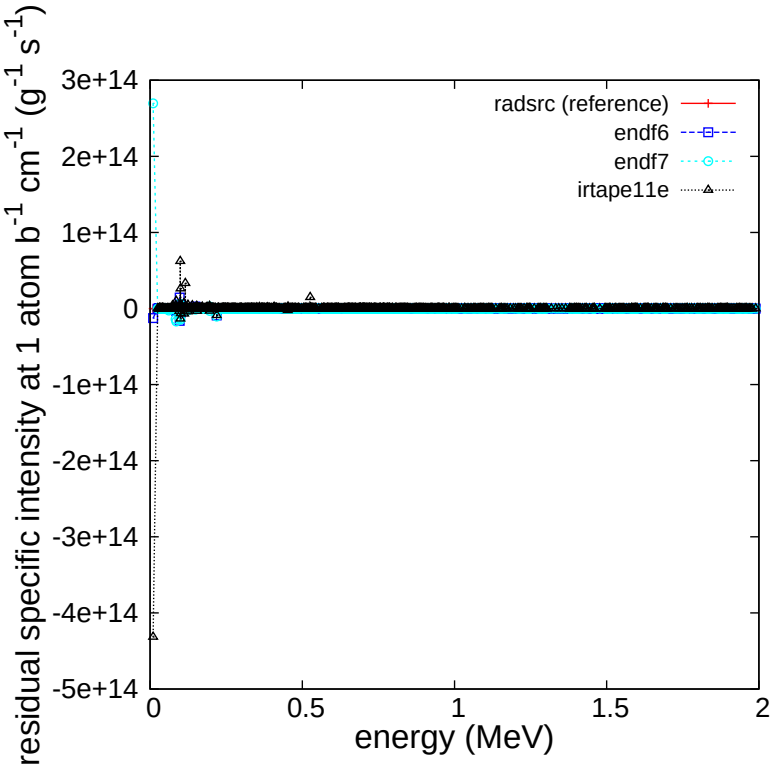

(b)

Fig. A.34. (a) photon emission intensity and (b) residual photon emission intensity with respect to the RadSrc database for Ac-225

A.35 Ac-227

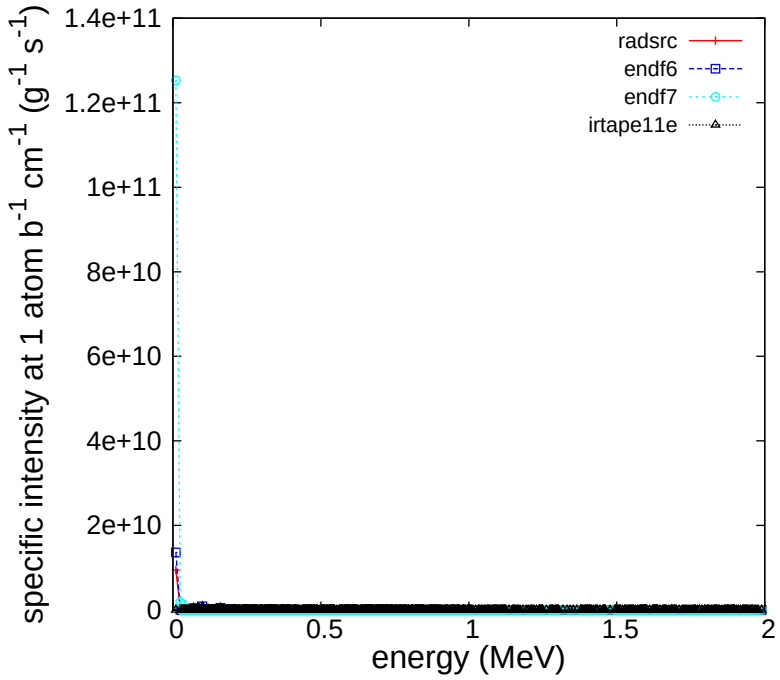

(a)

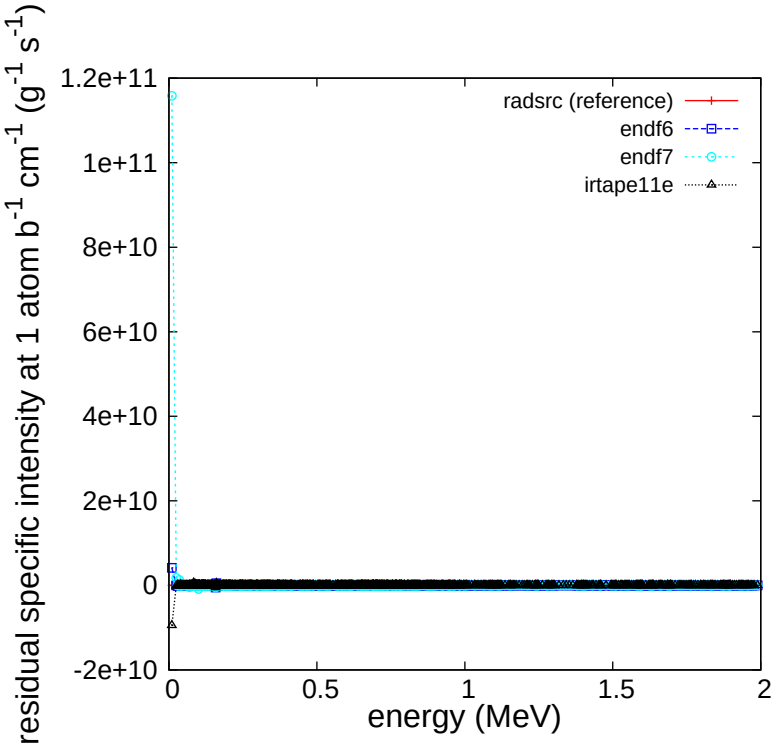

(b)

Fig. A.35. (a) photon emission intensity and (b) residual photon emission intensity with respect to the RadSrc database for Ac-227

A.36 Ac-228

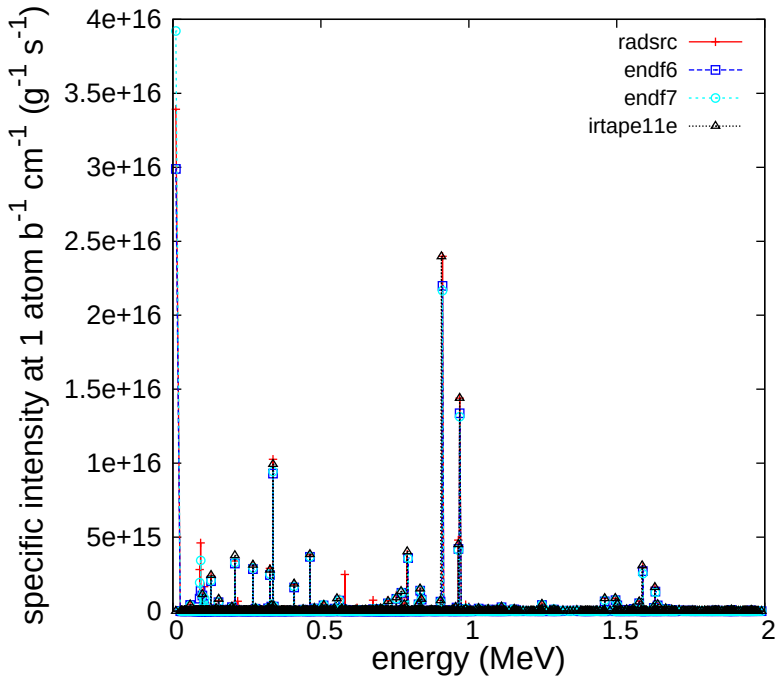

(a)

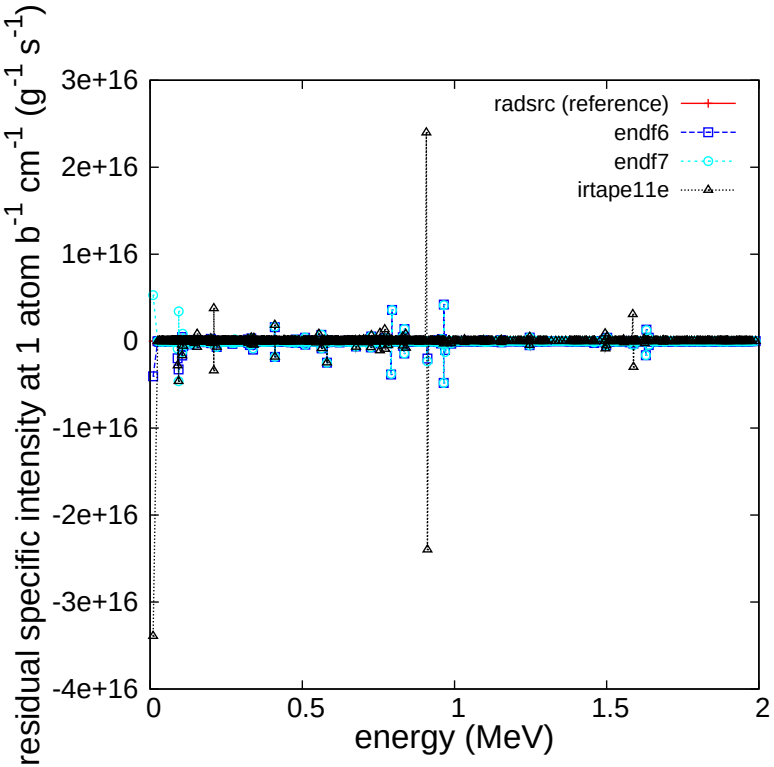

(b)

Fig. A.36. (a) photon emission intensity and (b) residual photon emission intensity with respect to the RadSrc database for Ac-228

A.37 Th-227

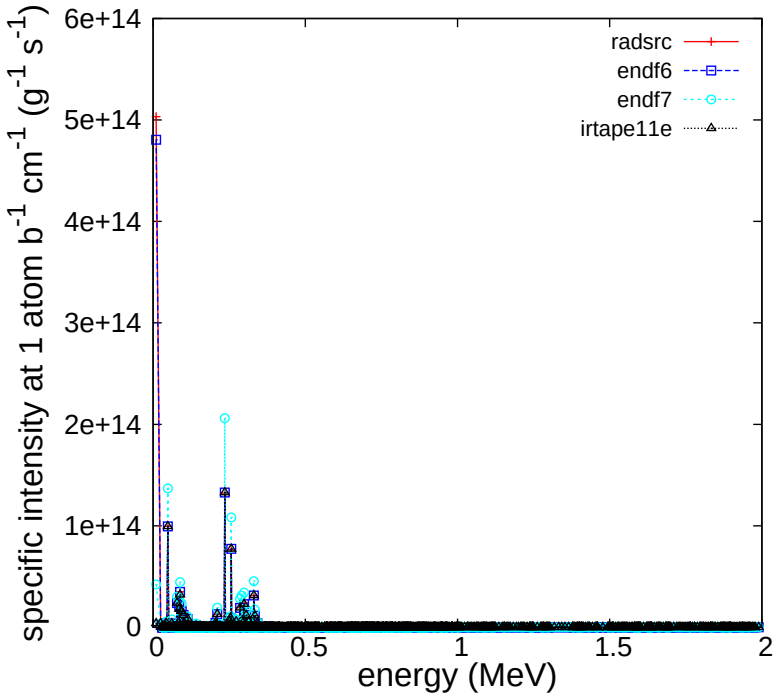

(a)

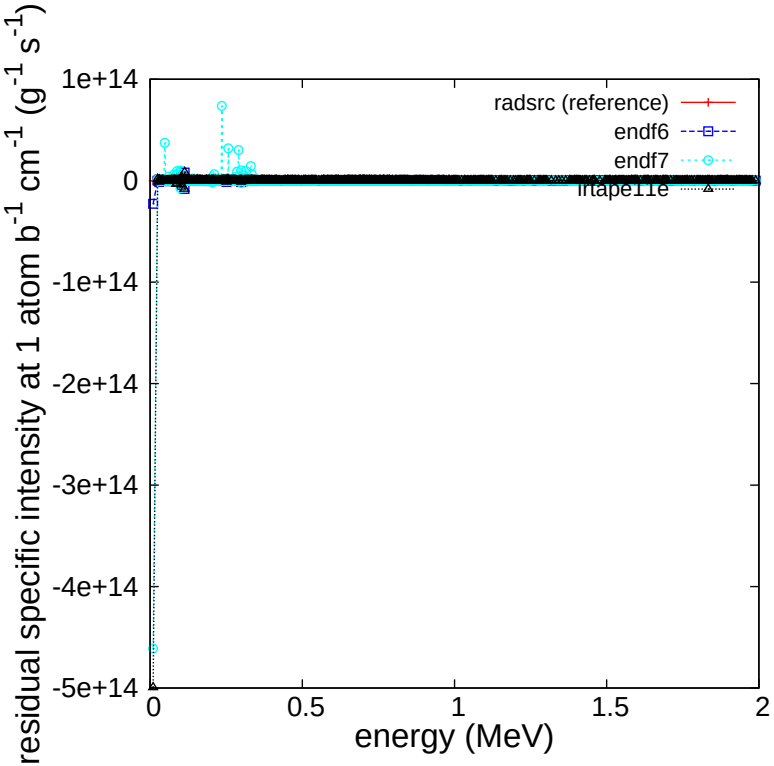

(b)

Fig. A.37. (a) photon emission intensity and (b) residual photon emission intensity with respect to the RadSrc database for Th-227

A.38 Th-228

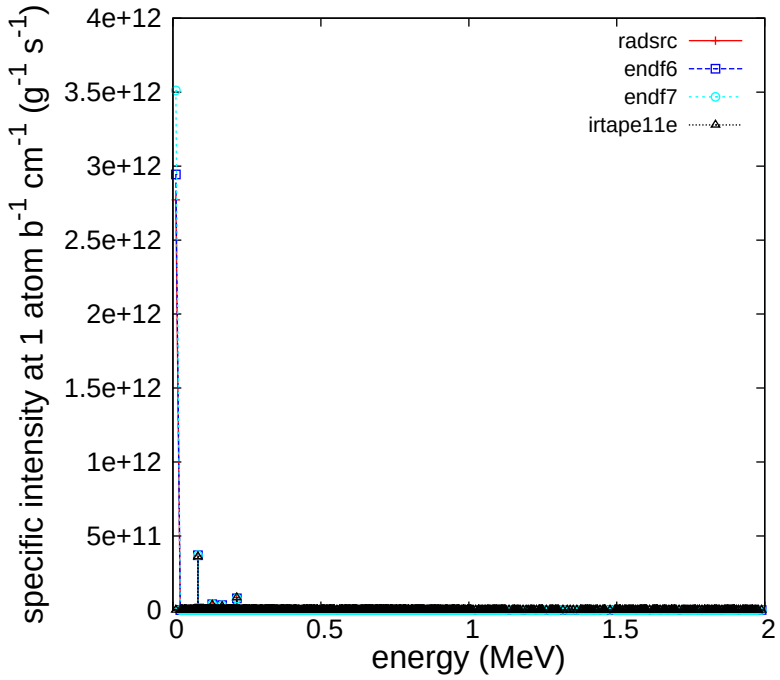

(a)

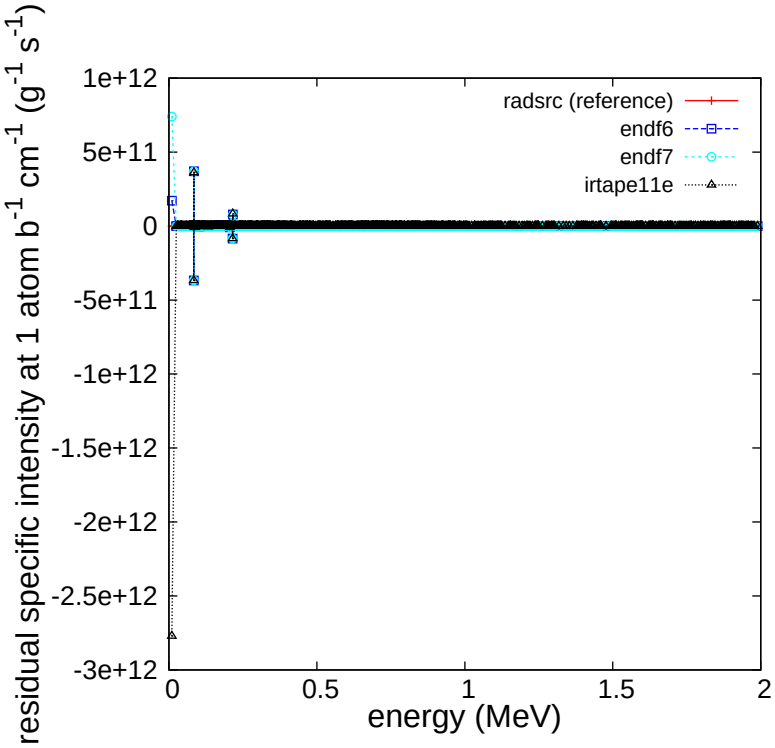

(b)

Fig. A.38. (a) photon emission intensity and (b) residual photon emission intensity with respect to the RadSrc database for Th-228

A.39 Th-229

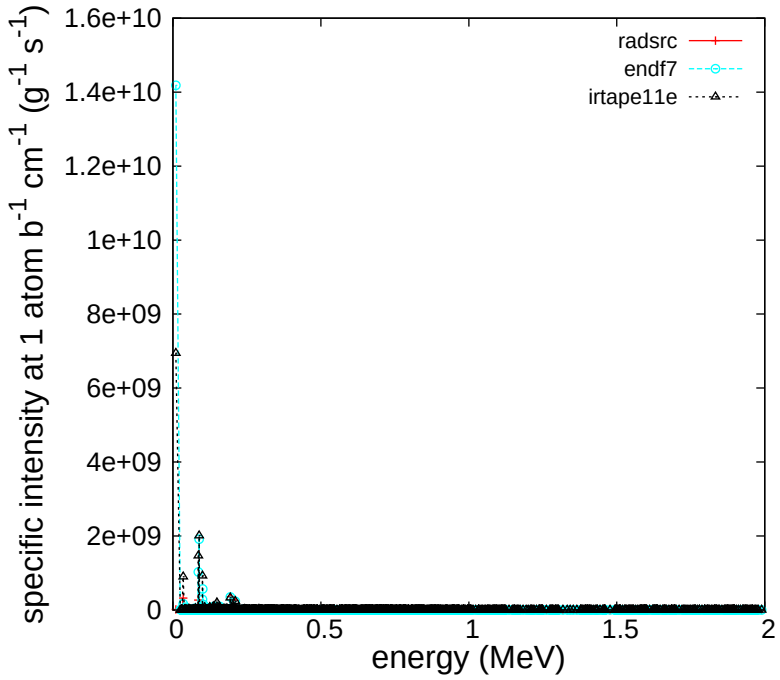

(a)

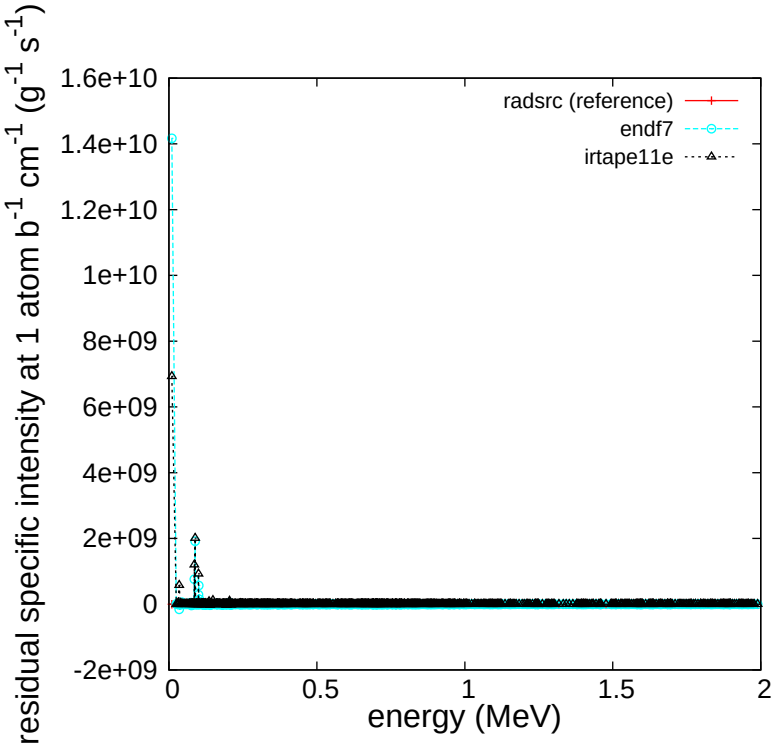

(b)

Fig. A.39. (a) photon emission intensity and (b) residual photon emission intensity with respect to the RadSrc database for Th-229

A.40 Th-230

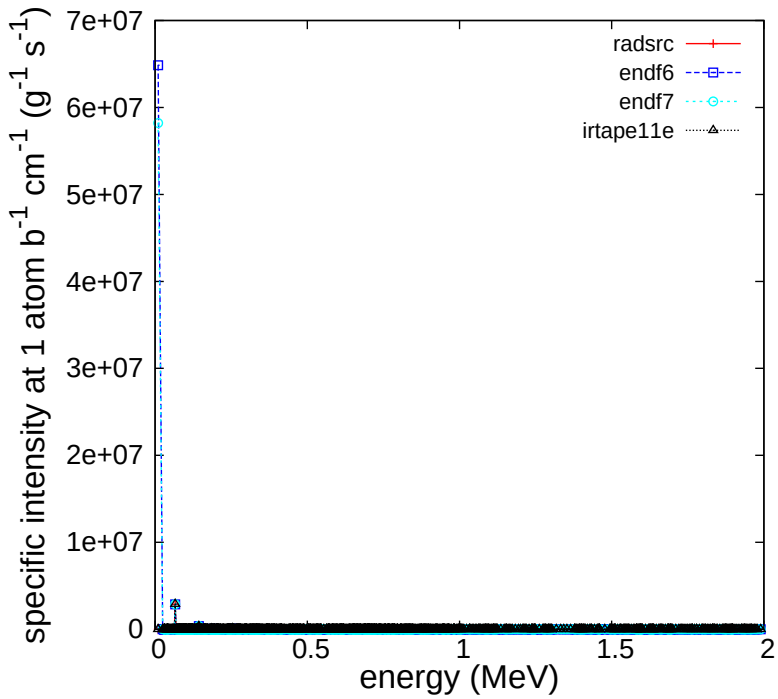

(a)

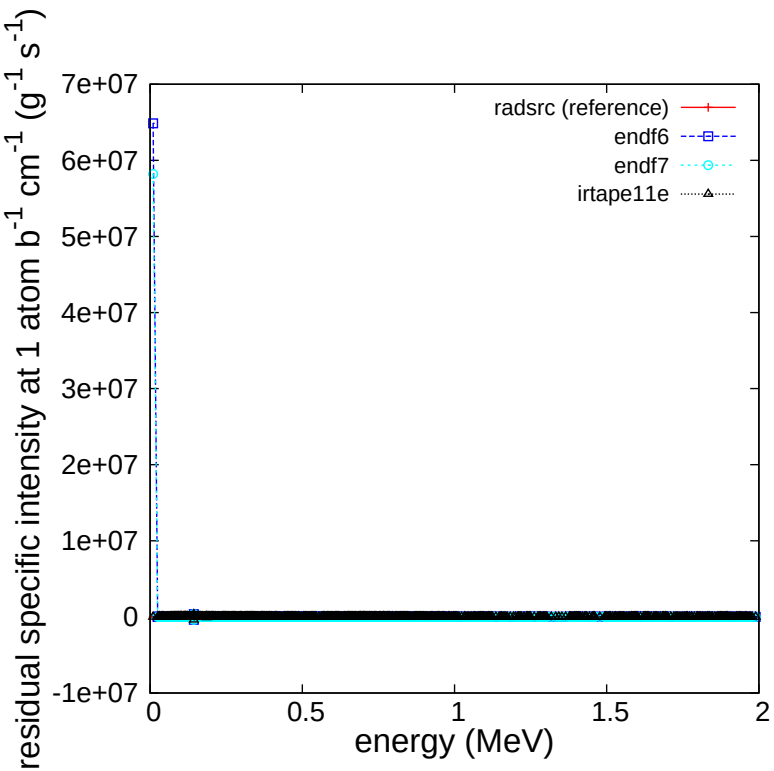

(b)

Fig. A.40. (a) photon emission intensity and (b) residual photon emission intensity with respect to the RadSrc database for Th-230

A.41 Th-231

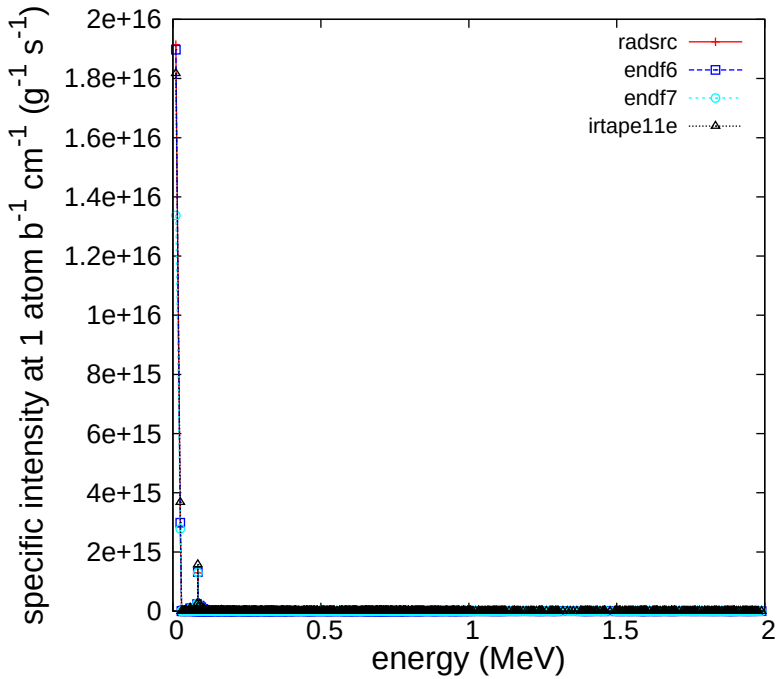

(a)

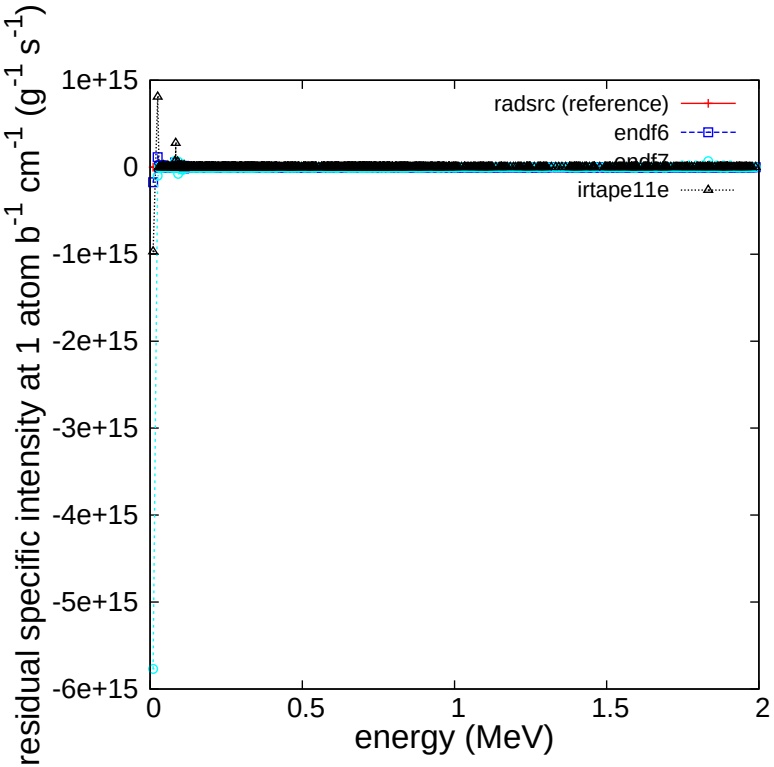

(b)

Fig. A.41. (a) photon emission intensity and (b) residual photon emission intensity with respect to the RadSrc database for Th-231

A.42 Th-232

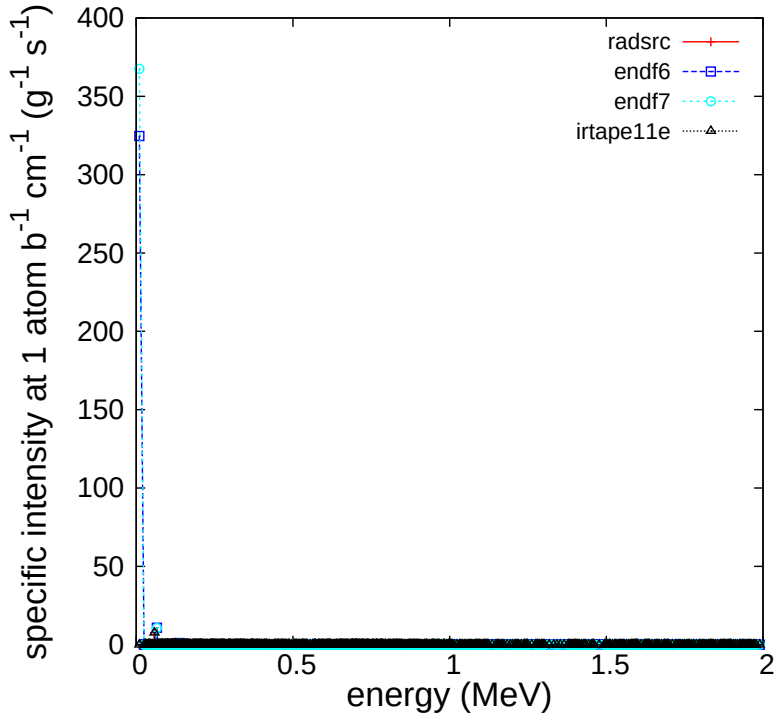

(a)

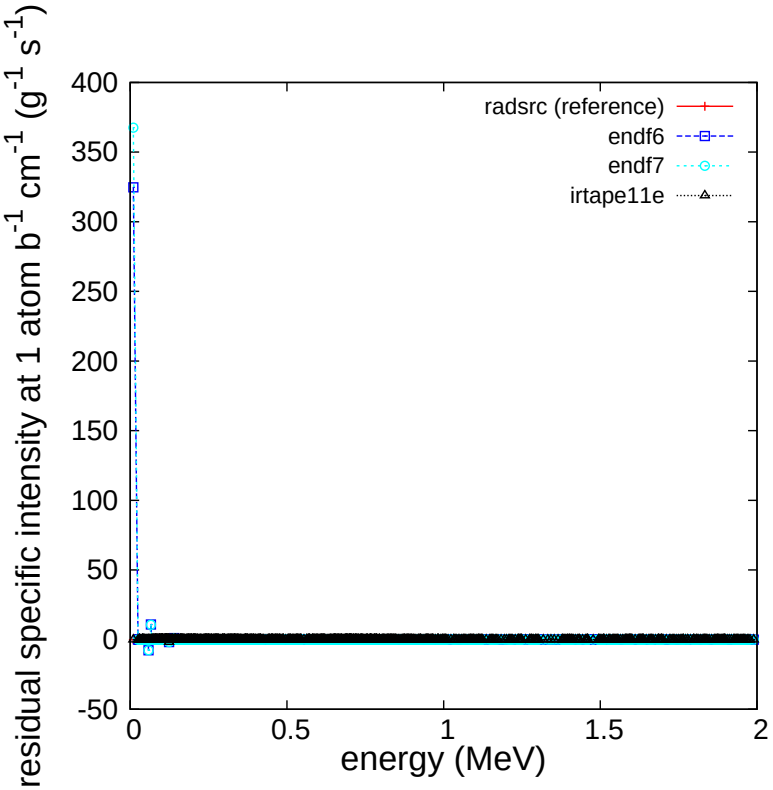

(b)

Fig. A.42. (a) photon emission intensity and (b) residual photon emission intensity with respect to the RadSrc database for Th-232

A.43 Th-234

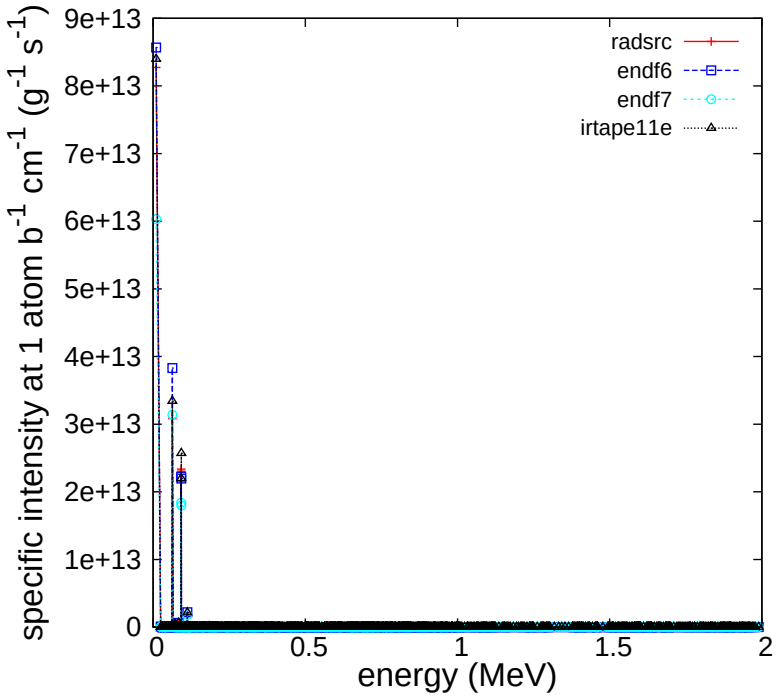

(a)

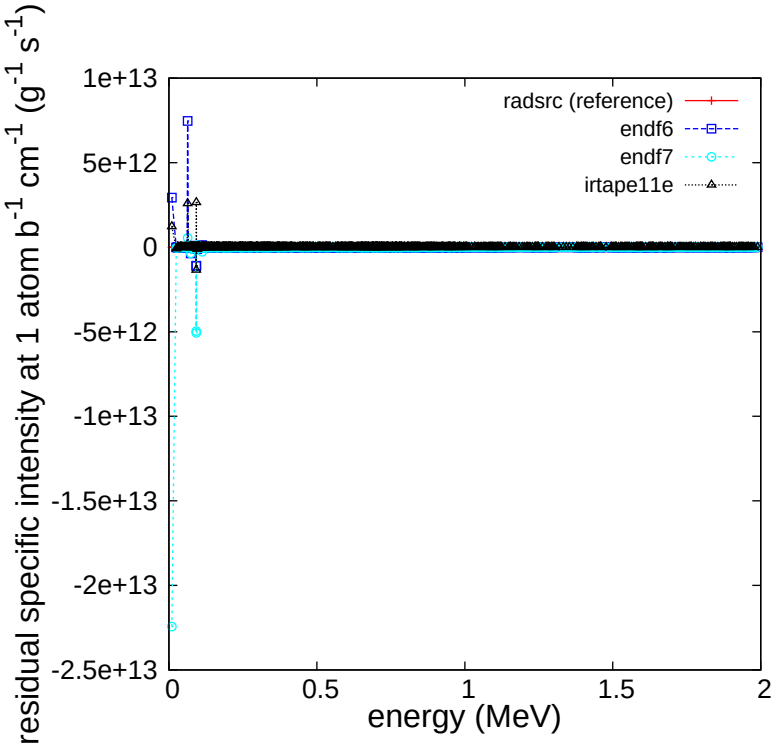

(b)

Fig. A.43. (a) photon emission intensity and (b) residual photon emission intensity with respect to the RadSrc database for Th-234

A.44 Pa-231

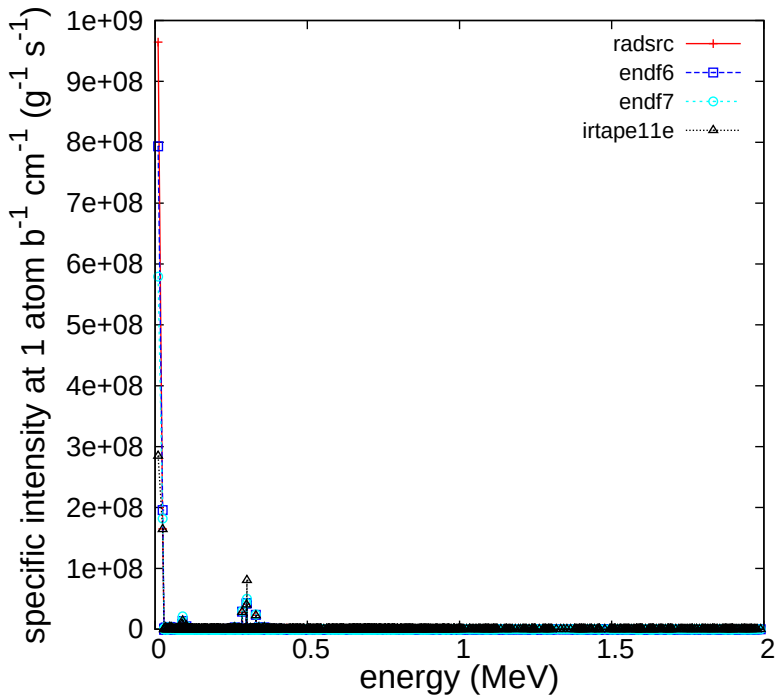

(a)

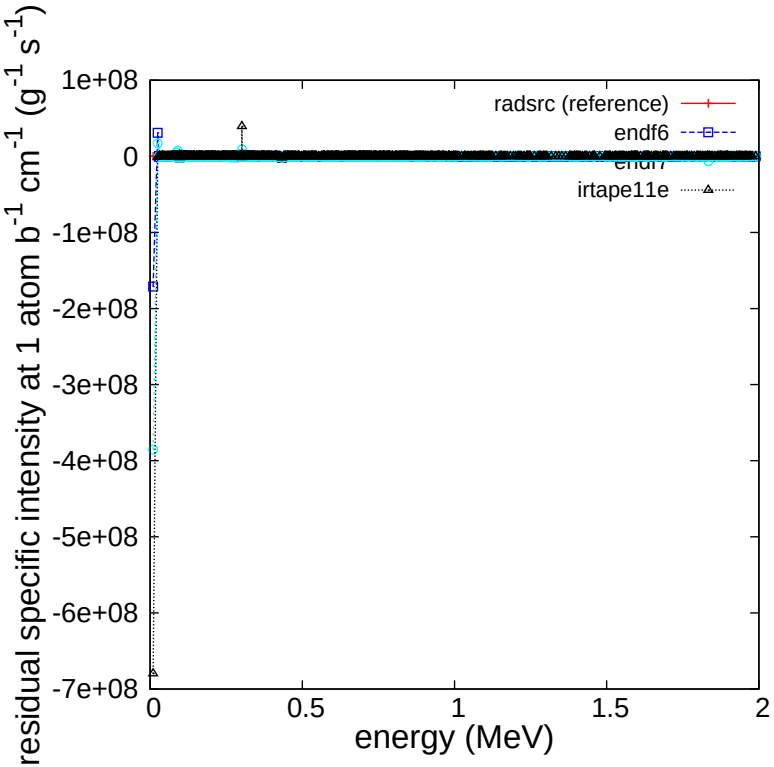

(b)

Fig. A.44. (a) photon emission intensity and (b) residual photon emission intensity with respect to the RadSrc database for Pa-231

A.45 Pa-233

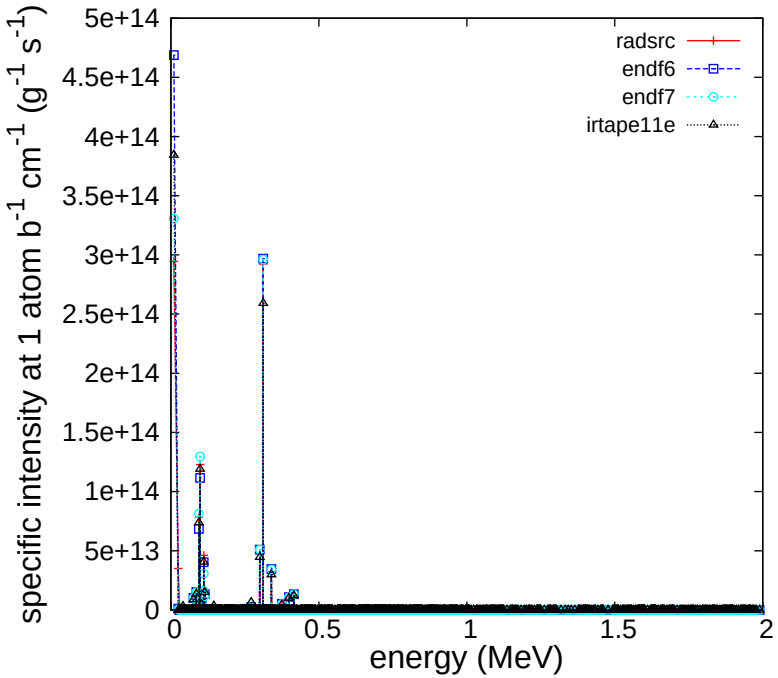

(a)

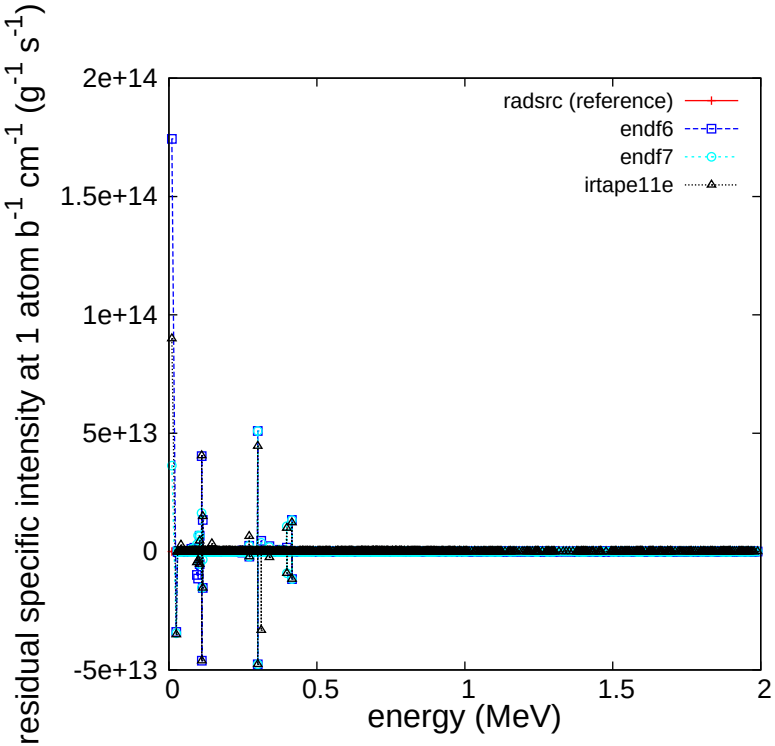

(b)

Fig. A.45. (a) photon emission intensity and (b) residual photon emission intensity with respect to the RadSrc database for Pa-233

A.46 Pa-234

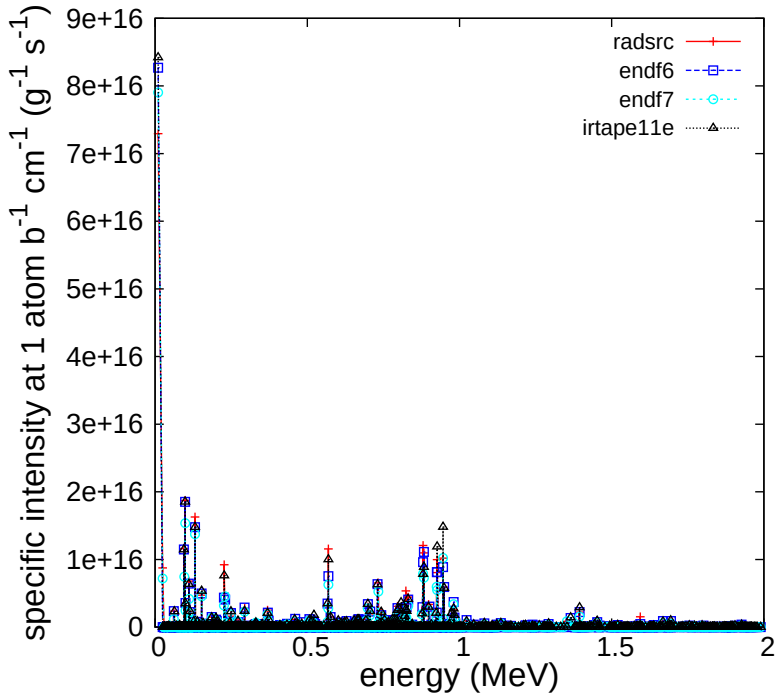

(a)

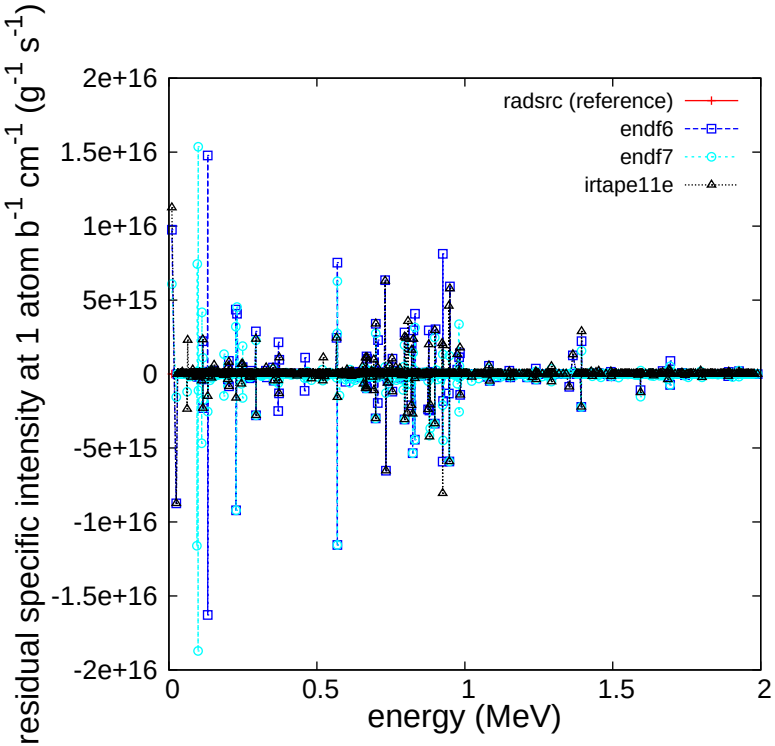

(b)

Fig. A.46. (a) photon emission intensity and (b) residual photon emission intensity with respect to the RadSrc database for Pa-234

A.47 Pa-234m

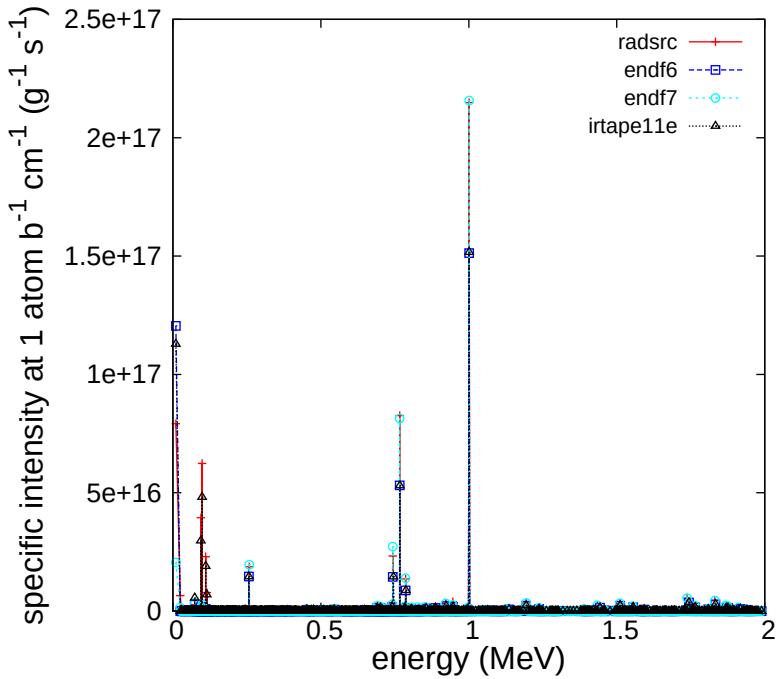

(a)

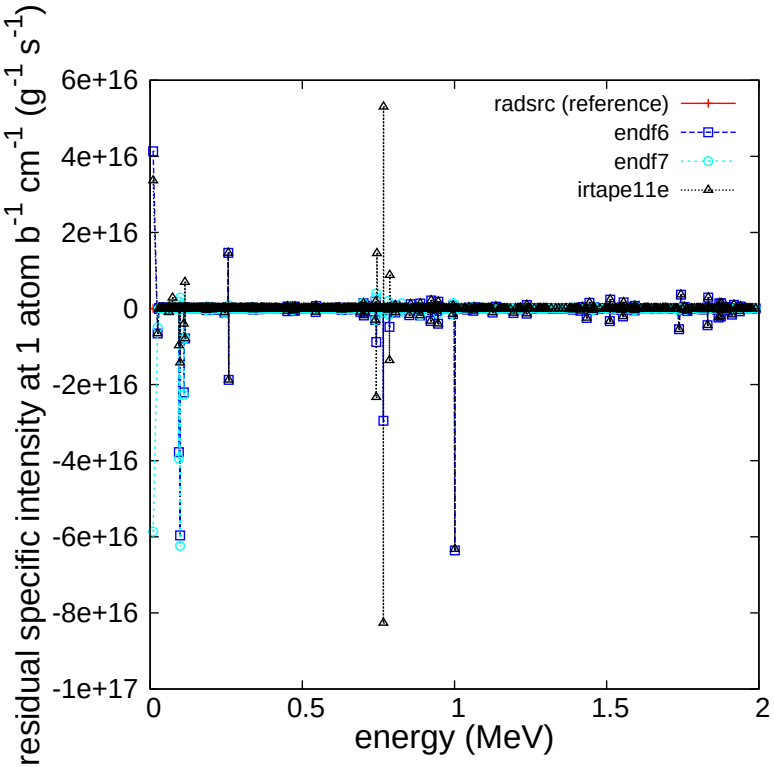

(b)

Fig. A.47. (a) photon emission intensity and (b) residual photon emission intensity with respect to the RadSrc database for Pa-234m

A.48 U-232

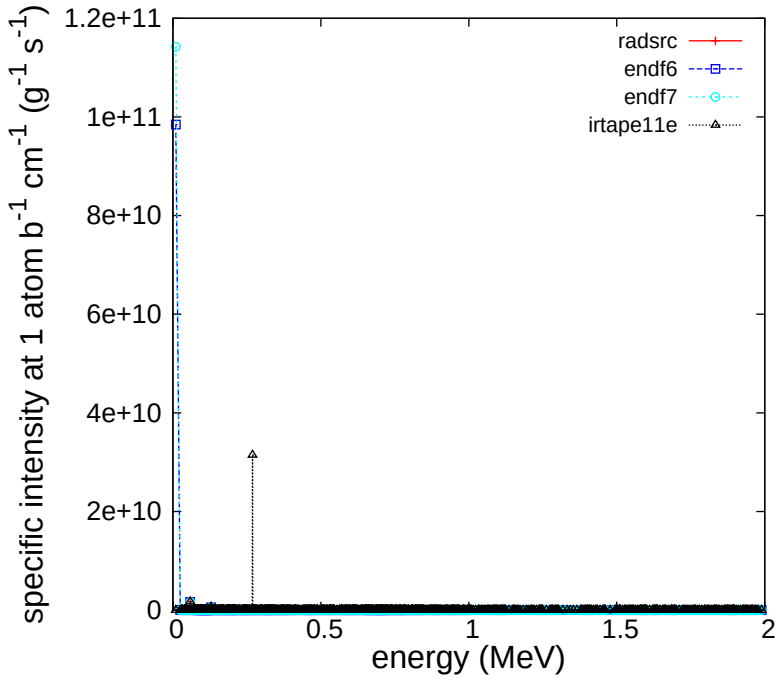

(a)

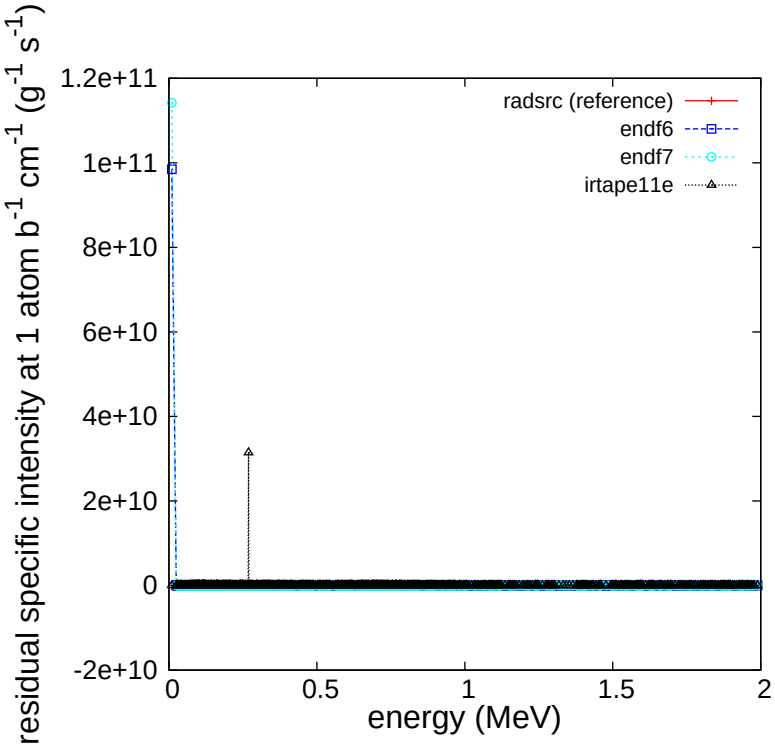

(b)

Fig. A.48. (a) photon emission intensity and (b) residual photon emission intensity with respect to the RadSrc database for U-232

A.49 U-233

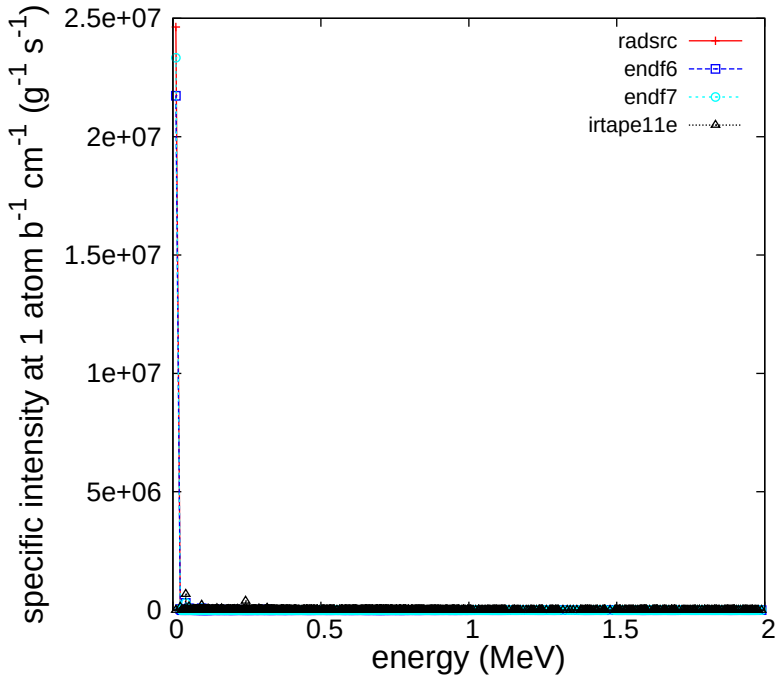

(a)

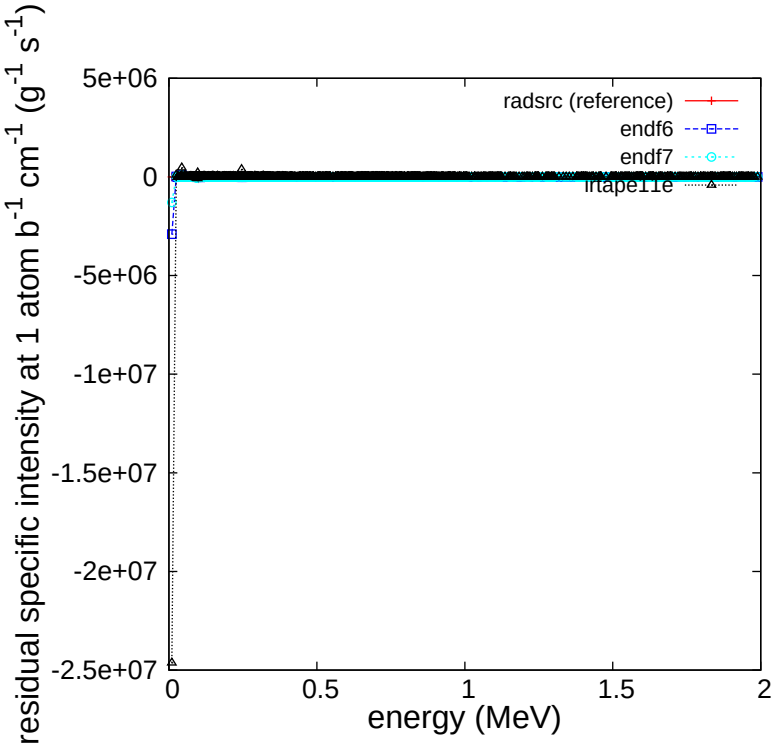

(b)

Fig. A.49. (a) photon emission intensity and (b) residual photon emission intensity with respect to the RadSrc database for U-233

A.50 U-234

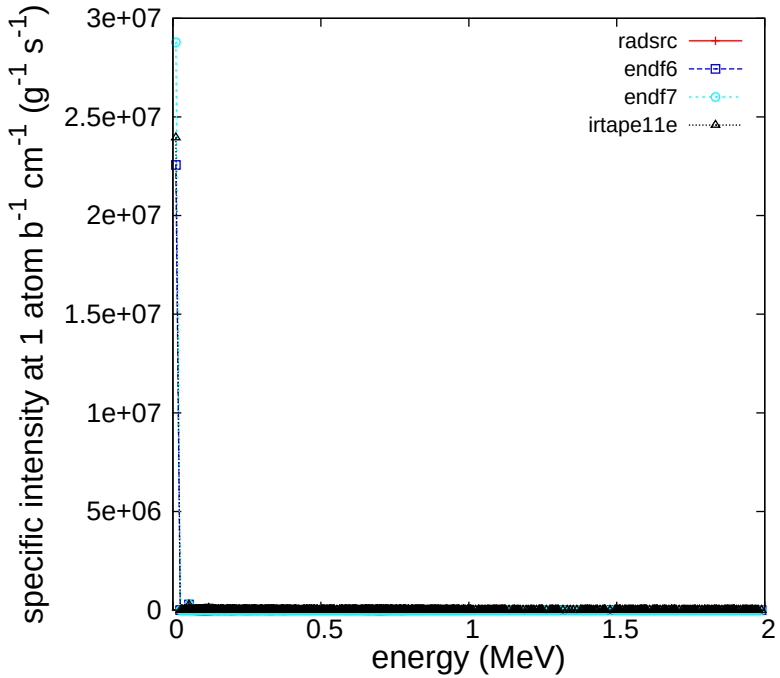

(a)

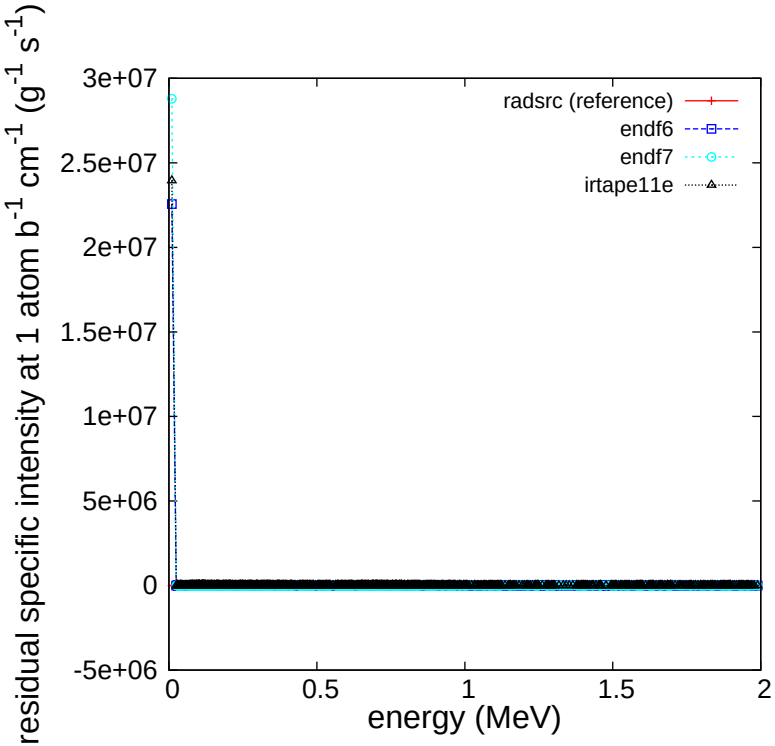

(b)

Fig. A.50. (a) photon emission intensity and (b) residual photon emission intensity with respect to the RadSrc database for U-234

A.51 U-235

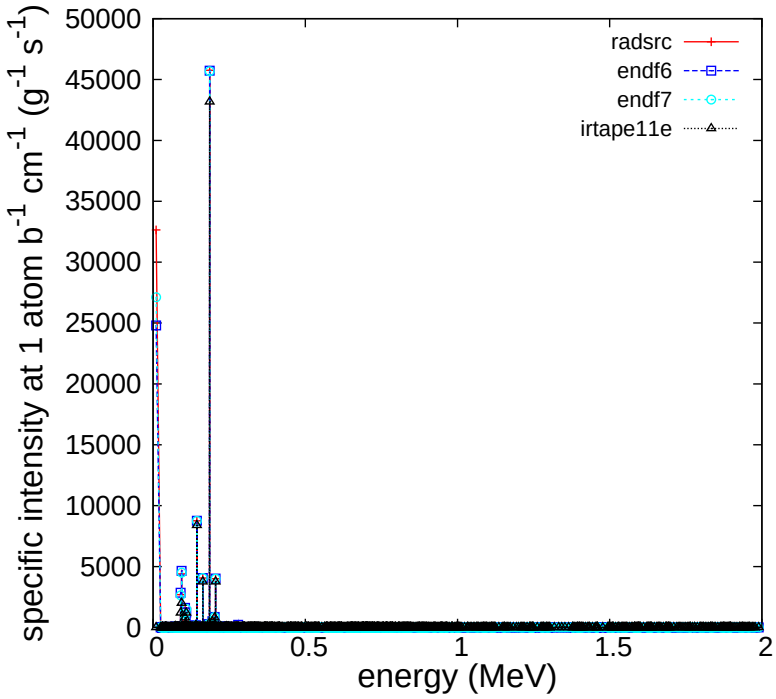

(a)

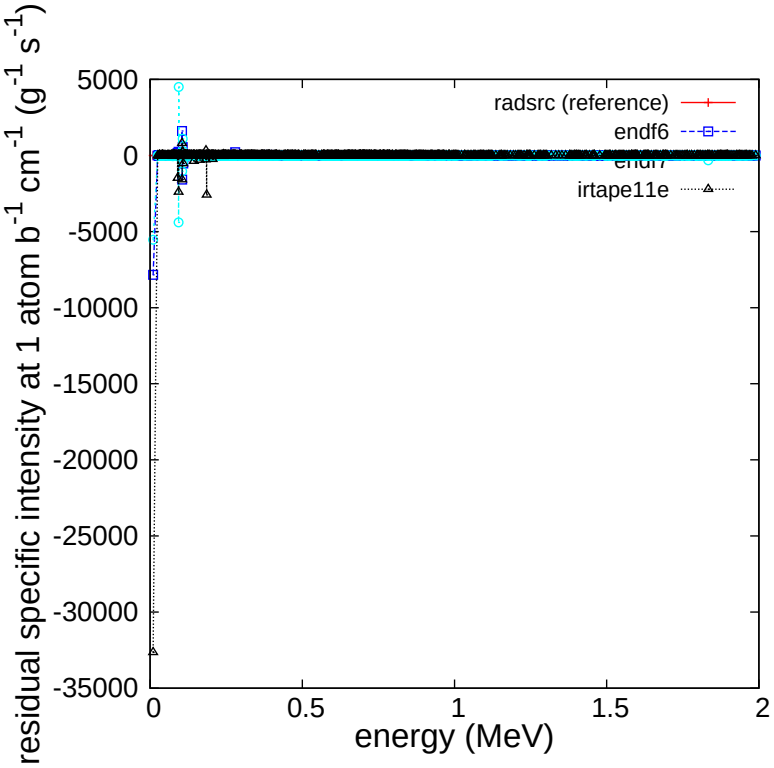

(b)

Fig. A.51. (a) photon emission intensity and (b) residual photon emission intensity with respect to the RadSrc database for U-235

A.52 U-236

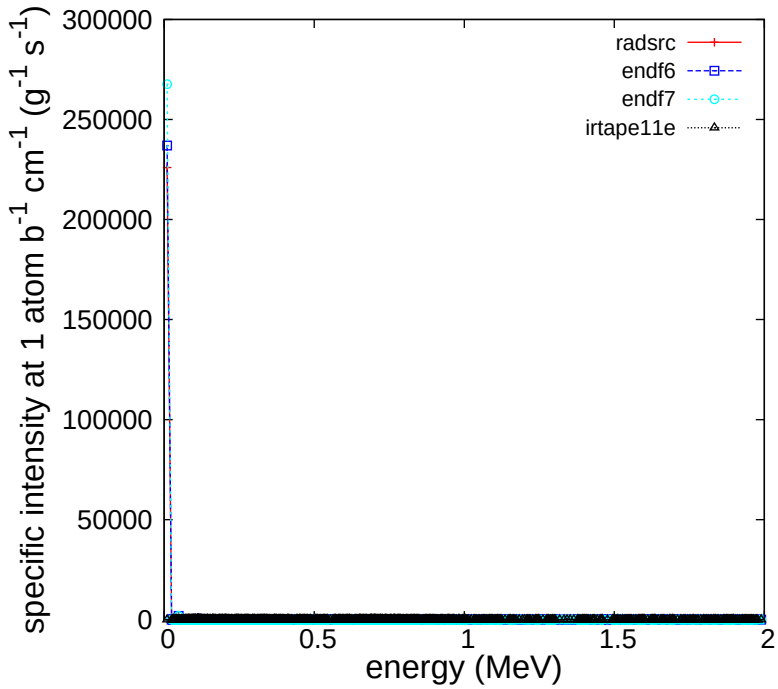

(a)

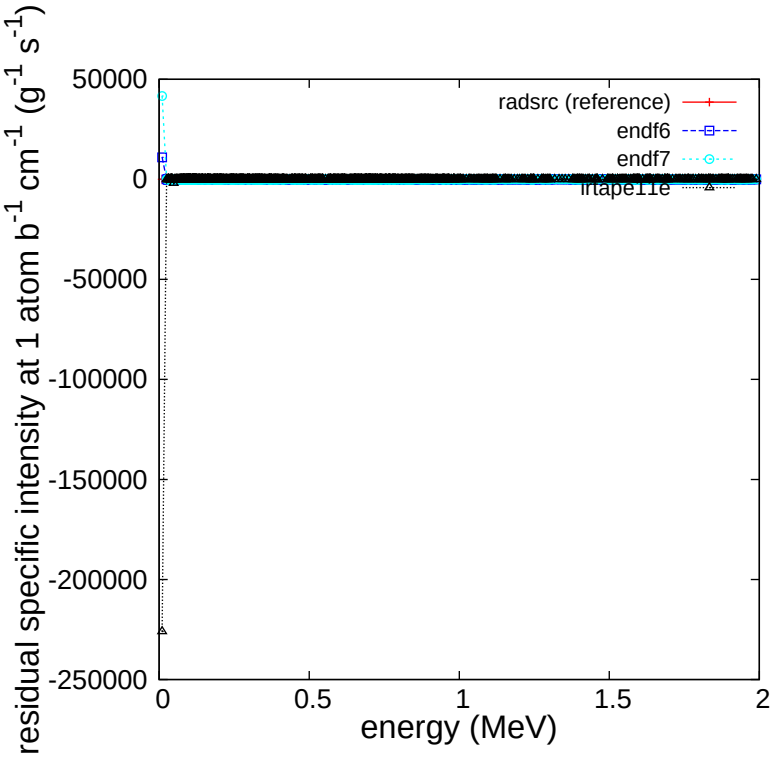

(b)

Fig. A.52. (a) photon emission intensity and (b) residual photon emission intensity with respect to the RadSrc database for U-236

A.53 U-237

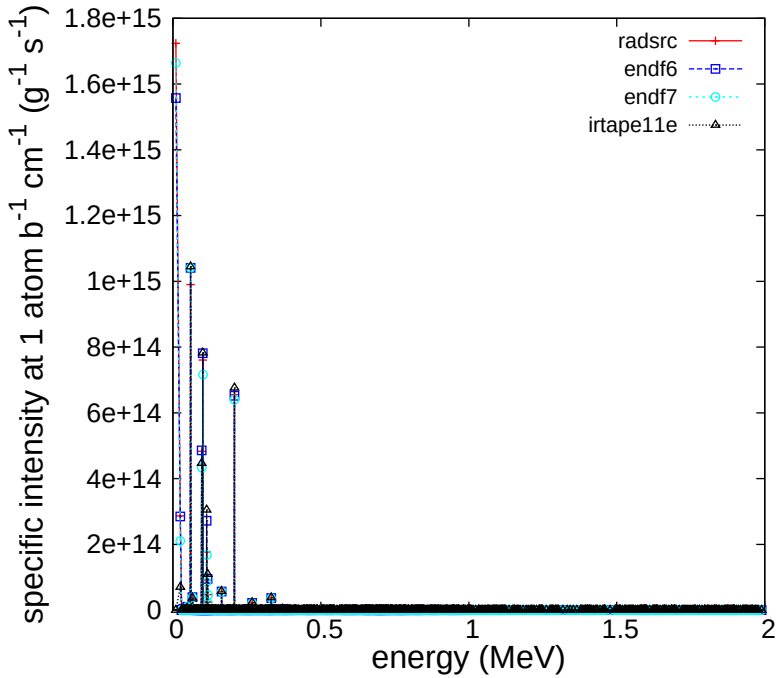

(a)

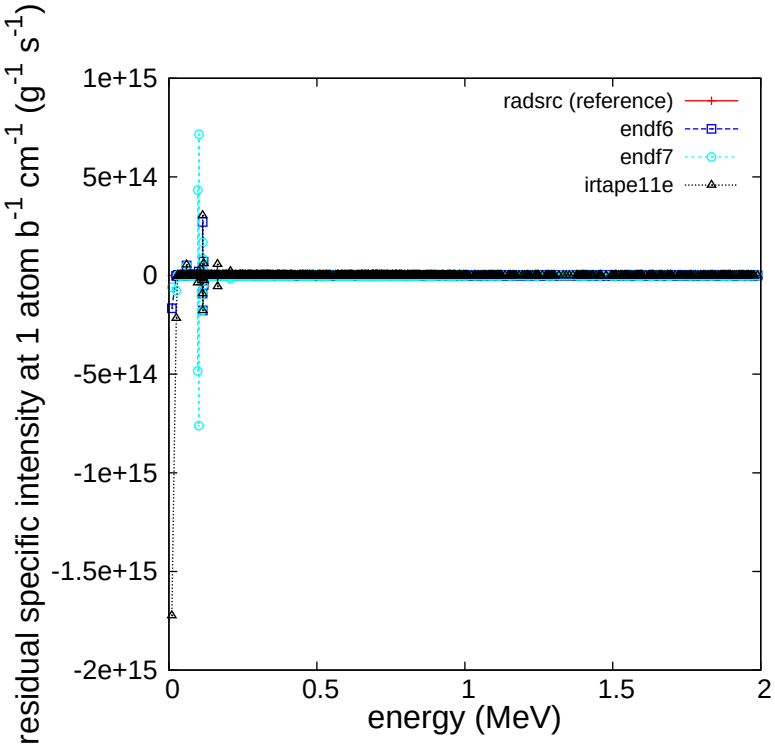

(b)

Fig. A.53. (a) photon emission intensity and (b) residual photon emission intensity with respect to the RadSrc database for U-237

A.54 U-238

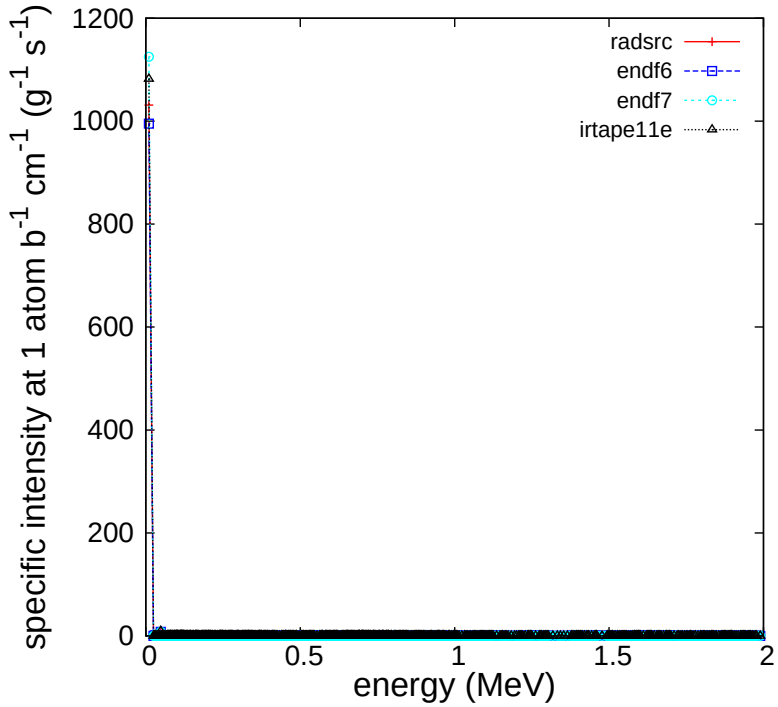

(a)

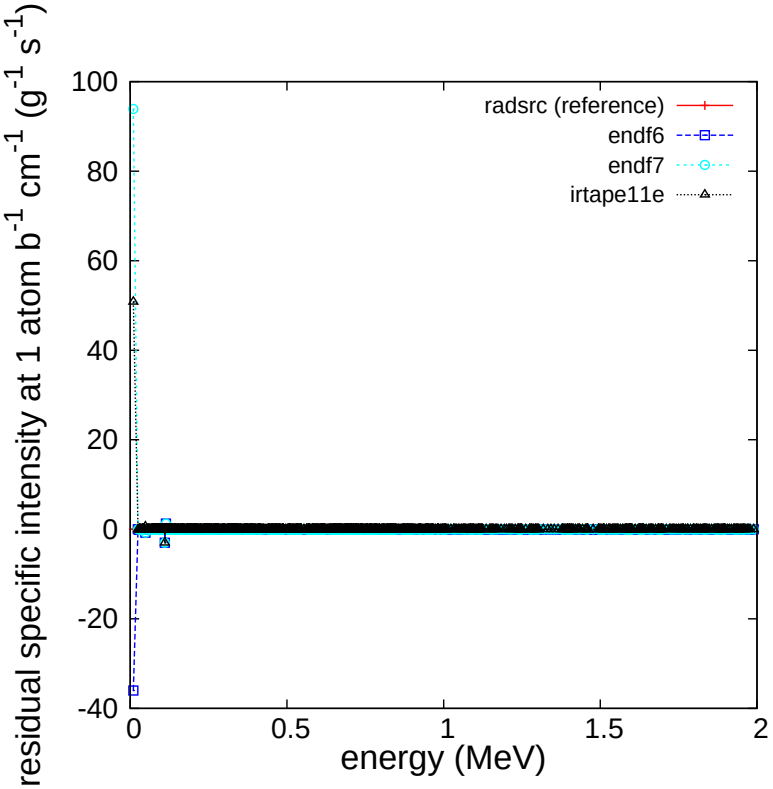

(b)

Fig. A.54. (a) photon emission intensity and (b) residual photon emission intensity with respect to the RadSrc database for U-238

A.55 Np-237

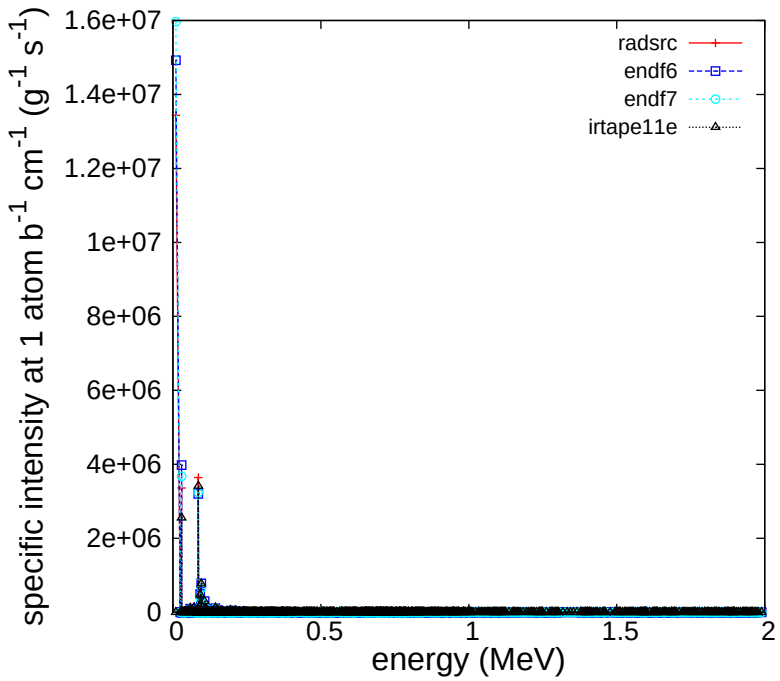

(a)

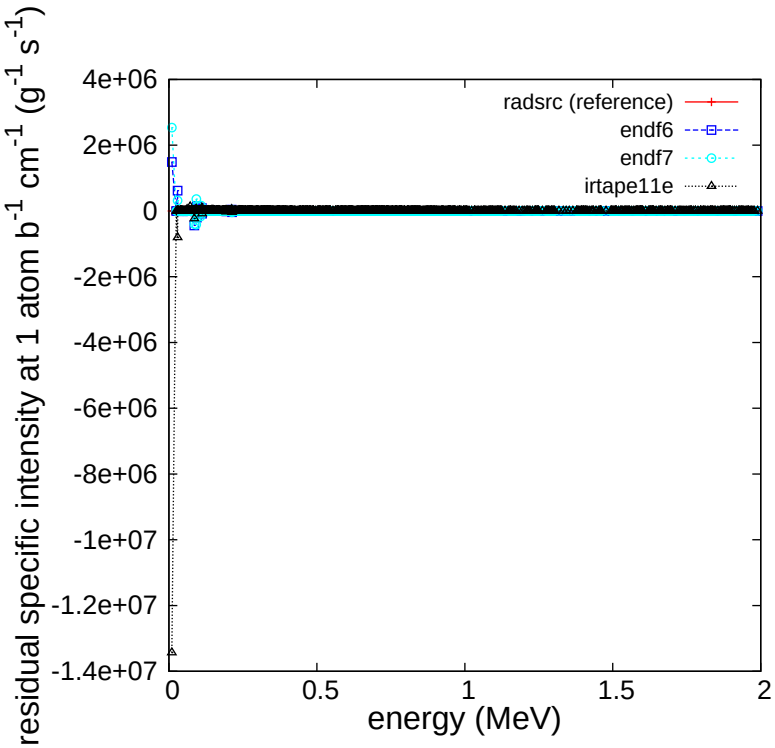

(b)

Fig. A.55. (a) photon emission intensity and (b) residual photon emission intensity with respect to the RadSrc database for Np-237

A.56 Np-239

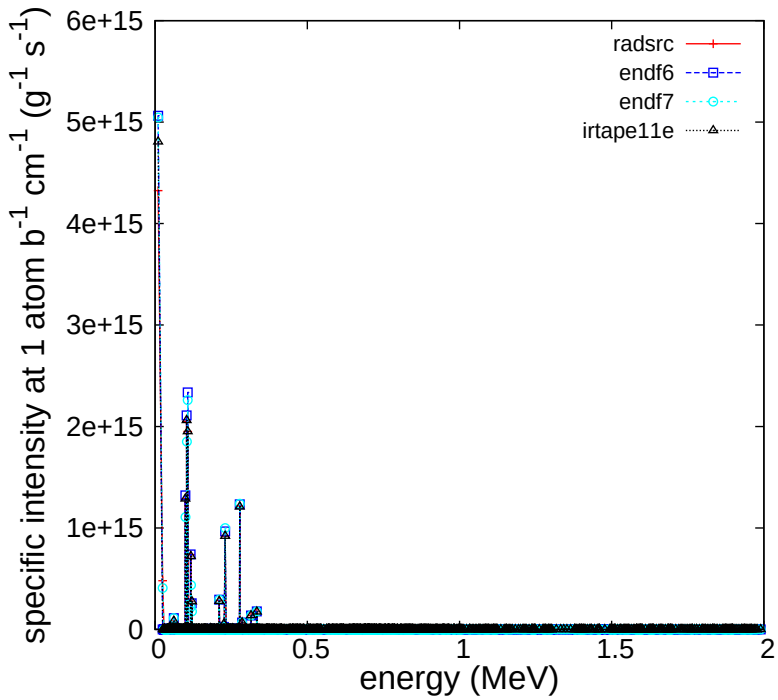

(a)

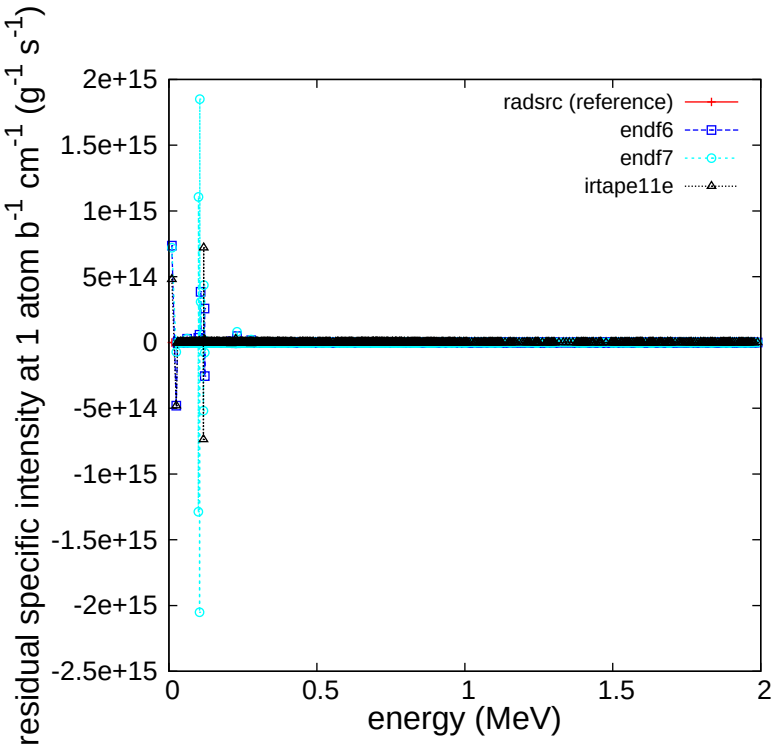

(b)

Fig. A.56. (a) photon emission intensity and (b) residual photon emission intensity with respect to the RadSrc database for Np-239

A.57 Pu-236

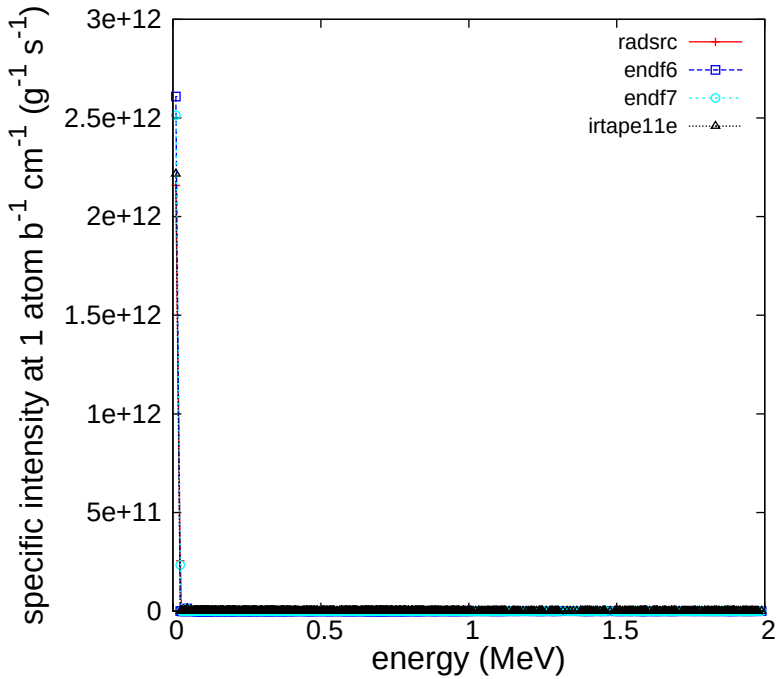

(a)

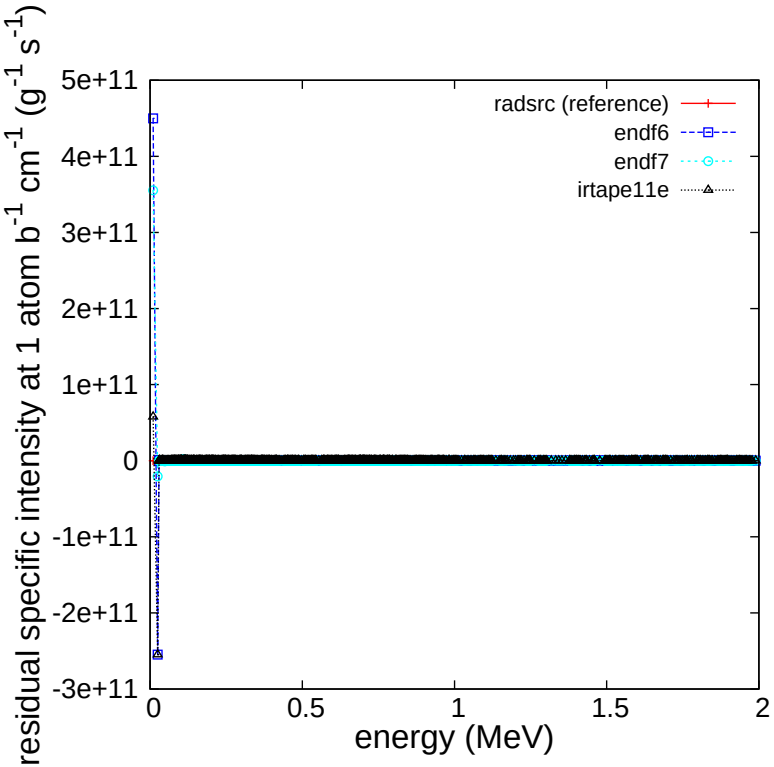

(b)

Fig. A.57. (a) photon emission intensity and (b) residual photon emission intensity with respect to the RadSrc database for Pu-236

A.58 Pu-238

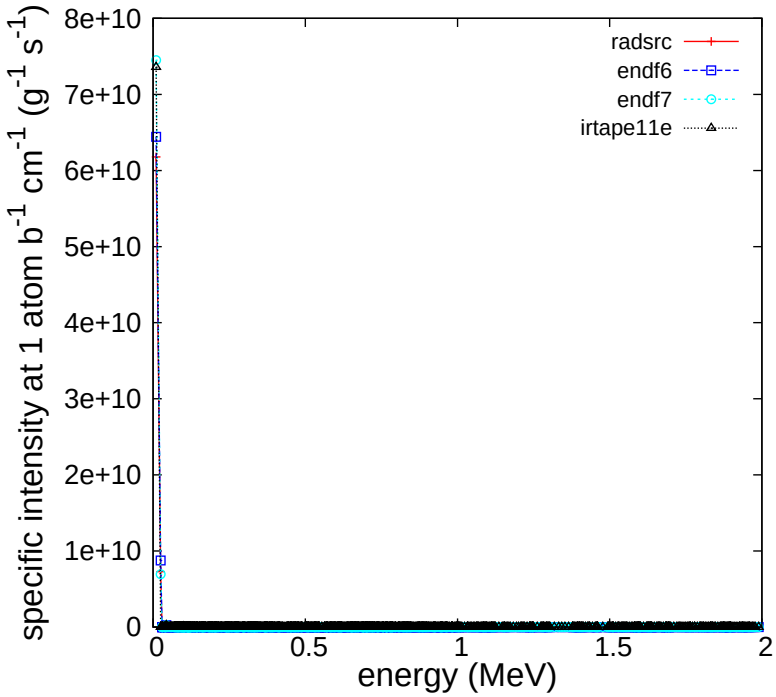

(a)

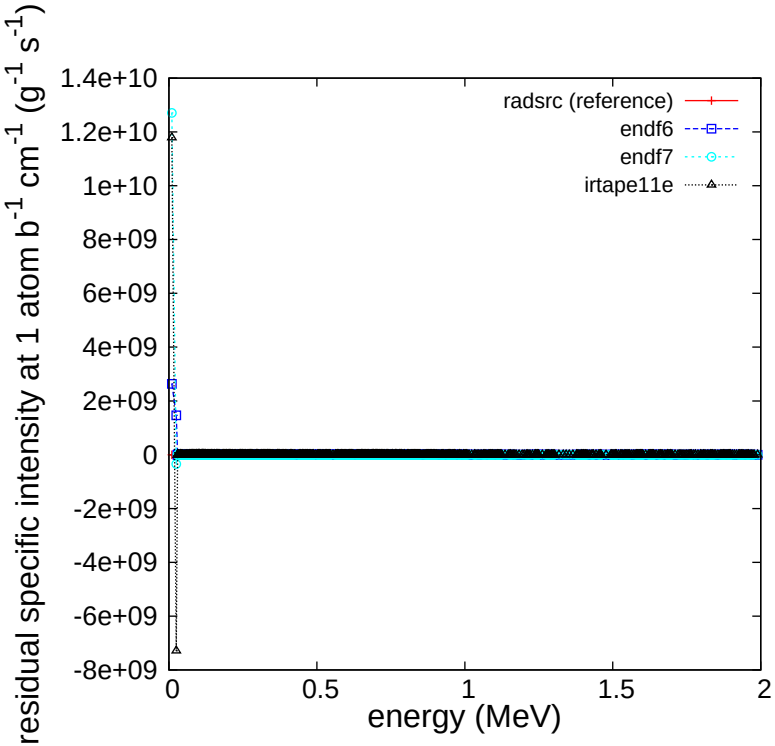

(b)

Fig. A.58. (a) photon emission intensity and (b) residual photon emission intensity with respect to the RadSrc database for Pu-238

A.59 Pu-239

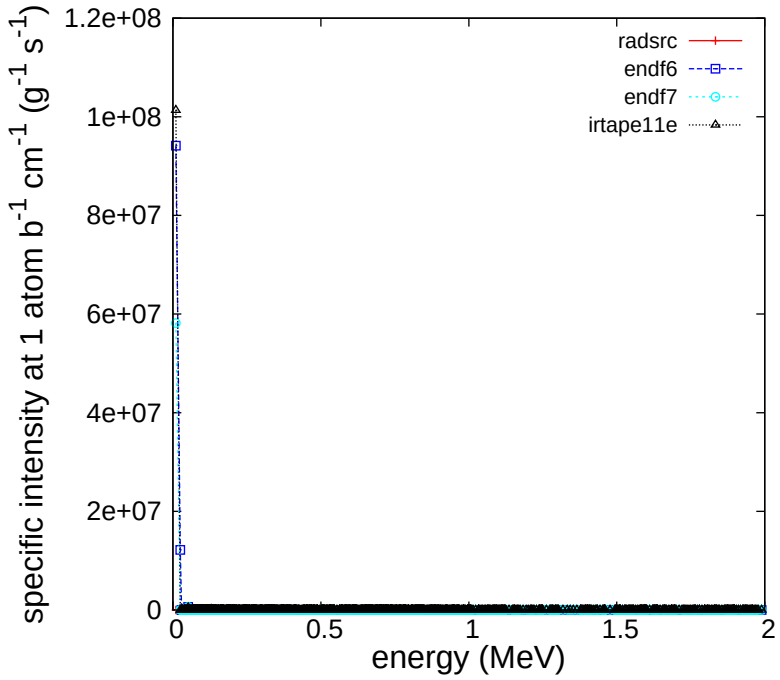

(a)

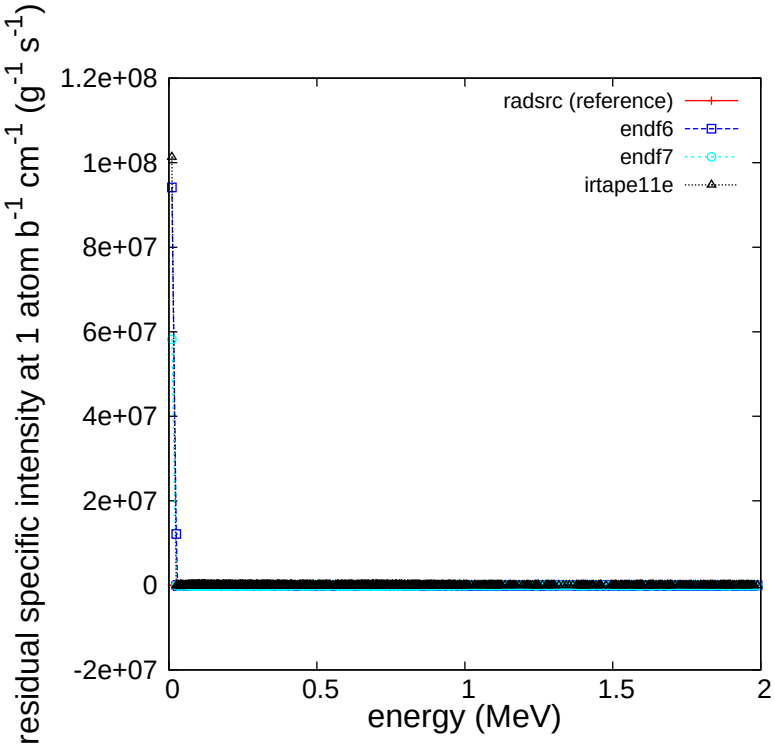

(b)

Fig. A.59. (a) photon emission intensity and (b) residual photon emission intensity with respect to the RadSrc database for Pu-239

A.60 Pu-240

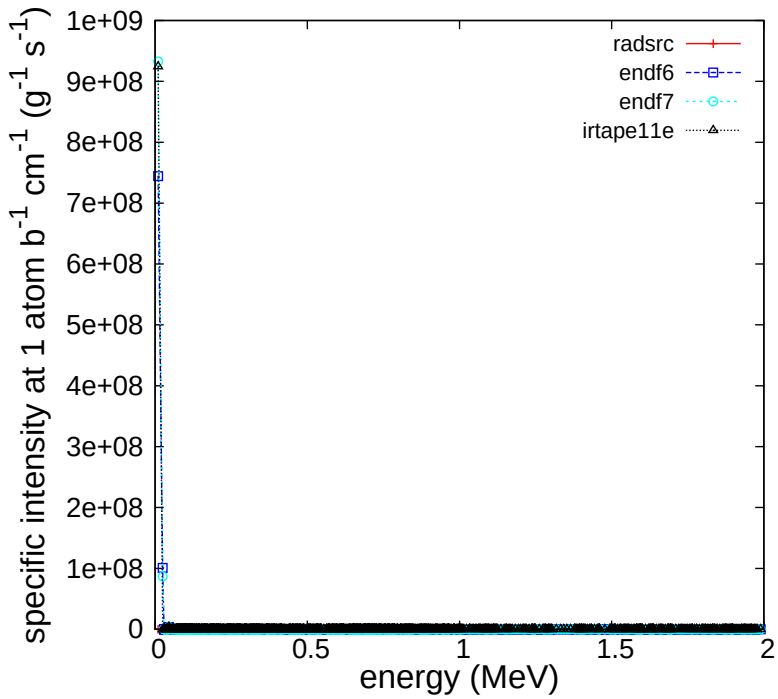

(a)

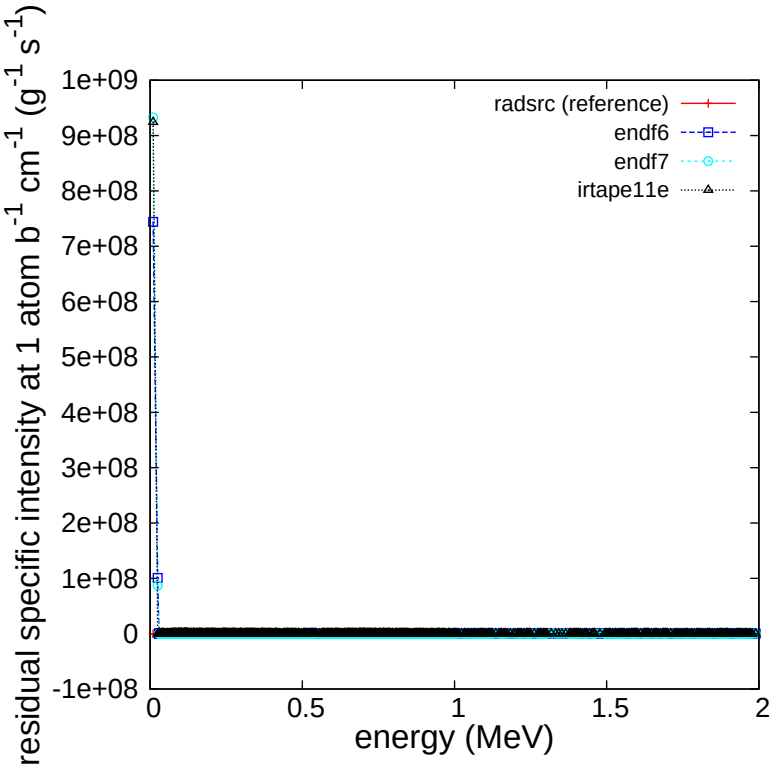

(b)

Fig. A.60. (a) photon emission intensity and (b) residual photon emission intensity with respect to the RadSrc database for Pu-240

A.61 Pu-241

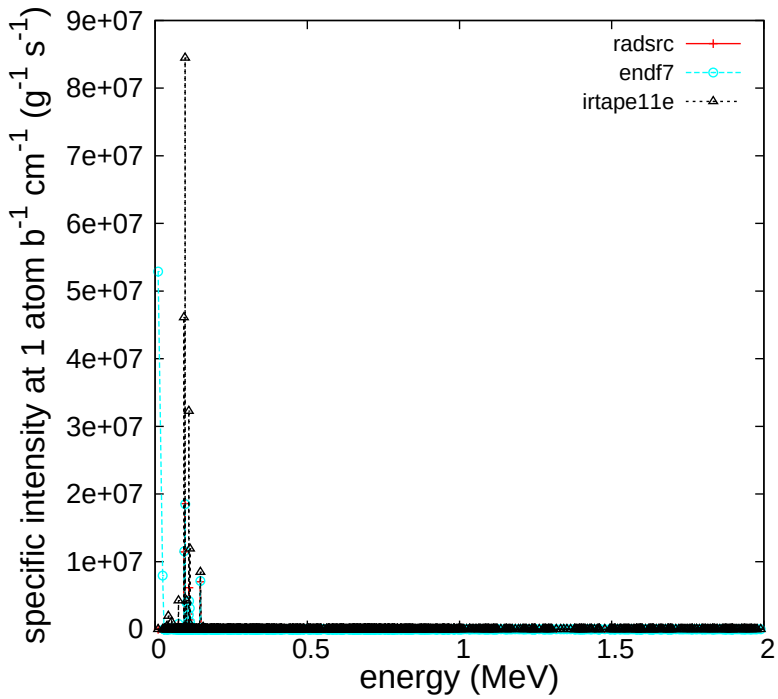

(a)

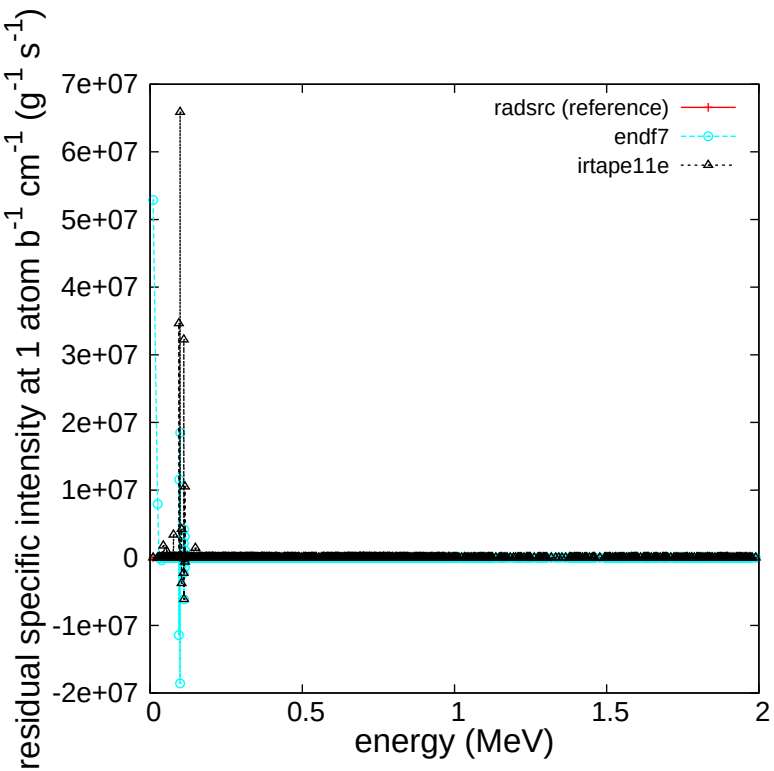

(b)

Fig. A.61. (a) photon emission intensity and (b) residual photon emission intensity with respect to the RadSrc database for Pu-241

A.62 Pu-242

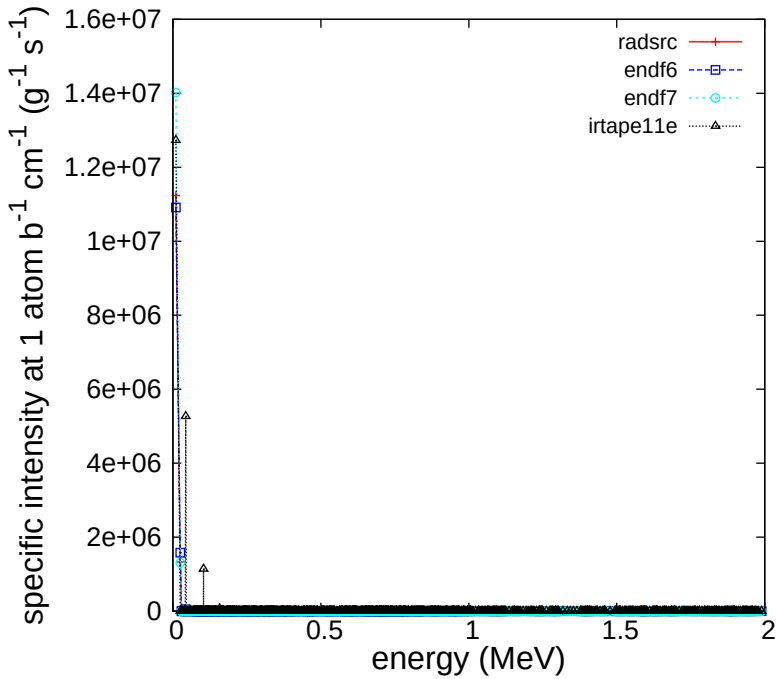

(a)

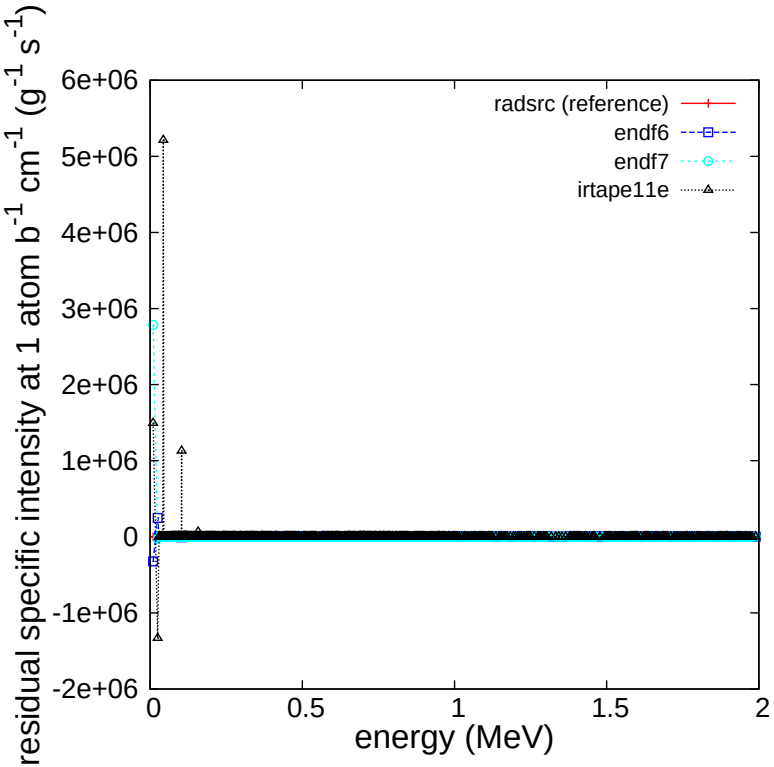

(b)

Fig. A.62. (a) photon emission intensity and (b) residual photon emission intensity with respect to the RadSrc database for Pu-242

A.63 Am-241

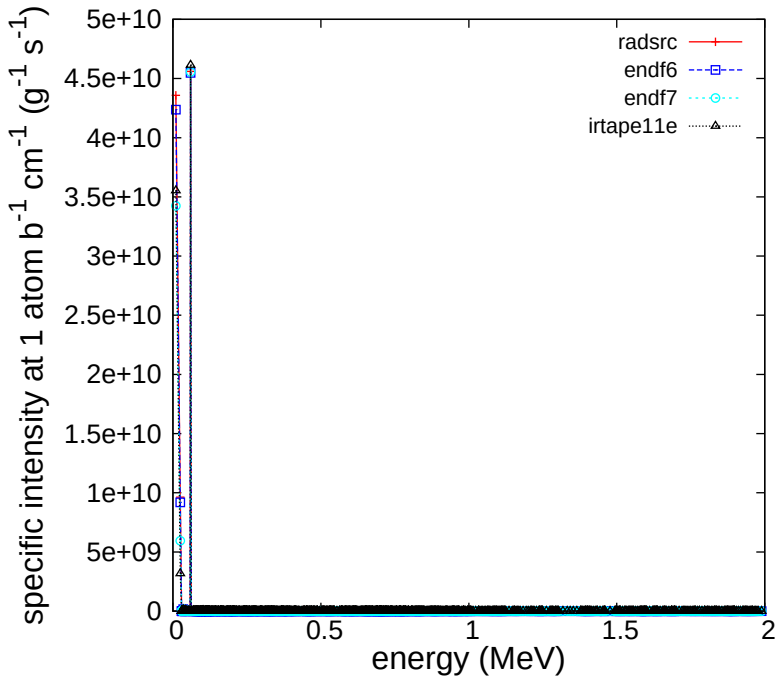

(a)

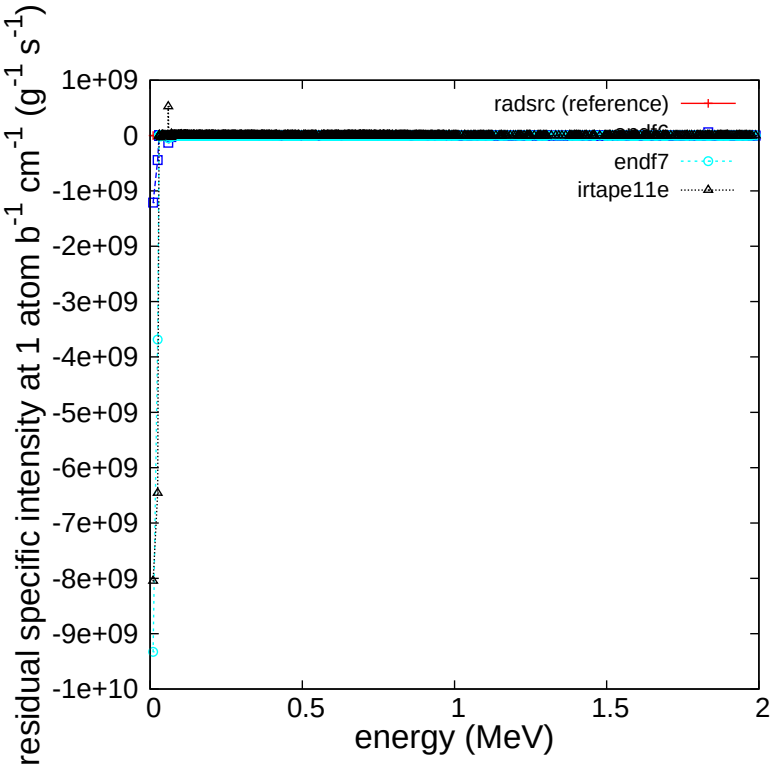

(b)

Fig. A.63. (a) photon emission intensity and (b) residual photon emission intensity with respect to the RadSrc database for Am-241

A.64 Am-243

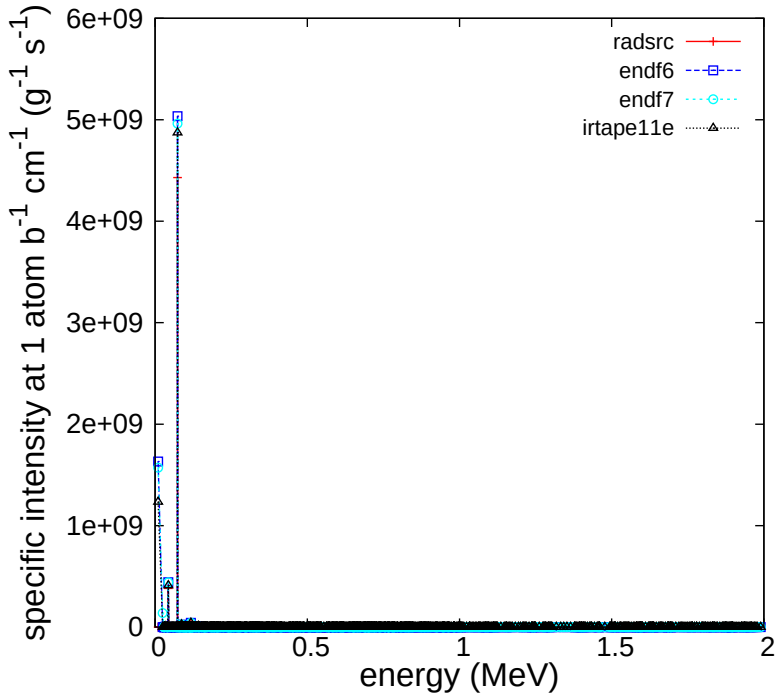

(a)

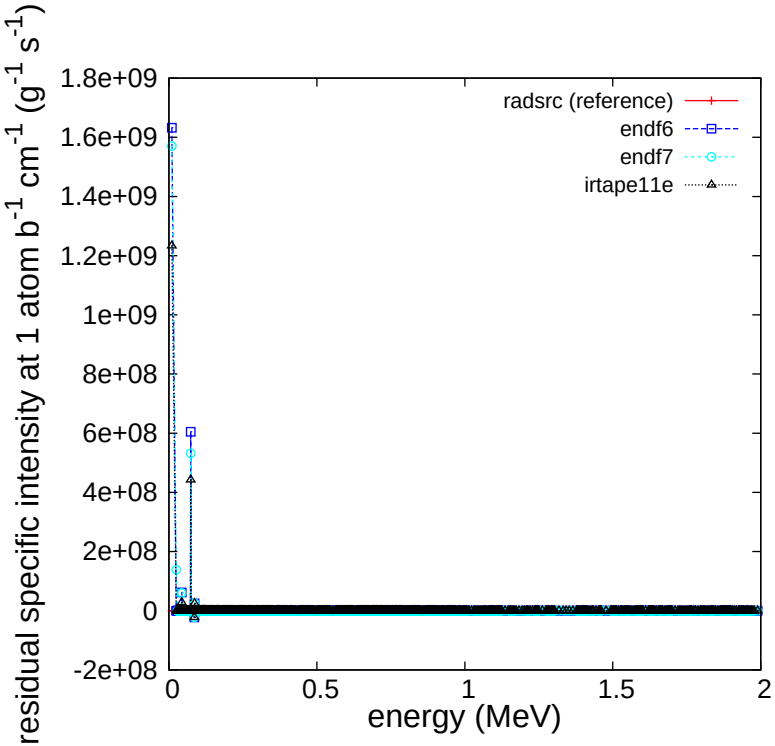

(b)

Fig. A.64. (a) photon emission intensity and (b) residual photon emission intensity with respect to the RadSrc database for Am-243

A.65 Am-245

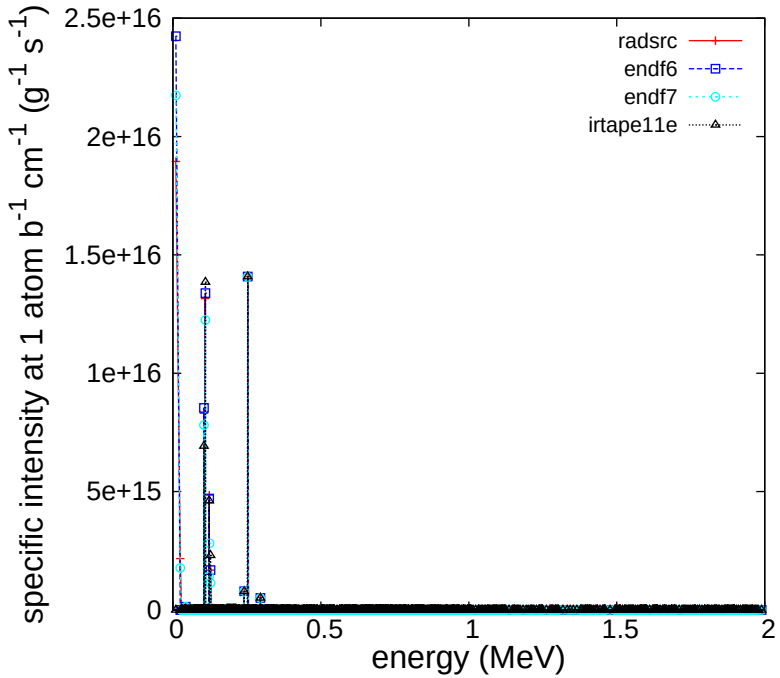

(a)

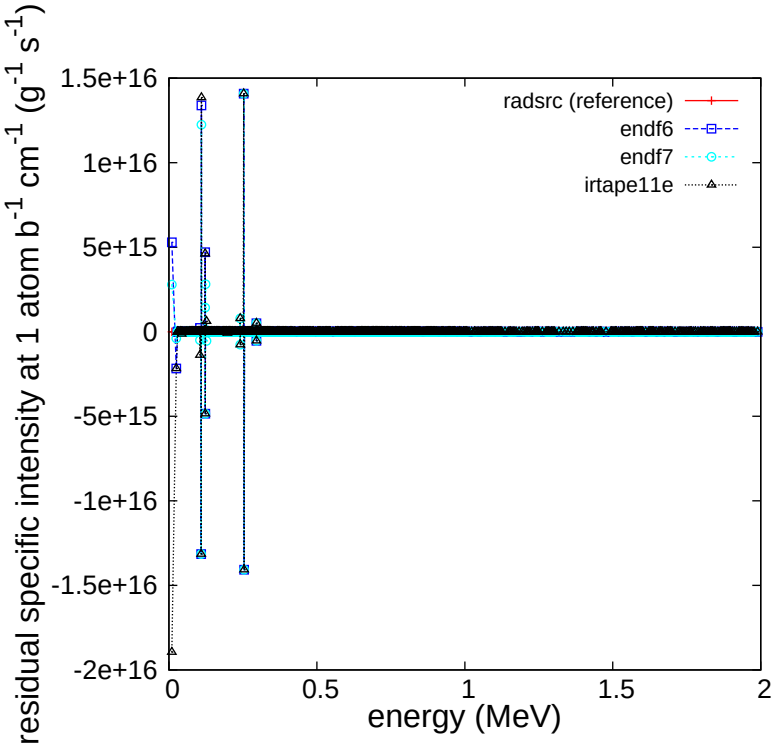

(b)

Fig. A.65. (a) photon emission intensity and (b) residual photon emission intensity with respect to the RadSrc database for Am-245

A.66 Cm-244

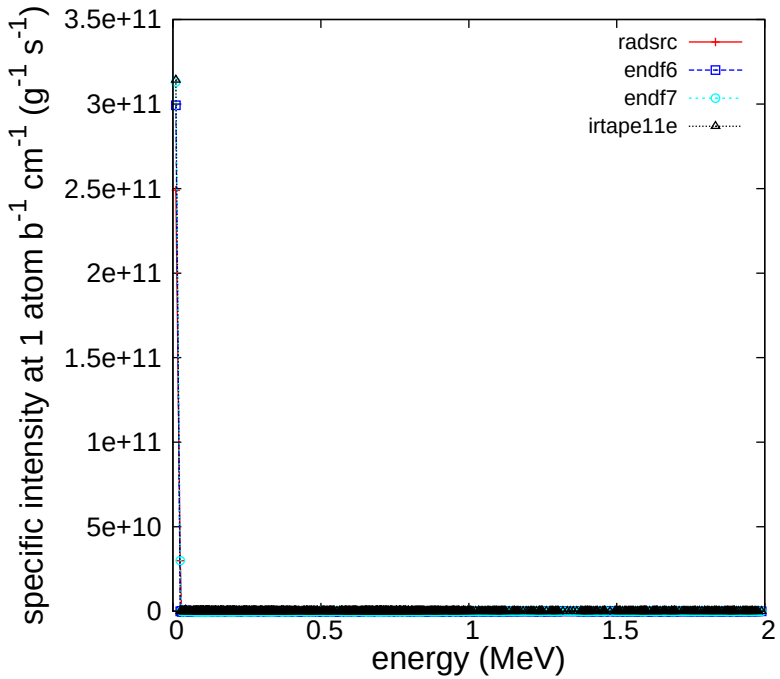

(a)

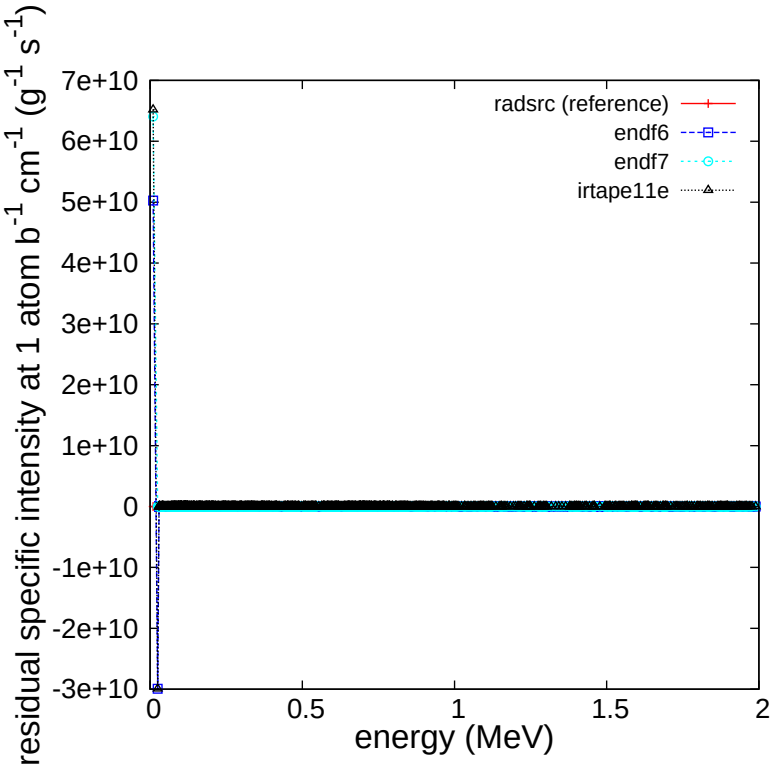

(b)

Fig. A.66. (a) photon emission intensity and (b) residual photon emission intensity with respect to the RadSrc database for Cm-244

A.67 Cm-245

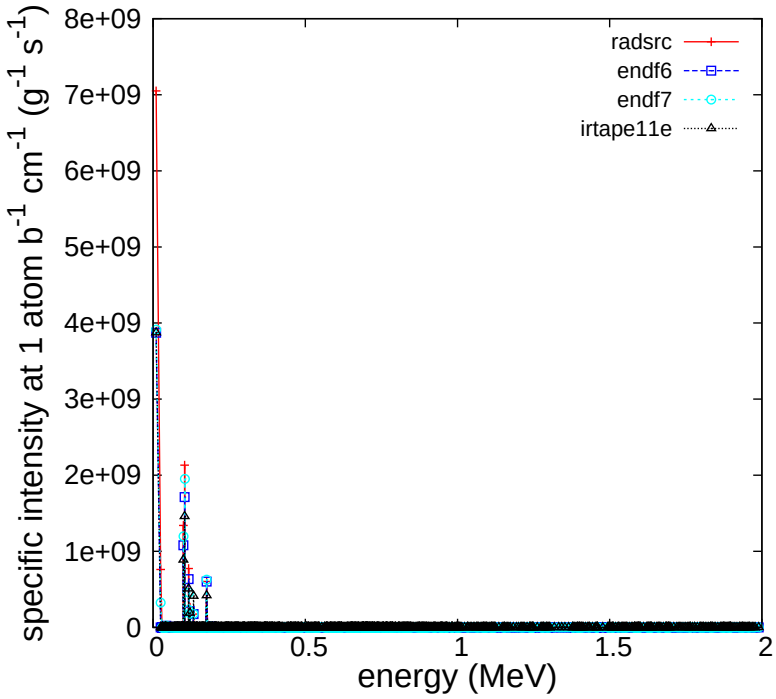

(a)

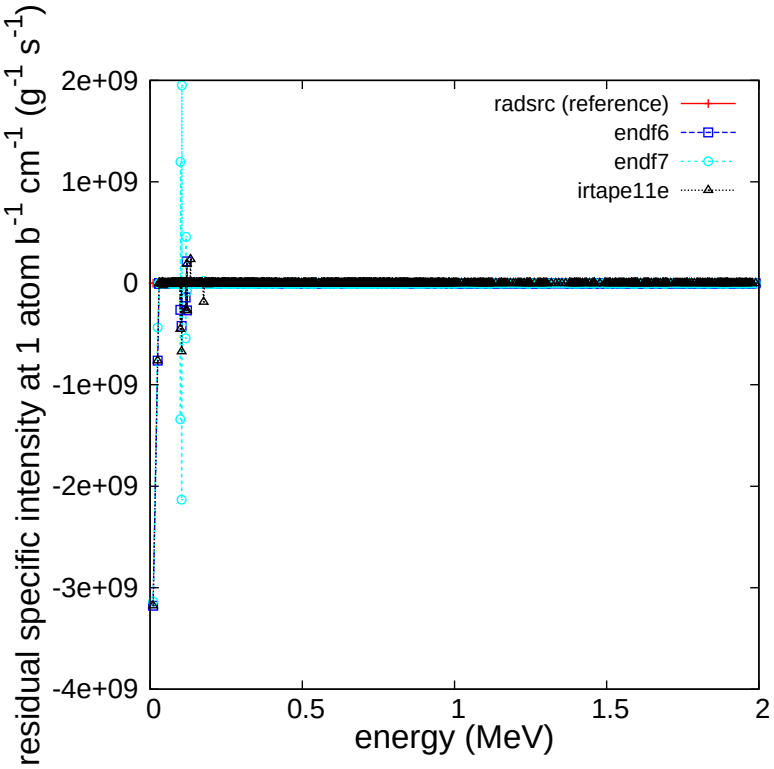

(b)

Fig. A.67. (a) photon emission intensity and (b) residual photon emission intensity with respect to the RadSrc database for Cm-245

A.68 Cm-249

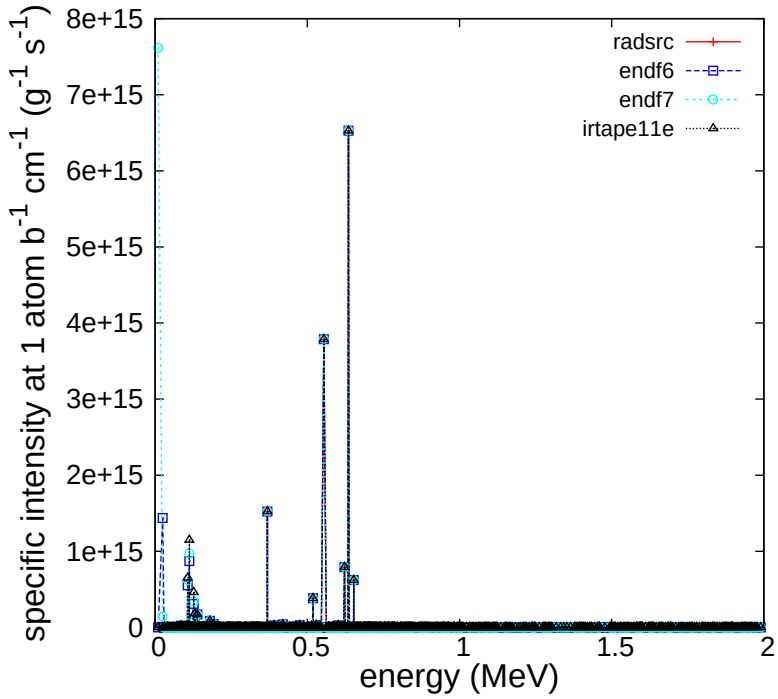

(a)

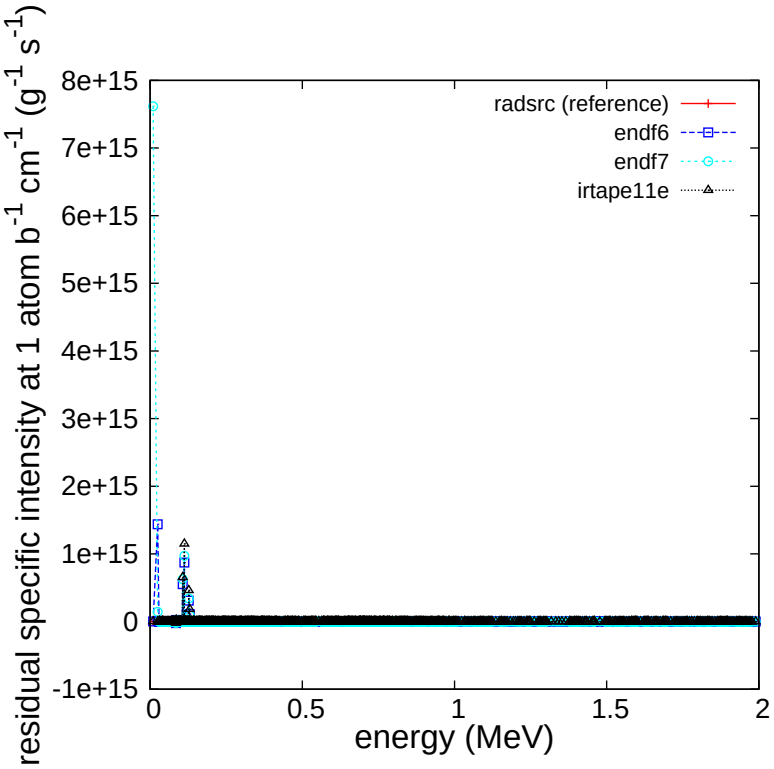

(b)

Fig. A.68. (a) photon emission intensity and (b) residual photon emission intensity with respect to the RadSrc database for Cm-249

A.69 Bk-249

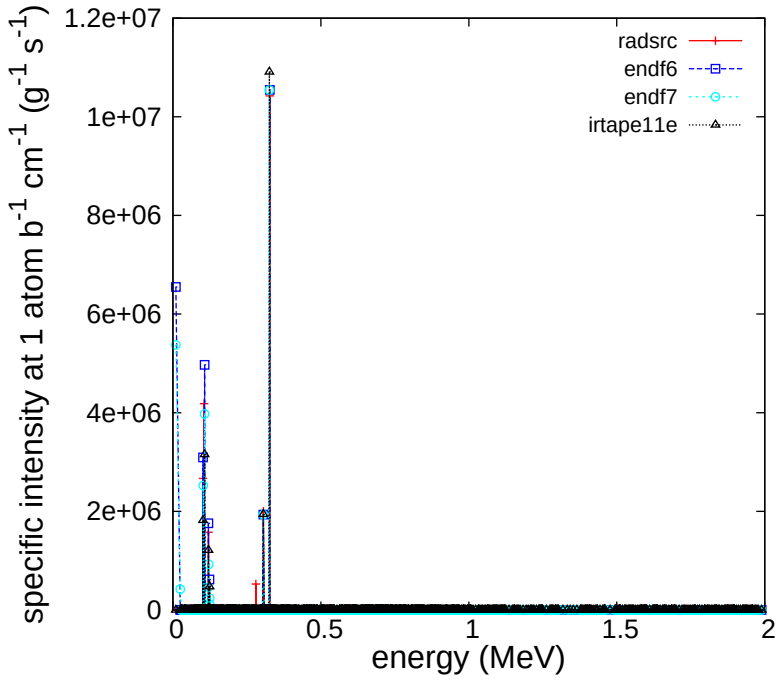

(a)

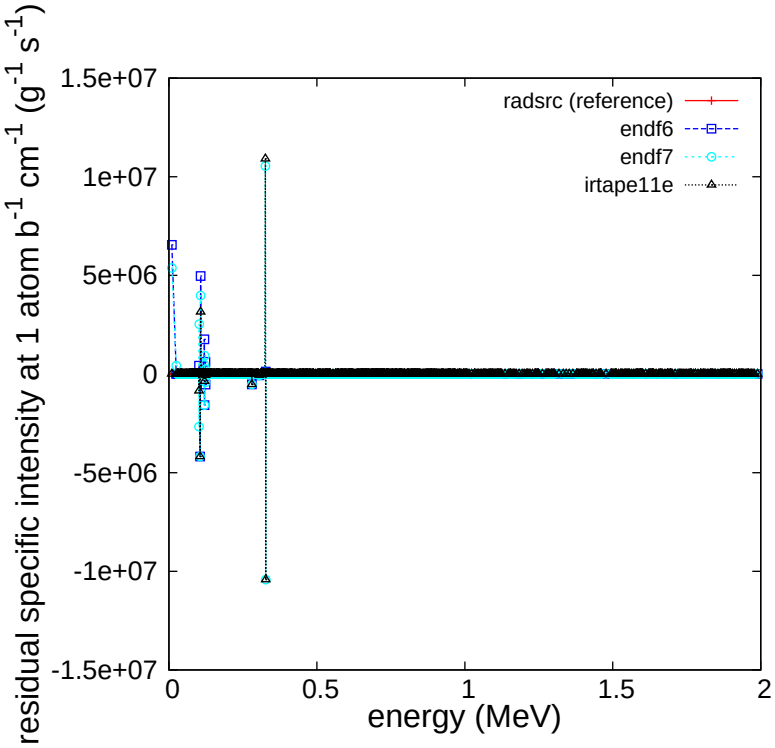

(b)

Fig. A.69. (a) photon emission intensity and (b) residual photon emission intensity with respect to the RadSrc database for Bk-249

A.70 Cf-249

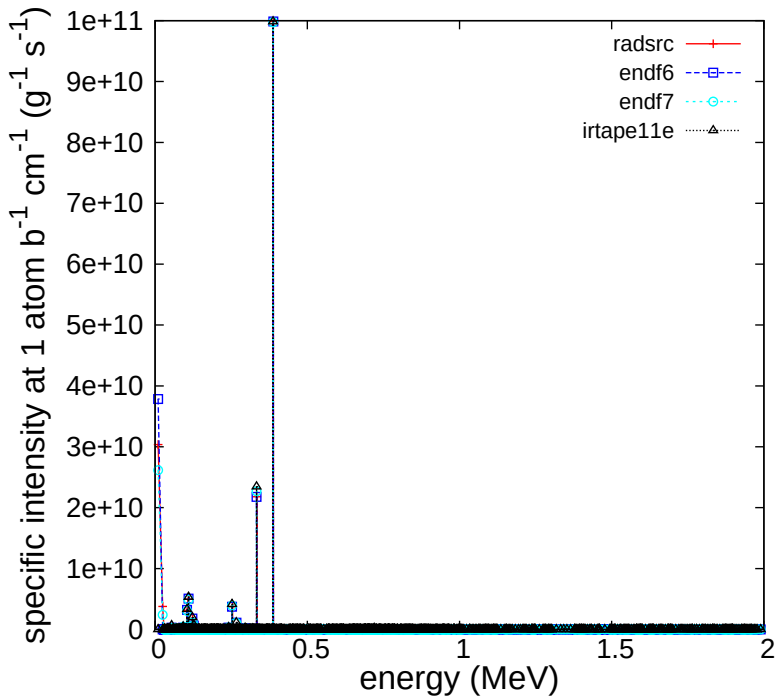

(a)

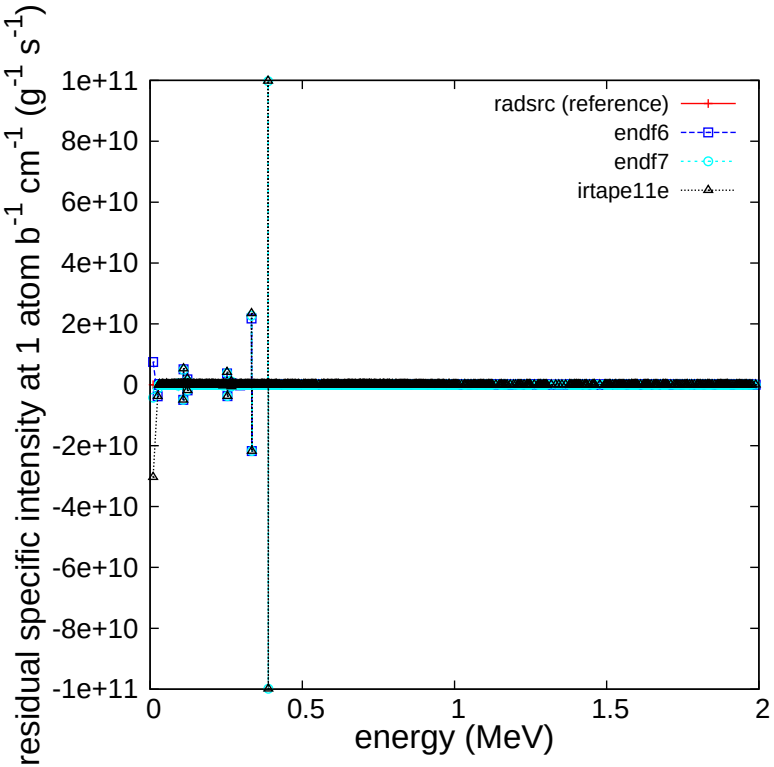

(b)

Fig. A.70. (a) photon emission intensity and (b) residual photon emission intensity with respect to the RadSrc database for Cf-249

A.71 Es-253

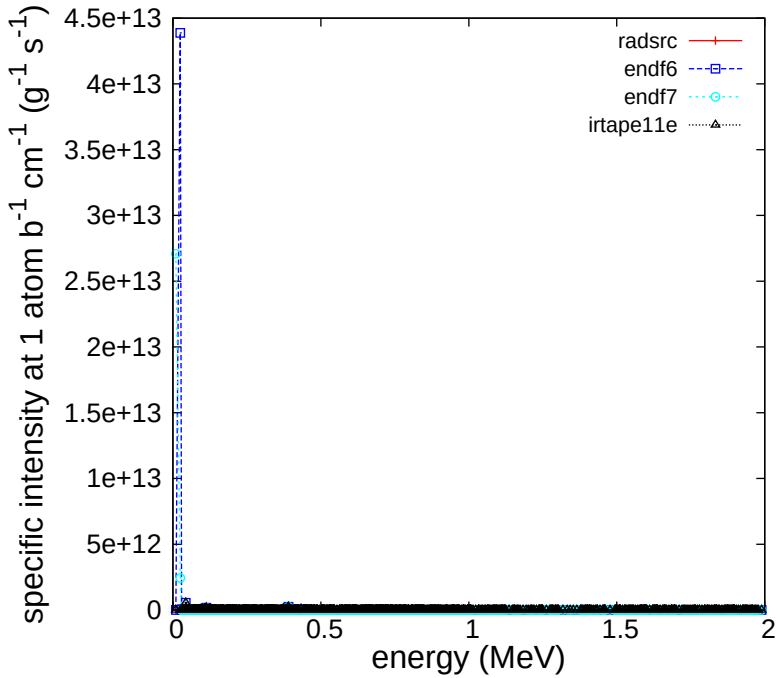

(a)

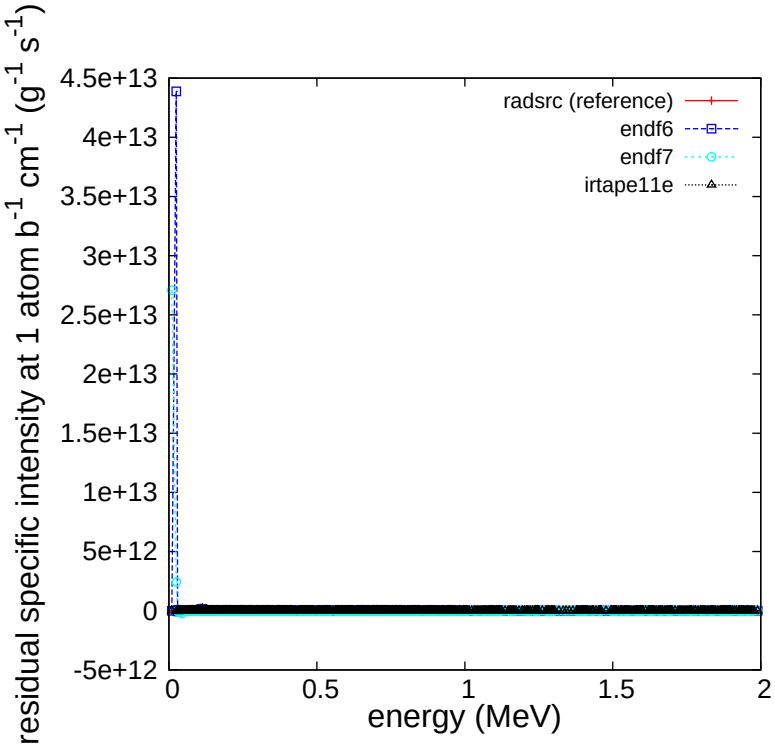

(b)

Fig. A.71. (a) photon emission intensity and (b) residual photon emission intensity with respect to the RadSrc database for Es-253